THEORETICAL AND EXPERIMENTAL STUDY OF A NEW, SMALL, HIGH SPEED, LINEAR TORQUE MOTOR (POLARIZED RELAY TYPE)

R. J. McNICHOLAS

THESIS
M265

Library
U. S. Naval Postgraduate School
Monterey, California

THEORETICAL AND EXPERIMENTAL STUDY

OF

A NEW, SMALL, HIGH SPEED, LINEAR TORQUE MOTOR

(POLARIZED RELAY TYPE)

by

Robert Joseph McNicholas

First Lieutenant U. S. Marine Corps

An essay submitted to the Advisory Board of the School of Engineering, The Johns Hopkins University, in conformity with the requirements for the degree of Master of Science in Engineering

THE JOHNS HOPKINS UNIVERSITY

Baltimore Maryland

MAY 1952

Thesis
M265

ACKNOWLEDGEMENT

The author gratefully expresses his indebtedness to Mr. Fletcher C. Paddison for his many helpful discussions and continuous encouragement during the progress of this test; to Dr. Walter A. Good and Dr. John M. Kopper for their most valuable comments and criticisms; to Mr. Loran A. Wenrich and Mr. Alan A. Hamilton for their cooperation, suggestions, and assistance in procuring and setting up equipment; and to Miss Ruth M. Mueller for the preparation of diagrams and photographs for inclusion in this manuscript.

8047

TABLE OF CONTENTS

		PAGE
	Acknowledgement	ii
	Table of Contents	iii
1.0	Summary	1
2.0	Introduction	2
	2.1 Statement of Problem	2
	2.2 General Description of Motor	2
3.0	Theory	8
	3.1 Derivation of Equations of Motion and Impedance	8
	3.11 Equivalent Circuits and Equations of Motion and Impedance	8
	3.12 Derivation of Mathematical Expressions for Constants Appearing in above Equations and Calculation of Set of Specific Values for Motor under Study	17
	3.2 Plots of Theoretical Impedance and Phase and Amplitude Curves	26
	3.21 Impedance Curves	26
	3.22 Frequency Response Curves	29
	3.23 Transient Response	29

4.0 Experiment 38

4.1 Experimental Determination of all Constants 38

4.2 Experimental Determination of Impedance 55

4.3 Experimental Determination of Phase and Amplitude Curves 55

4.4 Experimental Determination of Transient Response 76

5.0 Comparison of Theoretical and Experimental Results 78

5.1 Comparison of Theoretical and Experimental Impedance Curves 78

5.2 Comparison of Theoretical and Experimental Phase and Amplitude Curves 78

5.21 Survey of Linear and Non-linear Regions 84

5.3 Comparison of Theoretical and Experimental Transient Response Curves 86

6.0 Discussion of Effect of Motor Study on Closed Servo Loop 88

6.1 Determination of Effect of Current and Voltage Feedback 93

7.0 Conclusions 94

8.0 Appendix 95

8.1 Computation of Moment of Inertia of Armature 95

8.2 Flux Density Due to Armature Current 96

8.3 Table XVI Constants of Motors A and B Used in Study 99

8.4 Complete List of Symbols 100

8.5 References 103

Vita

1.0 SUMMARY

In this essay a detailed analytical and experimental study of a new, high speed, linear torque motor has been carried out. First, the need for such a motor is shown. This is followed by a general description of the actual motor. The equations of motion and impedance for the motor are developed theoretically and analytical expressions for all the constants appearing in these equations are derived. Experimental values of all the constants are then found and experimental runs are made of the phase and amplitude characteristics, the impedance, and the transient response to a step input. A comparison is made of the theoretical and experimental results including a discussion of linear and non-linear regions. The effect of the motor in the closed servo loop is then discussed as well as the effect of current and voltage feedback. Finally, the conclusions arrived at as a result of the study are stated.

2.0 INTRODUCTION

2.1 STATEMENT OF PROBLEM

At present there exists considerable interest in and need for small size, light weight, high speed, linear, torque motors at the Applied Physics Laboratory, The Johns Hopkins University, Silver Spring, Maryland. These motors are used in closed loop, electrohydraulic servomechanisms (see Fig. 1). To properly analyze these servomechanisms, the operating characteristics of all components should be known thoroughly. It is the object of this thesis to conduct a detailed analytic and experimental study of one of these high speed torque motors.

The motor was developed independently by the Applied Physics Laboratory and Curtiss-Wright for servosystem usage. A similar type was constructed by the Dynamics and Control Laboratory of the Massachusetts Institute of Technology. Two types of motors were built for the Applied Physics Laboratory--one by Curtiss-Wright Corporation and the other by Bendix Corporation (Eclipse-Pioneer Division). No thorough combined analytical and experimental studies have been conducted up to present due to the lack of time.

This analysis is conducted on the motor built by Eclipse-Pioneer since it is used in preference to the Curtiss-Wright motor in which the phase shift varies greatly with frequency because of large eddy current losses in the magnetic structure.

2.2 GENERAL DESCRIPTION OF MOTOR

The motor is essentially a polarized relay consisting of two magnetic yokes energized by a permanent magnet, a moving armature made of laminated iron, and two armature coils. The armature is pivoted at Point P, midway between the laminated pole faces of the yoke, as shown in Fig. 2. One end of the armature extends out beyond the gaps and is

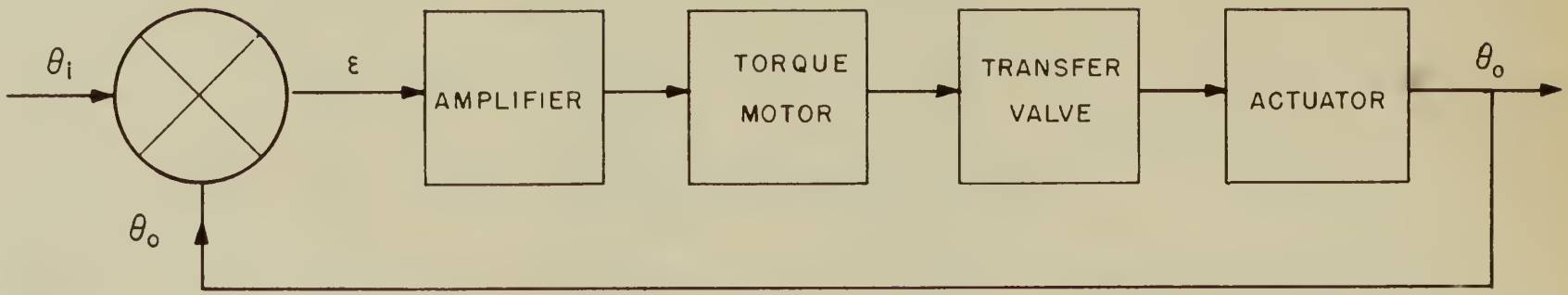

θ_i = EXTERNAL INPUT SIGNAL

θ_o = OUTPUT SIGNAL

ε = $\theta_i - \theta_o$ = ERROR SIGNAL (USUALLY A VOLTAGE)

FIG. 1. BLOCK DIAGRAM OF A CLOSED LOOP ELECTROHYDRAULIC SERVOMECHANISM

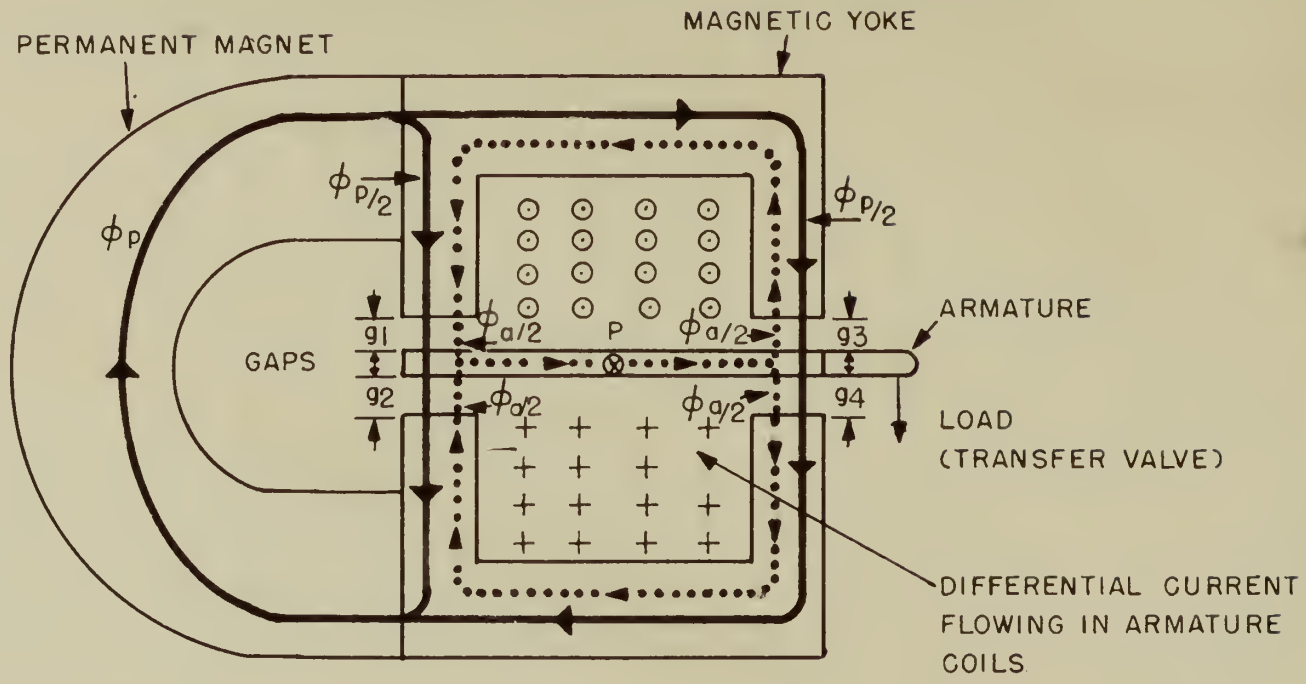

ϕ_p = PERMANENT FIELD FLUX

ϕ_a = ARMATURE FLUX

FIG. 2. SCHEMATIC OF HIGH SPEED TORQUE MOTOR (POLARIZED RELAY TYPE)

connected to the load.

The permanent magnet produces a constant flux, ϕ_p, which divides into two paths and generates equal flux densities at each of the four gaps when the armature is centered. If, under these conditions, currents are allowed to flow through the two armature coils then each current produces a flux. The difference of these two fluxes will be called the armature flux and will be considered to be produced by the difference of the two currents actually flowing or what can be called the differential current. This armature flux causes the armature to become polarized in such a way as to be attracted by one pair of diagonal poles and repelled by the other. There is a torsional spring restraining the armature motion which together with the design of the magnetic circuit causes the physical displacement of the armature to be proportional to the current in the coils. Reversing the direction of the differential current in the coils reverses the direction of motion. Torque is produced by simultaneously raising the current in one coil and lowering it in the other. The motor is operated with a quiescent current flowing in each coil. The motor operates with direct current power and is in principle similar to a Class A amplifier.

An exploded view of the motor is shown in Fig. 3 and the flux paths for the armature centered and off-center in Figs. 4A and 4B.

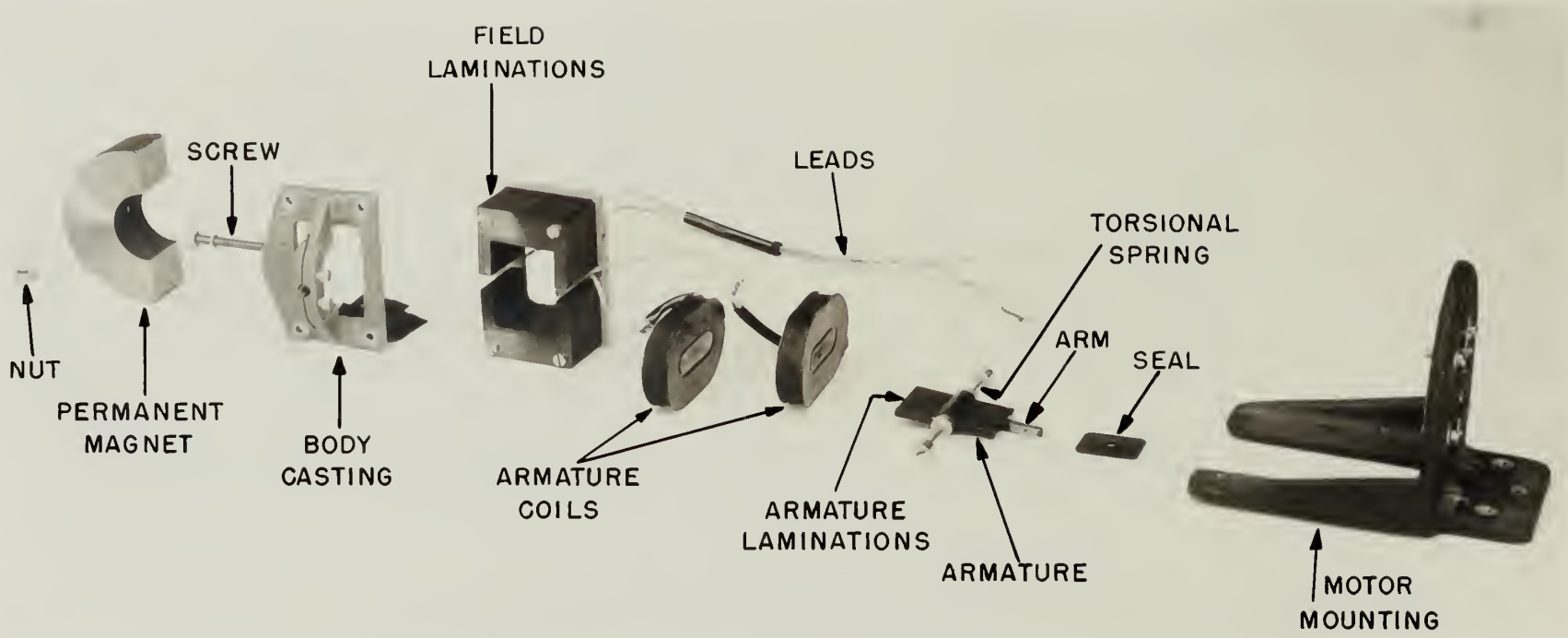

FIG. 3. EXPLODED VIEW OF LINEAR TORQUE MOTOR BUILT BY BENDIX, ECLIPSE-PIONEER, FOR THE APPLIED PHYSICS LABORATORY, THE JOHNS HOPKINS UNIVERSITY.

APPLIED
THE JOH
8621 GEORGIA AVENUE
DATE PRINTED
PHOTO NUMBER
9/5-8

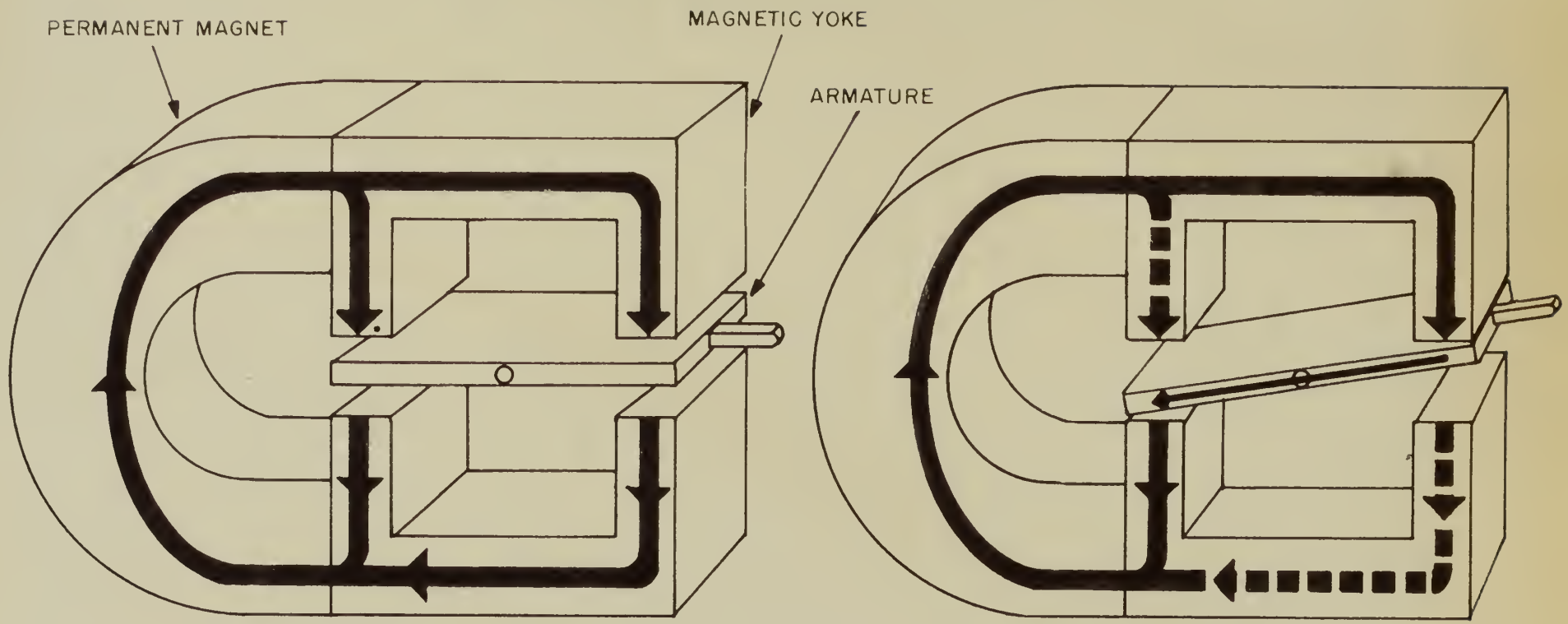

FIG. 4A. FLUX PATH — ARMATURE CENTERED.

FIG. 4B. FLUX PATH — ARMATURE OFF CENTER.

3.0 THEORY

In this section the theoretical equations of motion and impedance will be derived and theoretical values or expressions for all the constants appearing in them.

3.1 DERIVATION OF EQUATIONS OF MOTION AND IMPEDANCE

3.11 Equivalent Circuits and Equations of Motion and Impedance

3.111 Linear relationship between force produced by the motor and the differential armature current.

The first thing to be found is the relationship between the force exerted by the armature arm and the differential armature current. The flux in the armature, ϕ_a, is proportional to the difference of the currents, i, flowing in the armature coils, i.e. $\phi_a = a\,i$, where a is a constant as long as the iron is not saturated. In Fig. 2 it can be seen from the geometry of the relay that the gap lengths $g_1 + g_2$ always equal $g_3 + g_4$. The permanent flux, ϕ_p, emanating from the permanent magnet is considered constant. It will be assumed that as long as the movement of the armature is small and the permeance of the gaps low, the flux through the armature from the permanent magnet is negligible.

The force at any gap is given by the following formula according to Ref. 1, p. 202.

$$F = \frac{B^2 S}{72}$$

where F = force in lbs.
B = flux density, kilomaxwells/ sq. in.
S = area of gap, sq. in.

But, $B = \phi/S$ where ϕ_o is flux at any given gap

so $$F = \left[\frac{\phi_o}{S}\right]^2 \frac{S}{72}$$

If $\phi_a = 0$ and the armature is centered, there will be no force present to move it away from center, i.e. $F_1 = F_2$ and $F_3 = F_4$ in Fig. 5.

If $\phi_a \neq 0$, then the total flux at each gap will be (see Fig. 2)

At g_1 $\quad \phi_1 = \phi_p/2 + \phi_a/2$

g_2 $\quad \phi_2 = \phi_p/2 - \phi_a/2$

g_3 $\quad \phi_3 = \phi_p/2 - \phi_a/2$

g_4 $\quad \phi_4 = \phi_p/2 + \phi_a/2$

The force at each gap will then be:

$$F_1 = \frac{(\phi_p/2 + \phi_a/2)^2}{S^2} \frac{S}{72}$$

$$F_2 = \frac{(\phi_p/2 - \phi_a/2)^2}{S^2} \frac{S}{72}$$

$$F_3 = \frac{(\phi_p/2 - \phi_a/2)^2}{S^2} \frac{S}{72}$$

$$F_4 = \frac{(\phi_p/2 + \phi_a/2)^2}{S^2} \frac{S}{72}$$

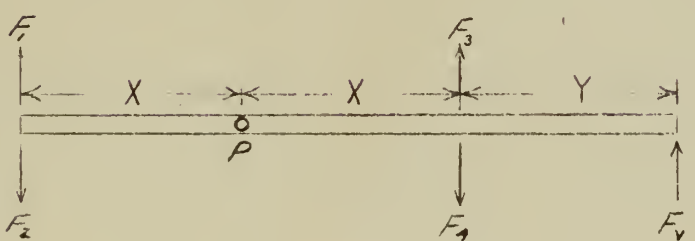

(force exerted by valve)

FIG. 5 FORCES ACTING ON ARMATURE.

The forces acting on the armature are as indicated in Fig. 5 (all attractive).

Writing the torque equation for the armature,

$$F_1X + F_4X = F_2X + F_3X + F_v(X + Y)$$

$$\text{or } F_1 + F_4 - F_2 - F_3 = F_v \frac{(X + Y)}{X}$$

Substituting for F_1, F_2, F_3, and F_4 the expressions just derived and at the same time putting in the numerical values of X and Y, namely X = 0.781 in. and Y = 0.625 in., one finds that

$$F_v = \frac{\phi_p \phi_a}{64.7S}$$

or $$F_v = b\,\phi_a \quad \text{where } b = \frac{\phi_p}{64.7S}$$

But $$\phi_a = a\,i$$

therefore, $F_v = a\,b\,i = K_M i$ where $K_M = ab$

K_M will be known as the electromechanical coupling constant and will be discussed in more detail later on. It is now seen that if the assumptions made in this derivation hold, the force is proportional to the differential current.

3.112 MECHANICAL SYSTEM

Now, considering the motor as a mechanical system, any force produced by the current in the armature coil must be numerically equal to the forces due to the inertia of the armature plus the moving mass of the piston and piston rod, to viscous friction, and to an effective spring force. By effective spring force is meant the combination of the force due to the torsional centering spring and the force due to permanent flux in the armature as a result of displacement. This mechanical system can be represented diagrammatically as follows:

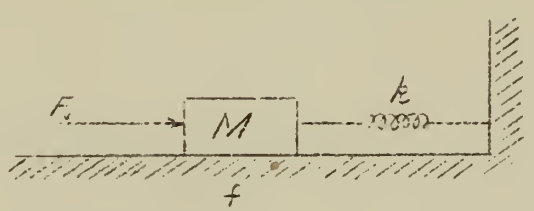

FIG. 6. DIAGRAMMATIC REPRESENTATION OF MECHANICAL SYSTEM

The symbolic diagram of Fig. 6 is:

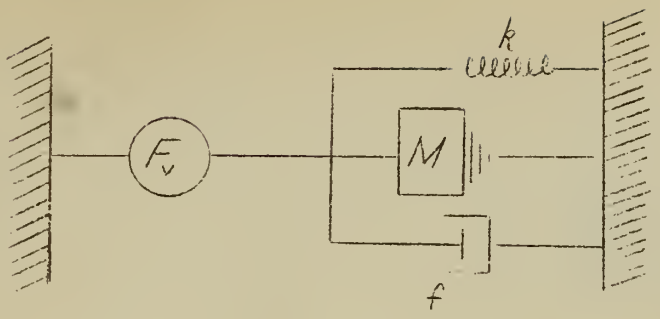

FIG. 7. SYMBOLIC DIAGRAM OF MECHANICAL SYSTEM

Writing the differential equation for this system,

$$F_v = M\frac{d^2x}{dt^2} + f\frac{dx}{dt} + kx$$

F_v = force produced, lbs.
M = total effective moving mass, lb sec^2/in.
f = viscous friction, lb sec/in.
k = effective spring coefficient, lb/in.
x = armature displacement, in.

Since $F_v = K_M i$,

$$F_v = K_M i - M\frac{d^2x}{dt^2} + f\frac{dx}{dt} + kx$$

3.113 ELECTRICAL SYSTEM

The electrical system for the motor may be represented as in Fig. 8.

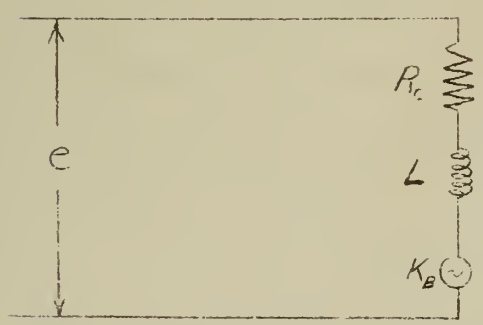

R_C = resistance of coil, ohms.
L = inductance of coil, henry.
K_B = back e.m.f., volt sec/in.
e = voltage feeding armature coil, volts.

FIG 8. ELECTRICAL SYSTEM FOR THE MOTOR

The output voltage of the last stage of the amplifier must feed the resistance and inductance of the armature coil and also overcome a back

electromotive force due to the velocity of the armature. An equivalent circuit is drawn in Fig. 9.

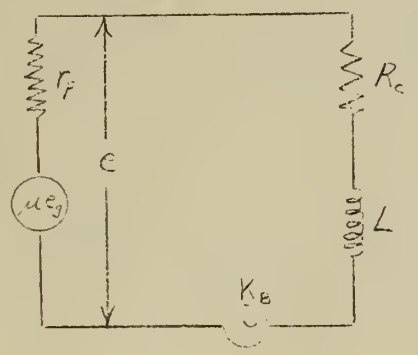

r_p = plate resistance, ohms.
amplification factor.
e_g = grid volts.

FIG. 9. EQUIVALENT ELECTRICAL CIRCUIT FOR THE MOTOR

The voltage equation, by Kirchhoff's law, is:

$$\mu e_g = Ri + \frac{Ldi}{dt} + K_B\frac{dx}{dt} \qquad \text{where} \quad R = r_p + R_c$$

3.114 EQUATIONS OF MOTION OF THE MOTOR

With these equations

$$K_M i = M\frac{d^2x}{dt^2} + f\frac{dx}{dt} + kx$$

and $$\mu e_g = Ri + \frac{Ldi}{dt} + K_B\frac{dx}{dt}$$

the output displacement per unit voltage input to the motor and also the impedance may be determined. Assuming that the system is initially at rest and using the Laplace transformation technique, one may write the following equations:

$$(Ms^2 + fs + k)\bar{x} - K_M\bar{i} = 0$$

$$(K_B s)\bar{x} + (Ls + R)\bar{i} = \mu\bar{e}_g$$

A bar (-) over a letter indicates the Laplace transform of that quantity. Solving for $\bar{x}$ and $\bar{i}$ by means of determinants,

$$\bar{x} = \frac{\begin{vmatrix} 0 & -K_M \\ \mu\bar{e}_g & Ls+R \end{vmatrix}}{\begin{vmatrix} Ms^2+fs+k & -K_M \\ K_Bs & Ls+R \end{vmatrix}} = \frac{K_M \mu \bar{e}_g}{(Ms^2+fs+k)(Ls+R)+K_MK_Bs}$$

$$= \frac{K_M\mu\bar{e}_g}{LMs^3+(fL+MR)s^2+(kL+fR+K_BK_M)s+kR}$$

$$\bar{i} = \frac{\begin{vmatrix} Ms^2+fs+k & 0 \\ K_Bs & \mu\bar{e}_g \end{vmatrix}}{\begin{vmatrix} Ms^2+fs+k & -K_M \\ K_Bs & Ls+R \end{vmatrix}} = \frac{(Ms^2+fs+k)\mu\bar{e}_g}{LMs^3+(fL+MR)s^2+(kL+fR+K_BK_M)s+kR}$$

The Laplace transform of the displacement per unit volt input is then

$$\frac{\bar{x}}{\mu\bar{e}_g} = \frac{K_M}{LMs^3+(fL+MR)s^2+(kL+fR+K_BK_M)s+kR}$$

$$= \frac{K_M/LM}{s^3+(f/M+R/L)s^2+(k/M+fR/LM+K_BK_M/LM)+kR/LM}$$ upon dividing

numerator and denominator by LM.

The Laplace transform of the impedance, Z, is $\bar{e}/\bar{i}$ where $\bar{e}=\mu\bar{e}_g$ when the plate resistance, r_p, is zero, or in other words, one has a zero impedance source.

$$\bar{Z} = \frac{\mu\bar{e}_g}{\bar{i}} = \frac{L\left[s^3+(f/M+R/L)s^2+(k/M+fR/LM+K_BK_M/LM)s+kR/LM\right]}{s^2+(f/M)s+k/M}$$

where R now equals only R_c.

The Laplace transform of the displacement per unit ampere is found by

dividing $\bar{x}$ by $\bar{i}$ and this reduces to

$$\frac{\bar{x}}{\bar{i}} = \frac{K_M}{(Ms^2 + fs + k)}$$

3.115 MORE EXACT EQUATIONS OF MOTION

It should be noted that the equations of motion derived in 3.114 are simplifications of the true situation. No attention has been paid to the characteristic of the connection from the motor armature to the piston valve. A symbolic diagram taking this into account is shown in Fig. 10.

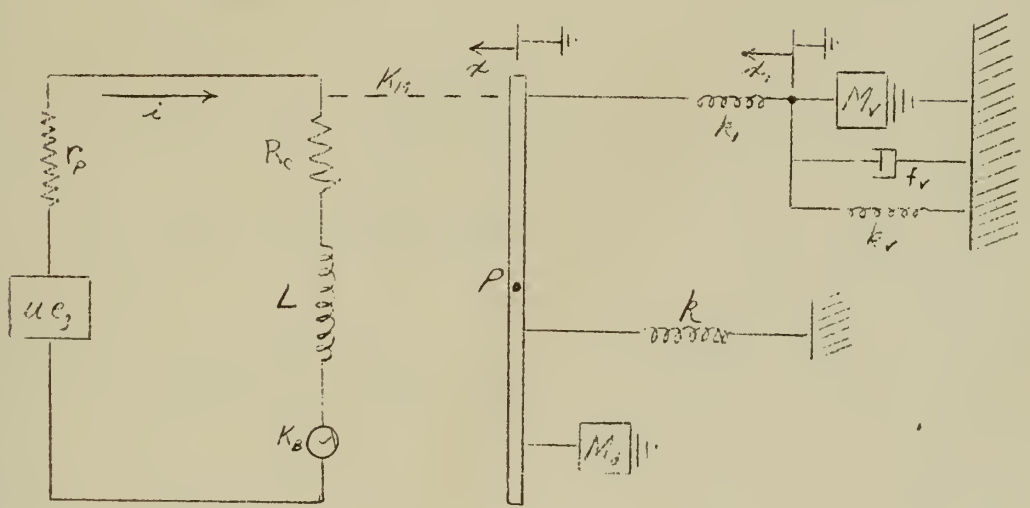

FIG. 10. SYMBOLIC DIAGRAM OF MOTOR TAKING INTO ACCOUNT ELASTANCE OF CONNECTION FROM MOTOR TO VALVE.

k_v = spring coefficient of valve.
k_1 = spring coefficient of connection.
x_1 = displacement of piston rod.
f_v = viscous friction of piston valve.
M_v = mass of valve and rod.
M_a = mass of armature.

Writing the equations of motion,

$$\mu e_g = (R_c + r_p)i + L\frac{di}{dt} + K_B\frac{dx}{dt}$$

and $K_M i = M_a\frac{d^2x}{dt^2} + kx + Q$

where $Q = k_1(x_1 - x) = M_v\ddot{x}_1 + f_v\dot{x}_1 + k_v x_1$

from which $x = \frac{1}{k_1}\left[M_v\ddot{x}_1 + f_v\dot{x}_1 + (k_v - k_1)x_1\right]$

A single dot over a letter indicates the first derivative with respect to time of that quantity and two dots the second derivative.

Taking the Laplace transforms,

$$\mu\bar{e}_g = (R_c + r_p + Ls)\bar{i} + K_B s\bar{x}$$

$$K_M\bar{i} = (M_a s^2 + k)\bar{x} + (M_v s^2 + f_v s + k_v)\bar{x}_1 = (M_a s^2 + k - k_1)\bar{x} + k_1\bar{x}_1$$

$$\bar{i} = \frac{1}{K_M}(M_a s^2 + k - k_1)\bar{x} + k_1\bar{x}_1$$

and $\bar{x} = -\frac{1}{k_1}(M_v s^2 + f_v s + k_v - k_1)\bar{x}_1$

Let $R = R_c + r_p$.

Then $\mu\bar{e}_g = (R + Ls)\bar{i} + K_B s\bar{x}$

or substituting for $\bar{i}$ and $\bar{x}$

$$\mu\bar{e}_g = (R + Ls)\frac{1}{K_M}\left[(M_a s^2 + k - k_1)\left\{-\frac{1}{k_1}(M_v s^2 + f_v s + k_v - k_1)\bar{x}_1\right\} + k_1\bar{x}_1\right]$$

$$- K_B s\frac{1}{k_1}(M_v s^2 + f_v s + k_v - k_1)x_1$$

Dividing through by $\bar{x}_1$ and then taking the reciprocal,

$$\frac{\bar{x}_1}{\mu\bar{e}_g} = \frac{1}{(R+Ls)\frac{1}{K_M}\left[(M_a s^2 + k - k_1)\left\{-\frac{1}{k_1}(M_v s^2 + f_v s + k_v - k_1)\right\} + k_1\right] - \frac{K_B s}{k_1}(M_v s^2 + f_v s + k_v - k_1)}$$

Multiplying the numerator and denominator by $K_M k_1$, we have

$$\frac{\bar{X}}{\mu \bar{e}_g} = \frac{K_M \quad k_1}{k_1 (R + Ls) \left[(M_a s^2 + k - k_1) \left\{ -\frac{1}{k_1} (M_v s^2 + f_v s + k_v - k_1) \right\} + k_1 \right] - K_B K_M (M_v s^2 + f_v s + k_v - k_1) s}$$

$$= \frac{- K_M k_1}{A^* s^5 + B^* s^4 + C^* s^3 + D^* s^2 + E^* s + F^*}$$

where $A^* = M_a M_v L$

$$B^* = M_a M_v R + M_a f_v L$$

$$C^* = M_a f_v R + L \left[M_v (k - k_1) + M_a (k_v - k_1) \right] + K_B K_M M_v$$

$$D^* = R \left[M_v (k - k_1) + M_a (k_v - k_1) \right] + L f_v (k - k_1) + f_v K_B K_M$$

$$E^* = f_v R (k - k_1) + L (k - k_1)(k_v - k_1) + K_B K_M (k_v - k_1) - k_1^2 L$$

$$F^* = (k - k_1)(k_v - k_1) R - k_1^2 R$$

When k_1 is very large, i.e. $k_1 \longrightarrow \infty$

$$A^* = 0$$

$$B^* = 0$$

$$C^* = -L (M_v + M_a)$$

$$D^* = -R (M_v + M_a) - L f_v$$

$$E^* = -f_v R - L (k_v + k) - K_B K_M$$

$$F^* = -(k + k_v) R$$

Substituting these values into the above equations and letting

$M = M_v + M_a$ and $f_v = f$,

$$\frac{\bar{X}}{\mu \bar{e}_g} = \frac{K_M}{LMs^3 + (fL + MR) s^2 + (kL + fR + K_B K_M) s + kR}$$

which is the same equation for displacement per unit input voltage derived in 3.114 for the simpler system assuming infinite elastance for the connection from the armature arm to the piston valve, an equivalent effective mass equal to the sum of the mass of the armature and valve, and that the viscous friction acts at the armature rather than in the valve itself.

3.12 Derivations of Mathematical Expressions for Constants Appearing in above Equations and Calculation of Set of Specific Values for Motor under Study.

In this section the various constants appearing in the equations of motion and impedance will be derived mathematically. Later these theoretical constants will be compared to those found experimentally.

3.121 Effective Mass M

As has already been noted the mass of the armature must be accelerated. Since this motor is to be used as a part of a system and it is the object of this thesis to determine its operating characteristics in that system an adjustment must be made in this term to take the moving mass of the piston rod and valve piston into account. For the purpose of simplification the mass of the armature can be combined in an equivalent mass with the total moving mass of the valve piston and rod.

$M = M_e + M_v$

M_e = mass equivalent of armature

M_v = total mass of valve piston and piston rod (measured and found to be 17 grams = 0.0375 pounds)

M = total effective moving mass converted to position of valve

To find the equivalent mass of the armature, the moment of inertia of the armature was calculated from its dimensions and shape using the fact that the moment of inertia of a body is equal to the integral of the elemental mass multiplied by the square of the distance

from this elemental mass to the axis about which the moment of inertia is sought and the parallel axis theorem. The calculation for I_a, the moment of inertia of the armature, will be found in appendix 8.1. Theoretically, $I_a = 48.12$ gm-cm^2. Therefore the equivalent mass is

$$M_e = \frac{I_a}{r^2} = 48.1/(3.57)^2 = 3.78 \text{ gram or } 0.00835 \text{ pound.}$$

$r = 3.57$ cm is distance from pivot point P to point of application of valve force.

Now the total effective moving mass, M, can be found. $M = M_e + M_v$

$$M = 3.78 + 17.0 = 20.8 \text{ gm or } 1.188 \times 10^{-4} \text{ lb sec}^2/\text{in.}$$

3.122 Effective Spring Coefficient k

For static equilibrium the forces on the armature arm must be equal, i.e. $F_v = k_s x = K_M i + k_f x$

where k_s = actual spring rate of torsional centering spring.

k_f = anti-spring rate due to the permanent flux through the armature when armature is off center.

K_M = electromechanical coupling constant

The force, $k_f x$, due to the permanent flux flowing through the armature when it is off center (see Fig. 4B) causes the armature to move farther off center. This force plus the force due to the flow of armature current must equal the force due to the centering spring for static equilibrium. The displacement sensitivity per ampere, x/i, is found as follows:

$$k_s x = K_M i + k_f x$$

$$x/i = K_M/(k_s - k_f)$$

If $(k_s - k_f)$ is set equal to k, k may be looked upon as an effective spring coefficient.

In order to find the value of k necessary to get mechanical resonance at, for example, 210 cycles per second, use is made of some well known relationships for second order systems. (These relationships may be found in any standard text on servomechanisms, for example, Ref. 2.)

$$\omega_n = \sqrt{\frac{k}{M}}$$

ω_n = angular velocity at undamped natural resonant frequency, rad/sec.

k = effective spring coefficient, lbs/in.

M = mass of system, lb sec^2/in.

or $$k = M\omega_n^2 = (1.188 \times 10^{-4})\ (1320)^2 = 207 \text{ lbs/in.}$$

This particular resonant frequency was chosen because of the effective spring rate found in the experimental section and it must be borne in mind that it is only the true resonant frequency for a system having no damping.

3.123 Viscous Friction f

Assume $\zeta = 0.1$ as a reasonable estimate as to the amount of damping present in the system, where ζ is defined as the ratio of the actual damping to the critical damping.

$$\omega_n = \sqrt{\frac{k}{M}} \text{ and } 2\zeta\omega_n = f/M$$

These relationships give $\zeta = \frac{f}{2M\omega_n} = \frac{f}{2\sqrt{Mk}}$ f = viscous friction coefficient

or $$f = \zeta\, 2\sqrt{Mk}$$

$$= (0.1)(2)\sqrt{1.188 \times 10^{-4} \times 207} = 0.0314 \text{ lb sec/in}$$

A useful parameter for calculations was found to be f/M which for $\zeta = 0.1$ was

$$\frac{f}{M} = \frac{0.0314}{1.188 \times 10^{-4}} = 264/\text{sec}$$

TABLE I. VALUES OF f/M CORRESPONDING TO DIFFERENT VALUES OF ζ

ζ	f/M
0.018	47.5
0.100	264
0.113	300
0.300	800

The value of ζ will be used as a parameter to show the variation of impedance and output displacement per volt as the amount of damping in the system is varied.

3.124 Inductance L

$$L = \frac{N\phi_a}{i \times 10^8} = \frac{7650 \times 6560}{0.060 \times 10^8} = 8.4 \text{ henries}$$

N = number of turns on armature coil
ϕ_a = armature flux in maxwells
i = differential current in amperes

The values of ϕ_a and i used to determine the theoretical value of inductance were taken from Fig. 55 in section 8.2.

3.125 Back Electromotive Force K_B

This method of determining the back electromotive force (e.m.f.) is due to Mr. R. B. Higley and Mr. J. Wheeler of Curtiss-Wright Corporation (see Ref. 3, p. 17). The leakage flux, ϕ_L, however, has been determined in a different and more rigorous manner.

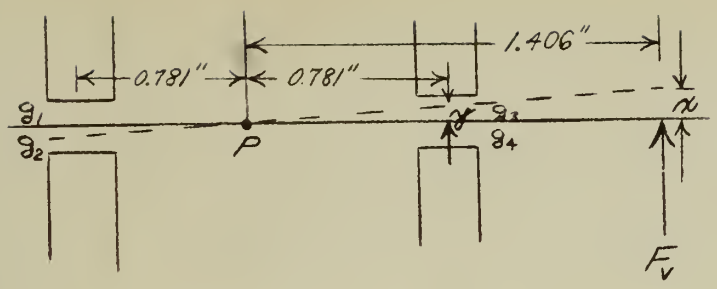

x = valve displacement, in.

y = armature displacement in air gap, in.

FIG. 11. RELATIONSHIP BETWEEN VALVE AND ARMATURE DISPLACEMENTS

It can be seen from Fig. 11 that $\frac{x}{1.406} = \frac{y}{0.781}$

or $$y = \frac{0.781}{1.406} = 0.6x$$

When the armature is centered all gap lengths are equal or

$$g_1 = g_2 = g_3 = g_4 = g.$$

When the armature is not centered, $g_2 = g_3 = g - 0.6x$

$$g_1 = g_4 = g + 0.6x$$

The permeance at any gap with the armature centered is

$$\mathcal{P} = \frac{\mu_o S}{g}$$

μ_o = permeability
S = area
g = gap length

with the armature off center, $\mathcal{P}_1 = \mathcal{P}_4 = \frac{\mu_o S}{g + 0.6x}$

and $$\mathcal{P}_2 = \mathcal{P}_3 = \frac{\mu_o S}{g - 0.6x}$$

Let us draw the magnetic circuit for the flux of the permanent magnet (see Fig. 12).

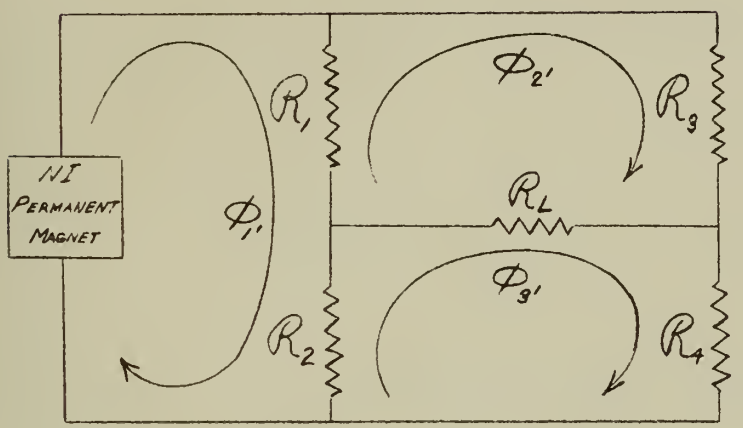

$\mathcal{R}_1$, $\mathcal{R}_2$, $\mathcal{R}_3$, and $\mathcal{R}_4$ are reluctance of air gaps 1, 2, 3, and 4.

$\mathcal{R}_L$ is reluctance of armature.

FIG. 12. MAGNETIC CIRCUIT FOR PERMANENT MAGNET FLUX

An expression for the flux, ϕ_L, flowing through the armature due to the permanent magnet can be found by solving the three magnetic loop equations. These equations are:

$$(\mathcal{R}_1+\mathcal{R}_2)\phi_{1'} - \mathcal{R}_1\phi_{2'} - \mathcal{R}_2\phi_{3'} = NI$$

$$-\mathcal{R}_1\phi_{1'} + (\mathcal{R}_1 + \mathcal{R}_3+\mathcal{R}_L)\phi_{2'} - \mathcal{R}_L\phi_{3'} = 0$$

$$-\mathcal{R}_2\phi_{1'} - \mathcal{R}_L\phi_{2'} + (\mathcal{R}_2+\mathcal{R}_4+\mathcal{R}_L)\phi_{3'} = 0$$

The flux we are seeking, ϕ_L, is equal to $\Phi_{2'} - \Phi_{3'}$

Actually solving we find

$$\phi_L = \frac{NI\ (\mathcal{R}_1\mathcal{R}_4 - \mathcal{R}_2\mathcal{R}_3)}{\mathcal{R}_L(\mathcal{R}_3+\mathcal{R}_4)(\mathcal{R}_1+\mathcal{R}_2)+\mathcal{R}_3\mathcal{R}_4(\mathcal{R}_1+\mathcal{R}_2)+\mathcal{R}_1\mathcal{R}_2(\mathcal{R}_3+\mathcal{R}_4)}$$

or, in terms of permeances, remembering $\mathcal{P}_1 = \mathcal{P}_4$ and $\mathcal{P}_2 = \mathcal{P}_3$

$$\phi_L = \frac{NI\ \left(\frac{1}{\mathcal{P}_2} - \frac{1}{\mathcal{P}_3^2}\right)}{\frac{1}{\mathcal{P}_L}\left(\frac{1}{\mathcal{P}_L}+\frac{1}{\mathcal{P}_3}\right)^2+\frac{1}{\mathcal{P}_1}\frac{1}{\mathcal{P}_3}\left(\frac{1}{\mathcal{P}_1}+\frac{1}{\mathcal{P}_3}\right) + \frac{1}{\mathcal{P}_1}\frac{1}{\mathcal{P}_3}\left(\frac{1}{\mathcal{P}_1}+\frac{1}{\mathcal{P}_3}\right)}$$

Dividing numerator and denominator by $\left(\frac{1}{\mathcal{P}_1} + \frac{1}{\mathcal{P}_3}\right)$

$$\phi_L = \frac{NI\left(\frac{1}{\mathcal{P}_1} - \frac{1}{\mathcal{P}_3}\right)}{\frac{1}{\mathcal{P}_L}\left(\frac{1}{\mathcal{P}_1} + \frac{1}{\mathcal{P}_3}\right) + \frac{2}{\mathcal{P}_1 \mathcal{P}_3}}$$

Putting the fractions over a common denominator and multiplying numerator and denominator by $\mathcal{P}_1 \mathcal{P}_3$

$$\phi_L = \frac{NI(\mathcal{P}_3 - \mathcal{P}_1)}{\frac{\mathcal{P}_1 + \mathcal{P}_3}{\mathcal{P}_L} + 2}$$

But we may justifiably assume, since the reluctance of the path through the armature is approximately zero, that the permeance, $\mathcal{P}_L$, is approximately infinite or certainly very much larger than $\mathcal{P}_3 + \mathcal{P}_1$.

Therefore, $\frac{\mathcal{P}_3 + \mathcal{P}_1}{\mathcal{P}_L} \cong 0$

or $$\phi_L = \frac{NI(\mathcal{P}_3 - \mathcal{P}_1)}{2}$$

Substituting for $\mathcal{P}_3$ and $\mathcal{P}_1$, one has

$$\phi_L = \frac{NI}{2}\left[\frac{\mu_0 S}{g - 0.6x} - \frac{\mu_0 S}{g + 0.6x}\right]$$

$$= \frac{NI}{2}\mu_0 S\left[\frac{2(0.6)x}{g^2 - 0.36x^2}\right]$$

$$= \frac{NI}{2}\mu_0 S\ 1.2\left[\frac{x}{g^2 - 0.36x^2}\right]$$

This checks with the expression given by Higley and Wheeler in Ref. 3, but solving in this manner requires only one assumption, namely, that $\mathcal{P}_L \gg \mathcal{P}_3 + \mathcal{P}_1$.

It should be noted that one can reduce ϕ_L, which is desired small, by either keeping x very small or by increasing g, the gap length, with the armature centered.

To get the back e.m.f. due to ϕ_L, use is made of the fact that ϕ_L is a function of displacement x, and x is a function of time. Therefore, ϕ_L is a function of time.

$$E = -\frac{N d\phi_L}{dt} 10^{-8} \text{ volts}$$

where N is number of turns of coil
ϕ_L is flux in maxwells

$$E = -\frac{N d\phi_L}{dx}\frac{dx}{dt} 10^{-8}$$

$$E = K_B \frac{dx}{dt} \quad \text{where} \quad K_B = -N \frac{d\phi_L}{dx} 10^{-8} \text{ volt sec/inch}$$

If we differentiate $\phi_L = \frac{NI}{2}\mu_o S \; 1.2 \left[\frac{x}{g^2-.36x^2}\right]$ with respect to x, we get

$$\frac{d\phi_L}{dx} = \frac{NI}{2}\mu_o S \; 1.2 \left[(g^2-.36x^2)^{-1} + 2(.36)x^2(g^2-.36x^2)^{-2}\right]$$

$$= \frac{NI}{2}\mu_o S \; 1.2 \left[\frac{(g^2 + .36x^2)}{(g^2-.36x^2)^2}\right]$$

Substituting this into our expression for K_B, we get

$$K_B = N \frac{(NI)}{2}\mu_o S \; 1.2 \left[\frac{g^2 + .36x^2}{g -.36x^2)^2}\right] 10^{-8} \text{ volt sec/inch}$$

To use this formula the NI of the permanent magnet must be determined. The method used to determine this was as follows. The flux flowing in the armature due to the permanent magnet with the armature centered was assumed negligible. Also there was assumed to be no leakage flux. With these conditions plus the further assumption that the reluctance of the iron path is negligible compared to the air gaps, all the magnetic potential difference of the permanent magnet will appear across air gaps 1 and 2

(see Fig. 2).

$$\mathcal{F} = \mathcal{R}\,\phi_p$$

$$\mathcal{R} = \frac{2g}{\mu_o S}$$

$$\phi_p = B_p S$$

$\mathcal{F}$ = magnetic potential difference, gilberts
$\mathcal{R}$ = reluctance, gilbert/maxwell
ϕ_p = permanent flux, maxwells
μ_o = permeability, maxwell/NI-cm
B_p = flux density in any gap due to permanent magnet, gauss

Substituting these expressions for $\mathcal{R}$ and ϕ_p into $\mathcal{F}$,

$$\mathcal{F} = \frac{2gB_p S}{\mu_o S} = \frac{2gB_p}{\mu_o}$$

But $\mathcal{F}$ gilberts $= 0.4\pi$ NI ampere-turns

so, $$NI = \frac{2gB_p}{0.4\pi\mu_o} = \frac{2(0.145)4170}{0.4\pi(1.259)} = 766 \text{ ampere-turns}$$

$g = 0.145$ cm. (measured)
$\mu_o = 1.259$ maxwell/NI-cm.
$B_p = 4170$ gauss (measured)

$B_p = 4170$ gauss was determined by use of a General Electric fluxmeter Model 32C248 which was calibrated at the National Bureau of Standards by the author for this purpose with the assistance of Mr. I. L. Cooter and A. R. Lindberg of the staff there on 24 August, 1951. Substituting in the equation for K_B and letting

$x = 0$, $K_B\text{min} = 9.01$ volt sec/inch

$x = 0.032$, $K_B\text{max} = 12.6$ volt sec/inch

3.126 Electromechanical Coupling Constant K_M

K_M, the electromechanical coupling constant, may be defined as follows:

$$K_M = \frac{F \text{ (force in lbs)}}{i \text{ (differential current in amps)}}$$

But $$F = \frac{(\phi_p + \phi_a)^2}{288S}$$ from section 3.111 upon making the proper substitutions in the formula for force.

Therefore, $K_M = \dfrac{(\phi_p + \phi_a)^2}{\frac{288S}{i}}$ where $\phi_p = 13.9$ kilomaxwells (measured)

$\phi_a = 6.56$ kilomaxwells (Fig. 55)

S = gap area, 0.262 sq. in.

i = 60 milliamperes

Upon substituting the numerics and solving, K_M is found to be:

$$K_M = \frac{(13.9 + 6.56)^2}{(288)(0.262)(0.060)} = 92.8 \text{ lbs/amp}$$

3.2 PLOTS OF THEORETICAL IMPEDANCE AND PHASE AND AMPLITUDE CURVES

3.21 Impedance Curves

In section 3.114 it was shown that the Laplace transform of the impedance was:

$$\bar{Z} = \frac{\mu \bar{e}_g}{i} = \frac{L\left[s^3 + (f/M + R/L)s^2 + (k/M + fR/LM + K_B K_M/LM)s + kR/LM\right]}{s^2 + fs/M + k/M}$$

or multiplying through by L,

$$\bar{Z} = \frac{Ls^3 + (fL/M + R)s^2 + (kL/M + fR/M + K_B K_M/M)s + kR/M}{s^2 + fs/M + k/M}$$

Making use of the properties of the Laplace transform, since $s = \sigma + j\omega$ with $\sigma = 0$, $s = j\omega$. Now, writing the impedance as a function of frequency by substituting $j\omega$ for s, one has:

$$Z(j\omega) = \frac{\mu e_g}{i}(j\omega) = \frac{L(j\omega)^3 + (fL/M + R)(j\omega)^2 + (kL/M + fR/M + K_B K_M/M)j\omega + kR/M}{(j\omega)^2 + f(j\omega)/M + k/M}$$

or separating the real and imaginary parts

$$Z(j\omega) = \frac{\left[R(k/M - \omega^2) - fL\omega^2/M\right] + j\omega\left[L(k/M - \omega) + fR/M + K_B K_M/M\right]}{(k/M - \omega^2) + j(f/M)\omega}$$

R in this case equals R_c only.

From this equation for impedance plots have been made in Fig. 13 of Z as a function of frequency. Also the variation of Z as the viscous damping term

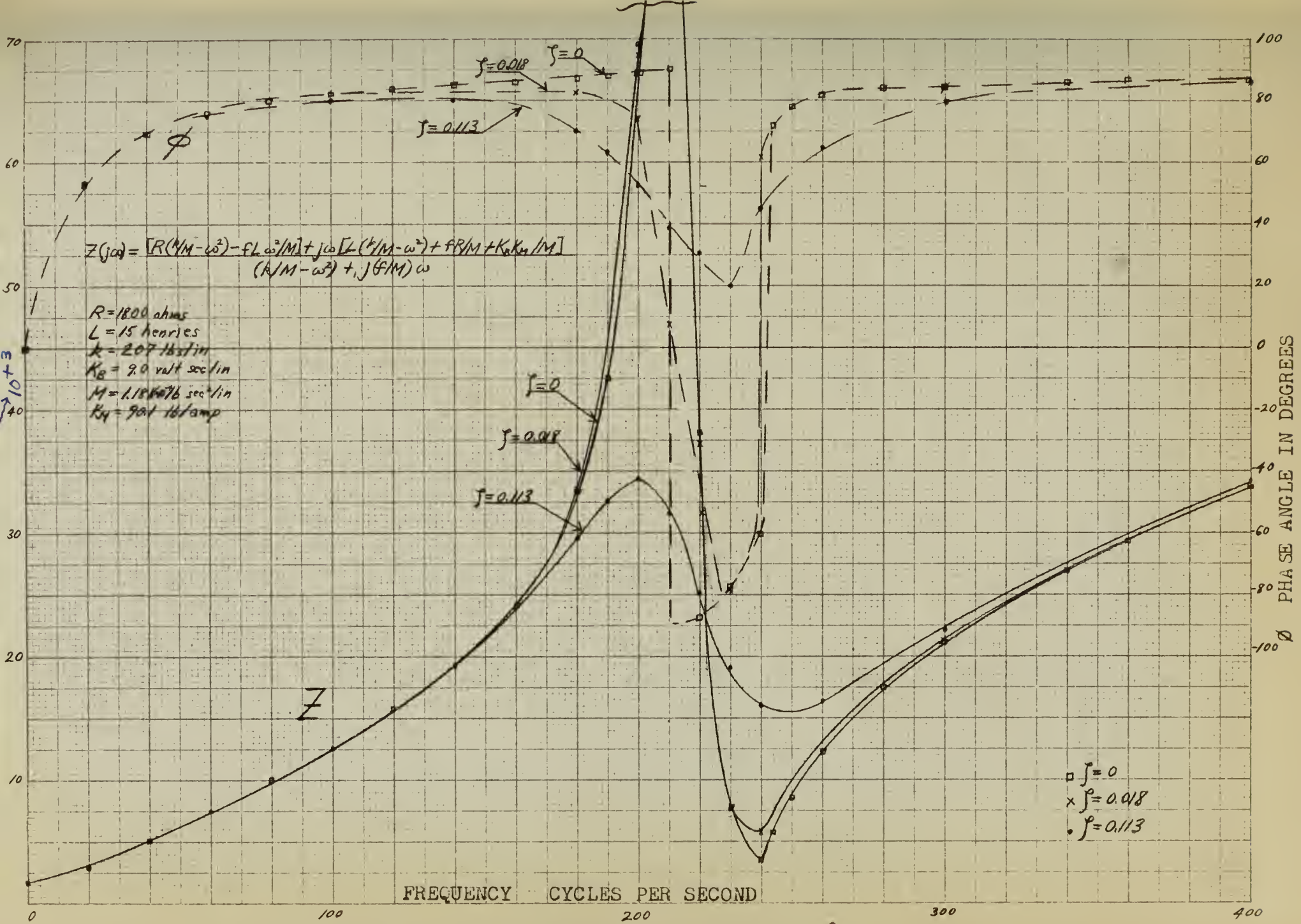

FIG. 13 IMPEDANCE CURVES FOR SEVERAL VALUES OF ζ

TABLE II CALCULATION DATA FOR THEORETICAL IMPEDANCE CURVES

		f/M = 0 ℑ = 0		f/M = 47.5 ℑ = 0.018		f/M = 300 ℑ = 0.113	
f	ω	Z	Ø	Z	Ø	Z	Ø
cps	rad/sec	ohms	degrees	ohms	degrees	ohms	degrees
0	0	1800	0.0	1800	0.0	1800	0.0
20	126	2990	52.0			3020	53.9
40	251	5120	69.4				
60	376	7450	76.0			7570	75.1
80	502	9970	79.6				
100	628	12700	81.9	12700	82.8	12700	79.9
120	754	15900	83.5				
140	880	19400	84.7			19400	79.8
160	1006	24200	85.7				
180	1130	33300	86.9	30700	83.3	29700	70.5
190	1191	42600	87.6			32700	63.5
200	1257	69600	88.5	68800	73.6	34500	53.1
210	1320	∞	-90.0	148000	7.7	31600	38.7
220	1380	38200	-87.3	37300	-53.0	25200	31.1
230	1442	7590	-76.8	7650	-78.6	19100	19.8
240	1507	3640	-60.3	5760	+61.7	16100	45.3
244	1532	5820	+72.0				
250	1570	8650	75.0				
260	1630	12300	81.6			16500	65.4
280	1760	17500	84.1				
300	1885	21100	85.1	21300	84.0	22100	80.1
340	2140	27000	86.2				
360	2260	29400	86.5				
400	2510	33800	86.9	33800	86.0	34200	86.0
450	2820	39200	87.4				

is varied. Calculation data for these theoretical curves may be found in Table II.

3.22 Frequency Response Curves

In section 3.114 it was shown that the Laplace transform of the displacement per unit volt was:

$$\frac{\overline{x}}{\mu \overline{e}_g} = \frac{K_M/LM}{s^3 + (f/M + R/L)s^2 + (k/M + fR/LM + K_B K_M/LM)s + kR/LM}$$

or writing this as a function of frequency as explained in 3.21

$$\frac{x(j\omega)}{\mu e_g} = \frac{K_M/LM}{\left[kR/LM - (f/M + R/L)\omega^2\right] + j\omega\left[k/M + fR/LM + K_B K_M/LM - \omega^2\right]}$$

Plots have been made of $x/\mu e_g$ versus frequency for various values of f. In Fig. 14 curves are plotted considering the tube as a zero impedance source, i.e. $r_p = 0$. The extremely large phase lags prohibit the use of such a source for driving the motor in the servo loop outlined in Fig. 1. In Fig. 15 curves are plotted considering the plate resistance, r_p, to be equal to 60,000 ohms and it is obvious from a comparison of the change in the phase and amplitude characteristics why pentodes with their high plate resistances are used to drive the motor. Calculation data for these curves may be found in Table III.

Plots have also been made of the displacement per unit ampere, x/i, versus frequency assuming a constant current source in Fig. 16. Calculation data may be found in Table IV.

3.23 Transient Response

To secure the transient response characteristic of the motor a step input voltage, K^*, is applied. That is,

$$\mu e_g = f(t) = \begin{cases} 0, & t<0 \\ K^*, & t>0 \end{cases}$$

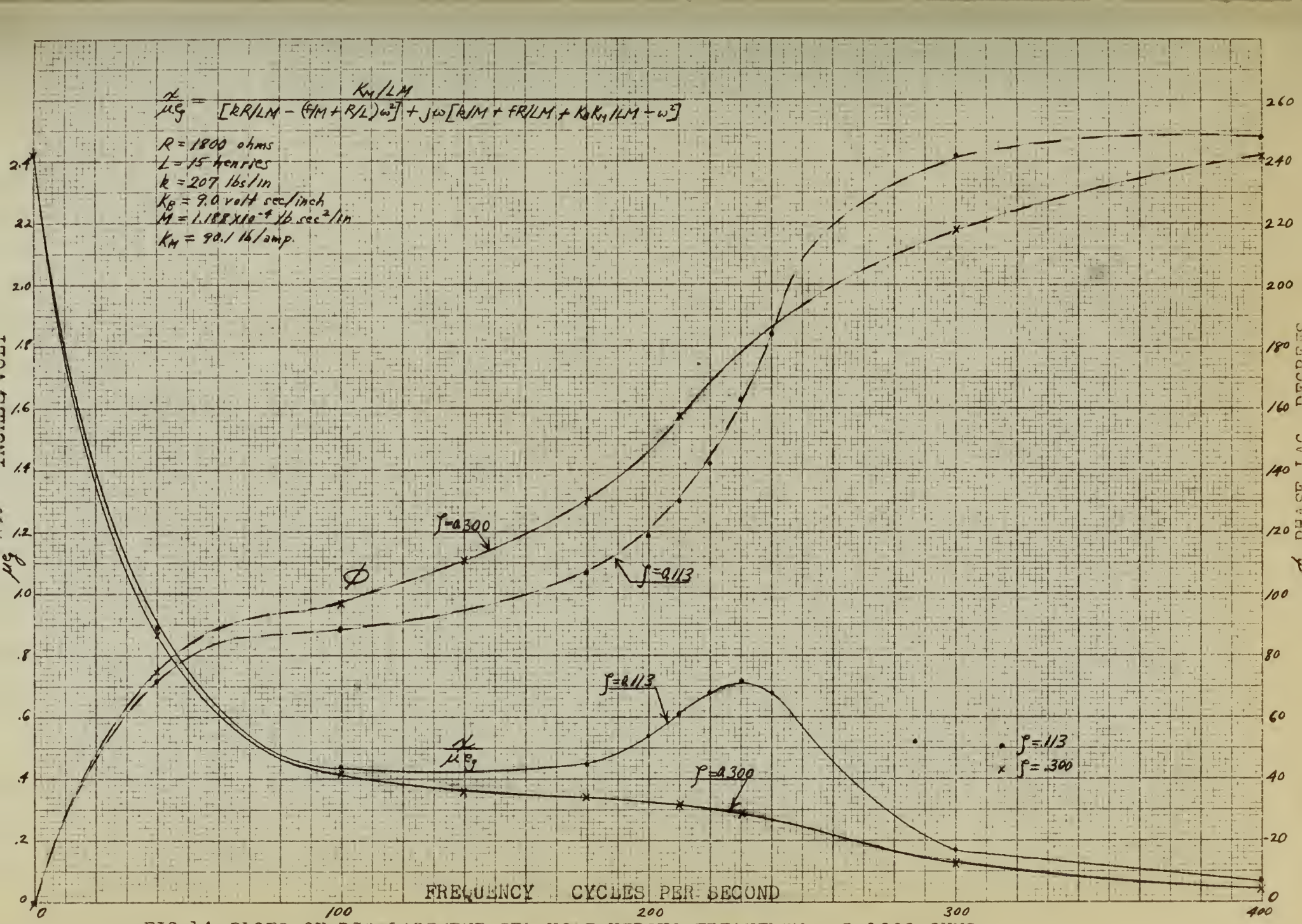

FIG.14 PLOTS OF DISPLACEMENT PER VOLT VERSUS FREQUENCY, R=1800 OHMS

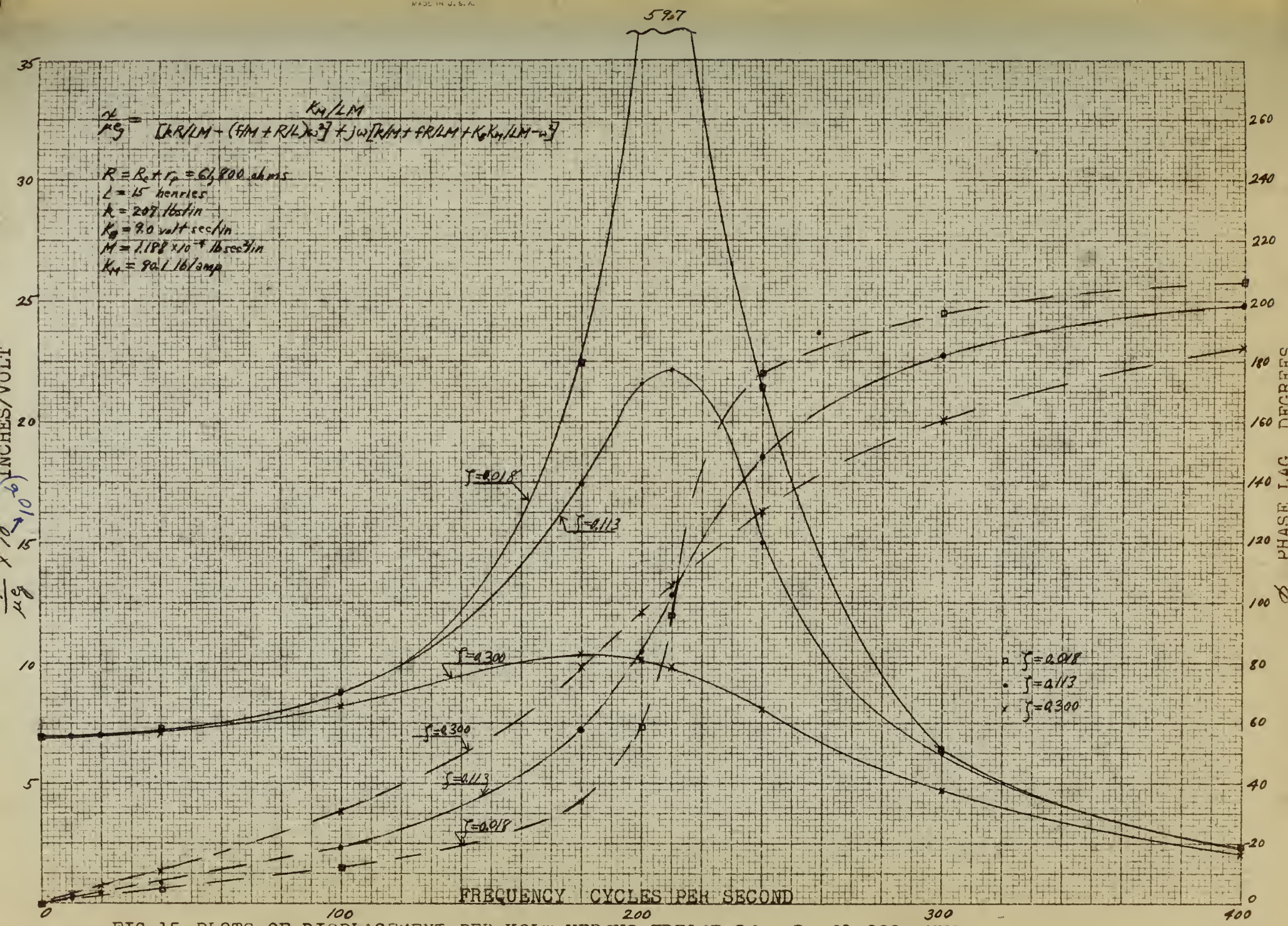

FIG.15 PLOTS OF DISPLACEMENT PER VOLT VERSUS FREQUENCY, R = 61,800 OHMS

TABLE III CALCULATION DATA FOR PLOTS OF DISPLACEMENT PER UNIT VOLT AS A FUNCTION OF FREQUENCY

	$R = 1800$				$R = 61,800$					
	$\zeta = 0.113$		$\zeta = 0.300$		$\zeta = 0.018$		$\zeta = 0.113$		$\zeta = 0.300$	
f	$\frac{x}{\mu e_g} \times 10^{-4}$	ϕ	$\frac{x}{\mu e_g} \times 10^{-4}$	ϕ	$\frac{x}{\mu e_g} \times 10^{-6}$	ϕ	$\frac{x}{\mu e_g} \times 10^{-6}$	ϕ	$\frac{x}{\mu e_g} \times 10^{-6}$	ϕ
0	2.42	0	2.42	0	7.04	0	7.04	0	7.04	0
10							7.05	-1.72		-2.76
20							7.11	3.5		5.58
40	.885	-71.7	.874	-74.9	7.30	-4.84	7.29	7	7.19	11.2
60										
80										
100	.440	88.6	.422	97.4	8.84	12.6	9.76	19.3	8.24	31.4
140			.357	110.7						
180	.452	107.0	.338	130.4	22.5	34.0	17.5	57.6	10.4	79.3
200	.542	119.2			42.2	58.7	21.6	84.4	10.2	96.6
210	.612	130.2	.322	157.8	59.7	96.1	22.2	103.2	9.84	105.8
220	.680	142.4								
230	.721	163.3	.291	170.3						
240	.684	183.5			21.5	176	15.0	148.9	8.06	129.5
300	.168	242.0	.130	217.8	6.39	196	5.96	181.5	4.65	160.5
400	.070	248.3	.044	241.5	2.37	207.3	2.32	199.2	2.13	184.8
1000							.186	233.4	.178	229.0

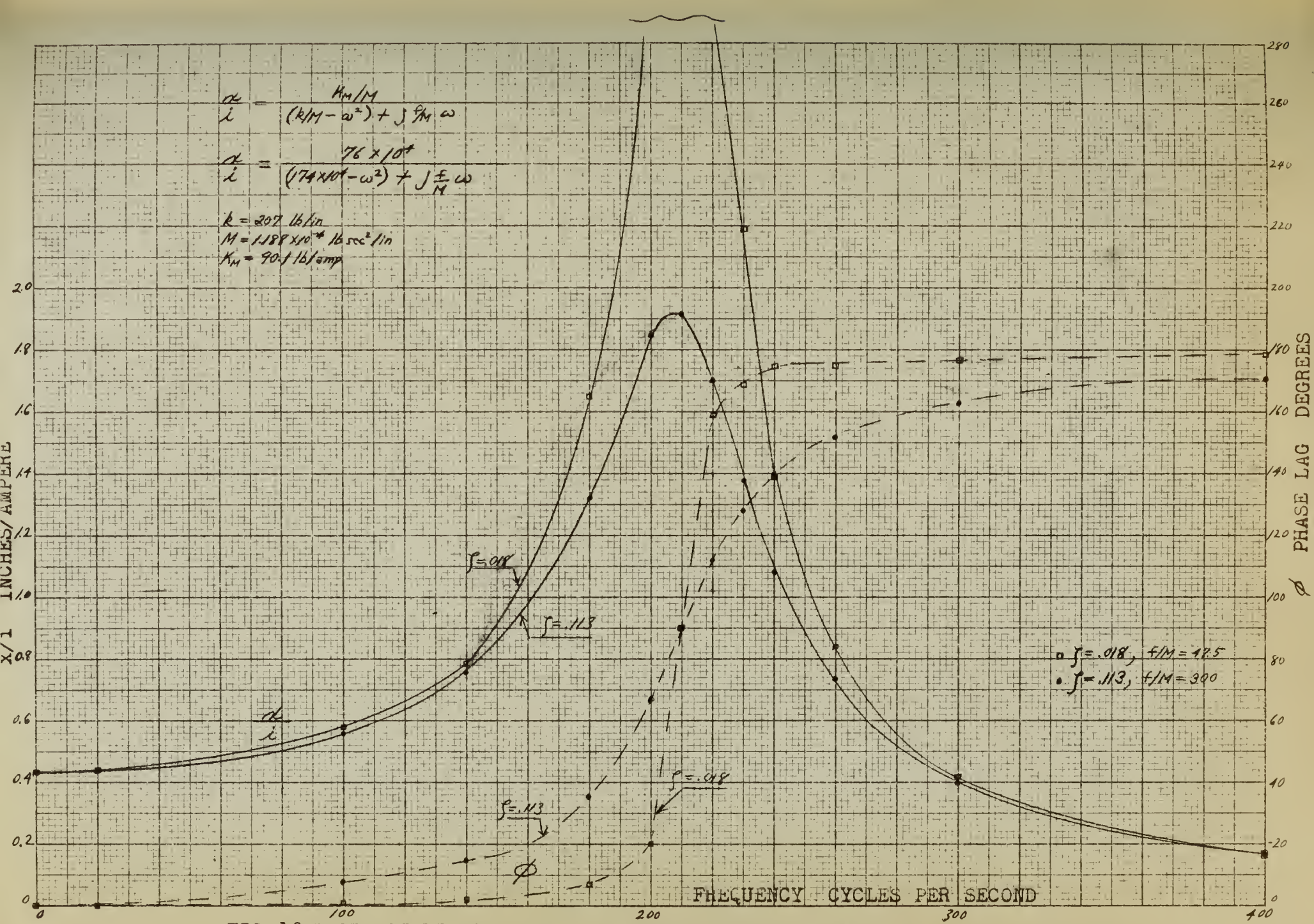

FIG. 16 PLOTS OF DISPLACEMENT PER AMPERE VERSUS FREQUENCY

TABLE IV CALCULATION DATA FOR PLOT OF OUTPUT DIS LACEMENT PER AMPERE VERSUS FREQUENCY

	ʃ =0.018		ʃ =0.113	
f	x/i	Ø	x/i	Ø
0	0.437	0	0.437	0
20	0.442	0	0.442	0
100	0.567	-1.3	0.559	-3
140	0.793	2.5	0.764	15.4
180	1.65	6.7	1.03	36.4
200	4.45	20.5	1.85	67.0
210	12.10	90.0	1.92	90.0
220	4.18	158.9	1.70	112.3
230	2.19	168.6	1.38	128.2
240	1.39	174.5	1.08	140.1
260	0.836	175.1	0.739	151.7
300	0.418	177.2	0.400	162.7
400	0.167	178.5	0.165	170.6

Taking the Laplace transform, $\mu\bar{e}_g = K^*/s$

Substituting this for $\mu\bar{e}_g$ in section 3.114, we have

$$\bar{x} = \frac{K_M K^*/s}{LMs^3 + (fL + MR)s^2 + (kL + fR + K_B K_M)s + kR}$$

or

$$\bar{x} = \frac{K_M}{s\left[LMs^3 + (fL + MR)s^2 + (kL + fR + K_B K_M)s + R\right]} \left\{K^*\right\}$$

Dividing the numerator and denominator by kR, we have:

$$\bar{x} = \frac{K_M/kR}{s\left[(LM/kR)s^3 + (fL/kR + M/k)s^2 + (L/R + f/k + K_B K_M/kR)s + 1\right]} \left\{K^*\right\}$$

and substituting in the numerical values (values listed in appendix — Table XVI under motor B)

$$\bar{x} = \frac{9.64 \times 10^{-6}}{s(2.29\times10^{-10}s^3 + 76.75\times10^{-8}s^2 + 6.07\times10^{-4}s + 1)} \left\{K^*\right\}$$

Factoring the cubic in the denominator,

$$\bar{x} = \frac{9.64 \times 10^{-6}}{s\left[s + 2.95\times10^{3}\right]\left[(s+203) + j1190\right]\left[(s+203) - j1190\right]} \left\{K^*\right\}$$

If now the inverse Laplace transform is taken,

$$x = 9.64\times10^{-6}\left[1.000 - 0.162e^{-2950t} + 1.000e^{-203t}\sin(1190t - 123.1^\circ)\right] K^*$$

At $t = 0$, $x = 9.64\times10^{-6}(1.000 - 0.162 - 0.838)K^*$

$= 0$

and at $t = \infty$, $x = 9.64\times10^{-6}K^*$

If $K^* = 1$, that is a unit step voltage is applied,

$$x = 9.64\times10^{-6} - 1.56\times10^{-2950t} + 9.64\times10^{-6}e^{-203t}\sin(1190t - 123.1^\circ)$$

A plot of the transient response to a step input of one volt is shown in Fig. 17 and the calculation data in Table V.

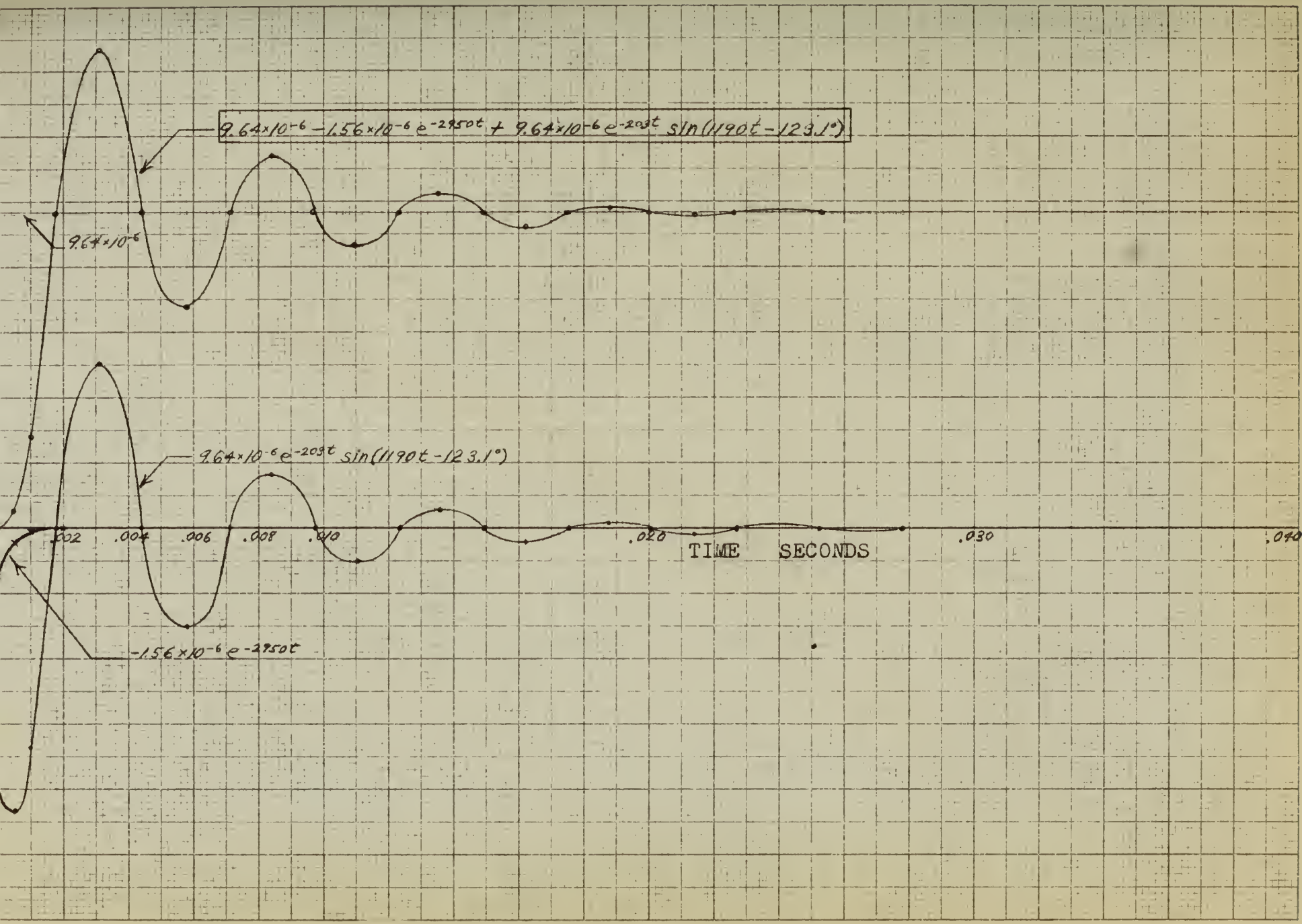

FIG. 17 TRANSIENT RESPONSE TO STEP INPUT

TABLE V CALCULATION DATA FOR THEORETICAL TRANSIENT RESPONSE TO A UNIT STEP INPUT

$$x=\left[9.64\times10^{-6}-1.56\times10^{-6}e^{-2950t}+9.64\times10^{-6}e^{-203t}\sin(1190t-123.1^\circ)\right]$$

t sec	$1.56\times10^{-6}e^{-2950t}$ inches$\times10^{-6}$	$9.64\times10^{-6}e^{-203t}\sin(1190t-123.1^\circ)$ inches$\times10^{-6}$
0	1.56	-8.08
.0005	0.356	-8.70
.0010	0.0816	-6.69
.0018	0.0076	0.00
.0031		+5.09
.0044		0.00
.0058		-2.99
.0071		0.00
.0084		+1.74
.0097		0.00
.0110		-1.04
.0123		0.00
.0136		+0.606
.0149		0.000
.0162		-0.356
.0175		0.000
.0187		+0.212
.0200		0.000
.0213		-0.125
.0226		0.000
.0239		+0.077
.0252		0.000
.0265		-0.048
.0278		0.000
.0291		+0.029

4.0 EXPERIMENT

In this section the actual experimental techniques used to determine the constants derived analytically in section 3.0 on theory will be described. It will be noted that two motors, called A and B, were used. When the analytical section was begun it had been planned to use Motor A throughout both the theoretical and the experimental phases but in the course of the determination of the phase and amplitude characteristics the laminations composing the armature of Motor A separated and therefore a different motor had to be substituted. This new motor has been called Motor B and differs from Motor A only in that it is a separate physical entity subject to the usual variations in manufacturing processes. For the comparison of theoretical and experimental results a new set of theoretical curves for Motor B was computed. The values of Motor A have been left in the report for the purposes of comparison and to retain the analytical studies already completed.

4.1 EXPERIMENTAL DETERMINATION OF ALL CONSTANTS

4.11 Effective Mass

The moment of inertia of a body can be determined experimentally from the following formula (see Ref. 4, p. 72).

$$I_a = \frac{T^2 w^2 M_a G}{4\pi^2 l}$$

where I_a = moment of inertia of armature in gm-cm^2.
T = period of oscillation sec/cycle.
$2w$ = suspension width in cm.
M_a = mass of armature in grams.
l = length of suspension in cm.
G = acceleration of gravity, cm/sec^2.

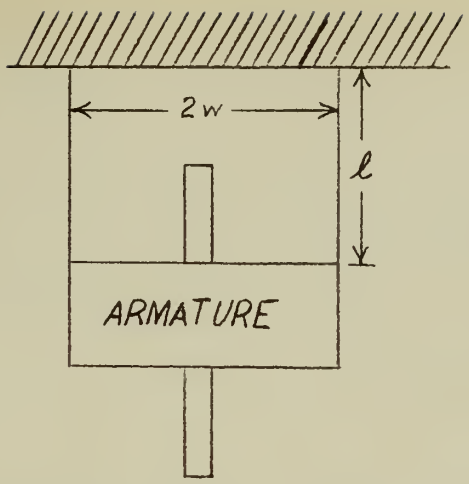

FIG. 18. BIFILAR SUSPENSION OF ARMATURE FOR EFFECTIVE MASS DETERMINATION

The armature was suspended as shown in Fig. 18. It was then set into motion with a very small amplitude of oscillation about its vertical axis. The period of this small oscillation was determined with the aid of an electric timer. The experimental values to be used in the formula for inertia were determined to be as follows:

$$T = \frac{1}{\frac{20 \text{ cycles}}{15.10 \text{sec}}} = 0.755 \text{ sec/cycle}$$

$w = 2.10$ cm.

$M_a = 43.7$ grams

$G = 980$ cm/sec^2

$l = 56.4$ cm.

Substituting these values into the formula,

$$I_a = \frac{0.755^2 \times 2.10^2 \times 43.7 \times 980}{4^2 \times 56.4} = 48.4 \text{ gm-cm}^2.$$

In order to determine the effective mass of the armature at the point of application of the valve force use was made of the fact that the moment

of inertia is equal to the product of the mass and the square of the distance to the axis about which it acts. Therefore,

$$M_e = \frac{I_a}{r^2} = \frac{48.4}{(3.57)^2} = 3.80 \text{ grams}$$

where $r = 3.57$ cm is the distance from the point of application of the valve force to the pivot point P of the armature.

M_e = effective mass of armature.

The total effective mass of the system, M, as defined in section 3.121 is the sum of $M_e + M_v$

or $M = 3.8 + 17.0 = 20.8$ grams $(1.188 \times 10^{-4}$ lb sec^2/in)

4.12 Effective Spring Coefficient k

The method used to determine the effective spring coefficient, k, was as follows. A quiescent current of 24 milliamperes was allowed to flow in each of the armature coils and then standard weights were added to the arm of the armature at the point of application of the valve force. The weights were added very carefully and then removed in inverse order of putting them on to preserve the hysteresis loop. A Brown and Sharpe dial indicator was mounted on the motor in order to read the inches displacement of the armature arm. This dial indicator read to the one one thousandth of an inch from zero up to thirty thousandths. After the plotting of the experimental points, a straight line was drawn through the middle of the resulting hysteresis loop and the slope of this line was determined to be 207 lbs/in for Motor A. This was taken as the value of the effective spring coefficient, k, (see Fig. 19).

The value of the natural (i.e. undamped) resonant frequency may now be determined.

$$\omega_n = \sqrt{\frac{k}{M}} = \sqrt{\frac{207}{1.188 \times 10^{-4}}} = 1320 \text{ rad/sec.}$$

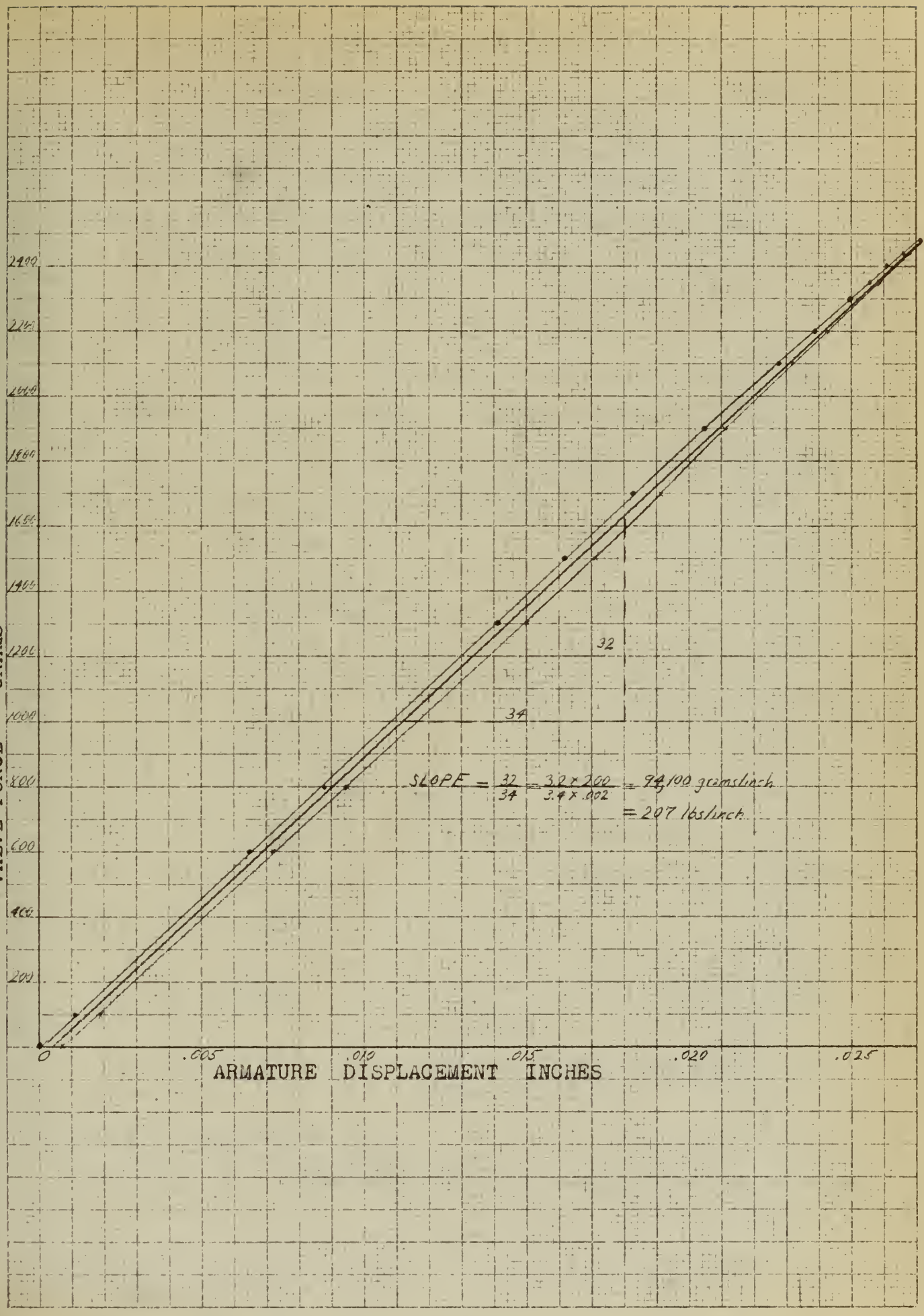

FIG.19 VALVE FORCE VERSUS ARMATURE DISPLACEMENT MOTOR A

or the frequency is $f = 1320/2\pi = 210$ cycles/sec for Motor A.

Table VI contains the experimental data for the effective spring coefficient for both Motors, A and B. The data for Motor B are plotted in Fig. 20 and the slope has been determined for displacements of the armature to either side of center. For Motor B, $k = 168$ lbs/in. and $f = 190$ cycles/second.

4.13 Viscous Friction f

The value of the viscous friction term, f, was determined in the following manner. An impulse was applied to the armature and a photographic record was taken by means of a Miller recorder. The value of $\int$ was obtained from the record as follows.

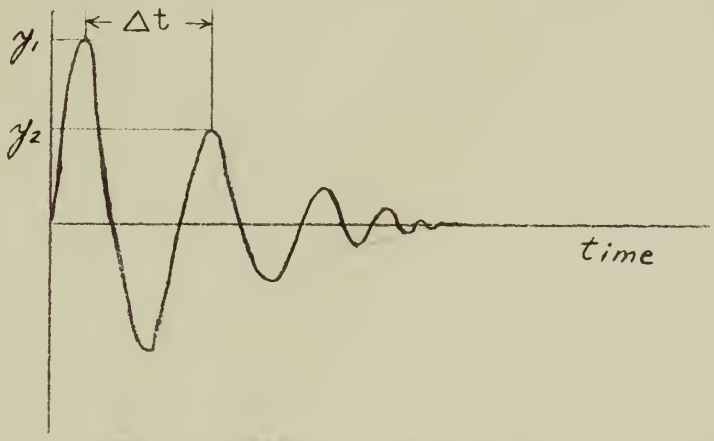

FIG. 21. SKETCH OF TYPICAL TRACE ON MILLER RECORDER

If in Fig. 21 we allow α to be the logarithmic decrement of the envelope of the decaying oscillation, then

$$\alpha = \frac{\ln y_1/y_2}{\Delta t}$$

where y_1 and y_2 are two consecutive values of amplitude of same sign read from record.

Δt is the time interval separating these amplitudes.

It is well known that $\alpha = \int \omega_n$

therefore, $\int = \frac{\alpha}{\omega_n} = \frac{\ln y_1/y_2}{\Delta t}$ where ω_n = undamped natural resonant frequency

TABLE VI EXPERIMENTAL DATA FOR EFFECTIVE SPRING COEFFICIENT

GRAMS	MOTOR A Left of Center INCHES		MOTOR B Left of Center INCHES		Right of Center INCHES	
0	0	.0007	0	.0004	0	.0008
100	.0011	.0019	.0009	.0013	.0009	.0021
600	.0065	.0078	.0070	.0082	.0079	.0092
800	.0088	.0095	.0096	.0106	.0103	.0118
1300	.0141	.0150	.0160	.0173	.0182	.0189
1500	.0162	.0171	.0186	.0199	.0208	.0216
1700	.0183	.0191	.0211	.0226	.0232	.0242
1900	.0205	.0211	.0240	.0254	.0260	.0267
2000			.0255	.0262	.0273	.0279
2050					.0283	
2100	.0228	.0232	.0269	.0278		
2140			.0279			
2200	.0239	.0243				
2300	.0250	.0252				
2350	.0256	.0259				
2400	.0261	.0263				
2440	.0266	.0268				
2480	.0271					

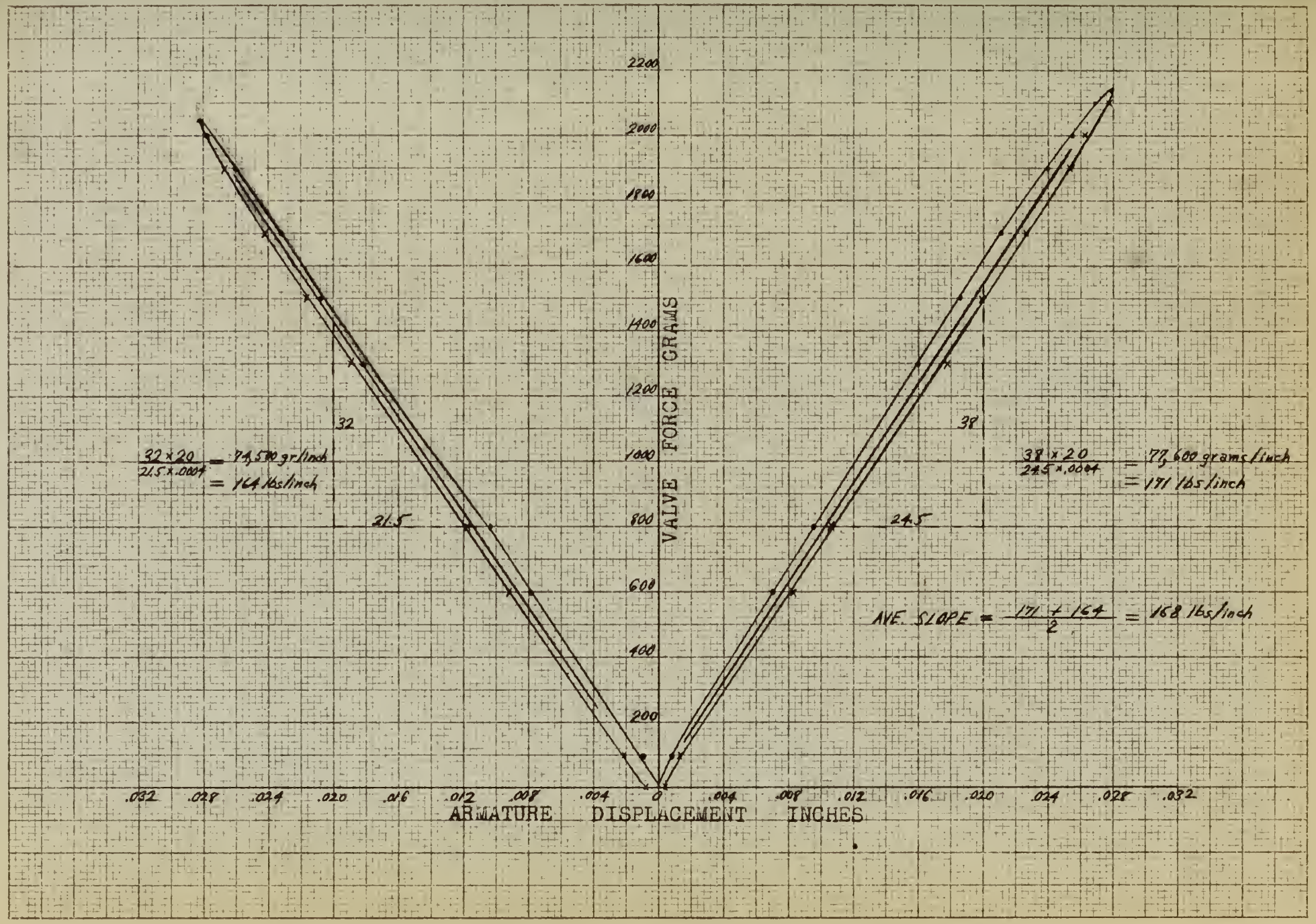

FIG.20 VALVE FORCE VERSUS ARMATURE DISPLACEMENT MOTOR B

$\omega_o = \omega_n\sqrt{1-\zeta^2}$ where ω_o = damped resonant frequency read on oscillographic record. (see Ref. 2, p. 49)

or $\omega_n = \dfrac{\omega_o}{\sqrt{1-\zeta^2}}$

Substituting,

$$\zeta = \frac{\ln \frac{y_1}{y_2}}{\frac{\omega_o \Delta t}{\sqrt{1-\zeta^2}}}$$

Multiplying numerator and denominator by $\sqrt{1-\zeta^2}$

$$\zeta = \frac{\ln \frac{y_1}{y_2}\sqrt{1-\zeta^2}}{\omega_o \Delta t}$$

Squaring and separating terms,

$$\zeta^2 = \left(\frac{\ln \frac{y_1}{y_2}}{\omega_o \Delta t}\right)^2 - \left(\frac{\ln \frac{y_1}{y_2}}{\omega_o \Delta t}\right)^2 \zeta^2$$

Rearranging terms,

$$\zeta^2 = \frac{\left(\frac{\ln \frac{y_1}{y_2}}{\omega_o \Delta t}\right)^2}{1+\left(\frac{\ln \frac{y_1}{y_2}}{\omega_o \Delta t}\right)^2} = \frac{\left(\ln \frac{y_1}{y_2}\right)^2}{(\omega_o \Delta t)^2 + \left(\ln \frac{y_1}{y_2}\right)^2}$$

Finally,

$$\zeta = \frac{\ln \frac{y_1}{y_2}}{\sqrt{(\omega_o \Delta t)^2 + \left(\ln \frac{y_1}{y_2}\right)^2}}$$

By means of this formula the values of ζ were computed from values of $\omega_o, \Delta t, y_1$, and y_2 given by oscillographic records. A plot of the values of amplitude on semi-log paper should have given a straight line, but this did not prove to be the case, showing that there are non-linearities in the system and that the damping present is not pure viscous damping. Average values of all the runs made (about three per set of given conditions) were used to calculate the final value given. It should be emphasized that these values are subject to some error due to the nonlinearity mentioned above and the difficulty in reading the record. Table VII shows the values of ζ for various conditions. Runs were made with and without the amplifier connected to the motor and with and without the 0.01 microfarad condensers across the motor coils.

TABLE VII. VALUES OF CRITICAL DAMPING RATIO,

CONDITIONS	ζ
No amplifier, no condensers	0.100
No amplifier, with condensers	0.062
Amplifier, no condensers	0.134
Amplifier, with condensers	0.257
Voltage across coils, with condensers, no pick-up	0.118
Voltage across coils, with condensers, with pick-up	0.229

Knowing ζ, it is an easy matter to determine the viscous friction of f, since $f = 2\zeta\omega_n M$. Taking a value of $\zeta = 0.1$, for the case of no amplifier and no condenser,

$$f = 2 \times 0.1 \times (190 \times 2\pi) \times 1.188 \times 10^{-4} = 0.0283 \text{ lb sec/in.}$$

This is the value of viscous friction for Motor B.

4.14 Coil Data--Resistance and Inductance R_c and L

The resistance, R_c, of the coil was determined by means of a Wheatstone bridge to be 1807 ohms for one coil and 1794 ohms for the other. A value of 1800 ohms was used in the calculations for Motor A. For Motor B, the value used was 1750 ohms.

The inductance, L, was determined as follows:

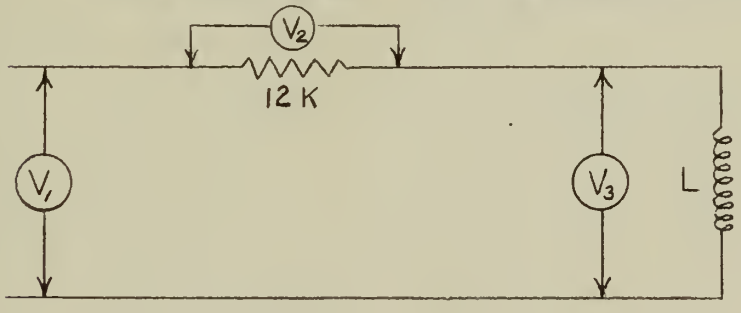

$V_1 = 140$ volts, 400 cycle.

$V_2 = 36$ volts.

$V_3 = 123$ volts.

FIG. 22. CIRCUIT USED TO MEASURE INDUCTANCE OF ARMATURE COIL

The coil was placed in series with a resistor of 12,000 ohms resistance and a source of 400 cycle per second power as shown in Fig. 22. Voltages V_1, V_2, and V_3 were measured. The current, I, flowing in the circuit can be determined since we know the voltage across the 12,000 ohm resistor.

$$I = 36/12K = 3 \times 10^{-3} \text{ amps.}$$

The magnitude of the impedance of the coil, Z_c, is the voltage across the coil divided by the current flowing through it.

$$V_3 = Z_c I = 123 \text{ volts}$$

$$Z_c = 123/3 \times 10^{-3} = 41 \times 10^3 \text{ ohms}$$

The source impedance, Z_o, is the voltage, V_1, divided by the current, or with $V_1 = 140$ volts

$$Z_o = 140/3 \times 10^{-3} = 46.7 \times 10^3 \text{ ohms.}$$

By drawing a vector diagram and actually plotting these values as in Fig. 23, one finds that

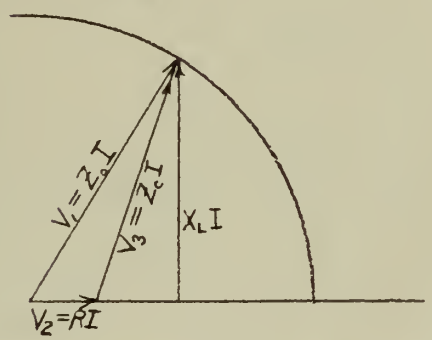

$$X_L I = 115.0 \text{ volts}$$

$$X_L = 115/3 \times 10^{-3} = 38.3 \times 10^3 \text{ ohms}$$

$$L = 38.3 \times 10^3 / 2\pi 400 = 15.3 \text{ henries}$$

FIG. 23. VECTOR DIAGRAM OF VOLTAGES

The same procedure for finding inductance, L, was followed at 60 cycles per second, a 60 c.p.s. source being used in place of the 400 c.p.s. source used above. The following voltage readings were obtained:

$V_1 = 45$ volts
$V_2 = 36$ volts
$V_3 = 17$ volts

$L = 14.1$ henry.

The value of inductance used for Motor A was 15.0 henry. Similar measurements on Motor B indicated that the inductance L was approximately 20.0 henries.

4.15 Back Electromotive Force K_B

To determine the back electromotive force experimentally a small variable speed motor was connected to the torque motor through an eccentric cam. When the motor made one revolution, the cam caused the torque motor armature to move a certain distance x in simple harmonic motion. In other words, $x = A\omega\sin\omega t$ where A = maximum displacement of armature from neutral. ω = angular velocity of motor

The derivative of x with respect to time, or the linear velocity of the armature, is $dx/dt = A\omega\cos\omega t$. The voltage produced by the motion of the armature in the magnetic field is proportional to the velocity of the armature.

i.e. $V_g = K_B\, dx/dt$

or $K_B = V_g / dx/dt$

where V_g = voltage generated by the motion of the armature in the magnetic field.
K_B = factor of proportionality

The velocity of the armature in simple harmonic motion will be maximum when x is zero. Therefore, the voltage, V_g, may be written as $V_g = V_{gmax}\cos\omega t$. Substituting this into the expression for K_B and at the same time substituting for dx/dt, we may write

$$K_B = \frac{V_{gmax}\cos\omega t}{A\ \omega\ \cos\omega t} = \frac{V_{gmax}}{A\ \omega}$$

We can now find K_B experimentally by measuring the maximum or peak voltage generated, the maximum displacement of the armature from neutral, and the angular velocity of the motor. The voltage was measured by placing a Hewlitt-Packard voltmeter across one of the coils; the maximum displacement of the armature was determined by the eccentric cam; and the angular velocity

of the motor was found by the use of a stroboscope.

Runs were made with eccentric throws of 0.00725 in., 0.011 in., and 0.0285 in. In each case graphs were plotted of the voltage generated versus armature linear velocity. These graphs are shown in Figs. 24, 25, and 26. In order to determine the value of K_B from these figures, the actual slope in volts per inch per second must be multiplied by 1.414 as the ordinate is the voltage read on a high input impedance voltmeter or, in other words, the root mean square value of the voltage whereas the peak voltage is desired. The experimental data are tabulated in Table VIII. In Fig. 27 a graph was plotted showing the variation of K_B with the amplitude of the armature motion and on the same figure the theoretical values of K_B from section 3.125 as well. It can be seen that for Motor A the theoretical and the experimental results agree very well. Only the theoretical values for Motor B have been plotted. It was felt that since the theoretical and experimental curves for Motor A agreed so well and time was at a premium that a satisfactory value of K_B for Motor B could be read off the graph as long as the maximum amplitude was kept below 0.015 inches.

4.16 Electromechanical Coupling Constant K_M

To determine the electromechanical coupling constant, K_M, experimentally, standard weights were hung on the armature arm and then the differential current necessary to bring the armature back to its center position was recorded. This procedure was repeated in taking off the weights and then the whole process was repeated for displacements on the other side of the center position by turning the motor over. This gave values of K_M for both positive and negative differential currents. To maintain the center position of the armature, a Brown and Sharpe dial indicator was mounted on the motor with the indicator set at zero. This

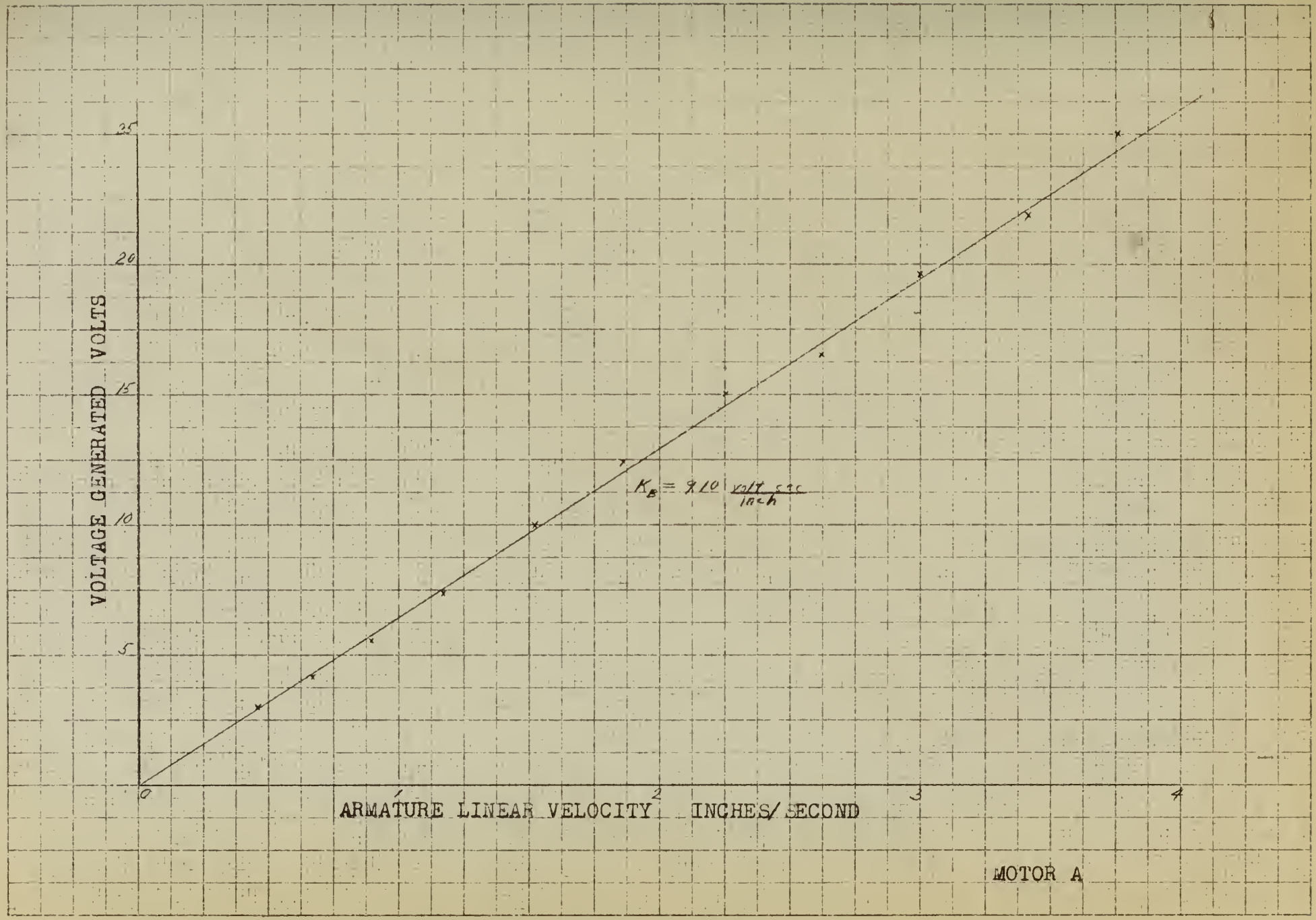

FIG. 24 VOLTAGE GENERATED VERSUS ARMATURE LINEAR VELOCITY, A = 0.00725 INCHES

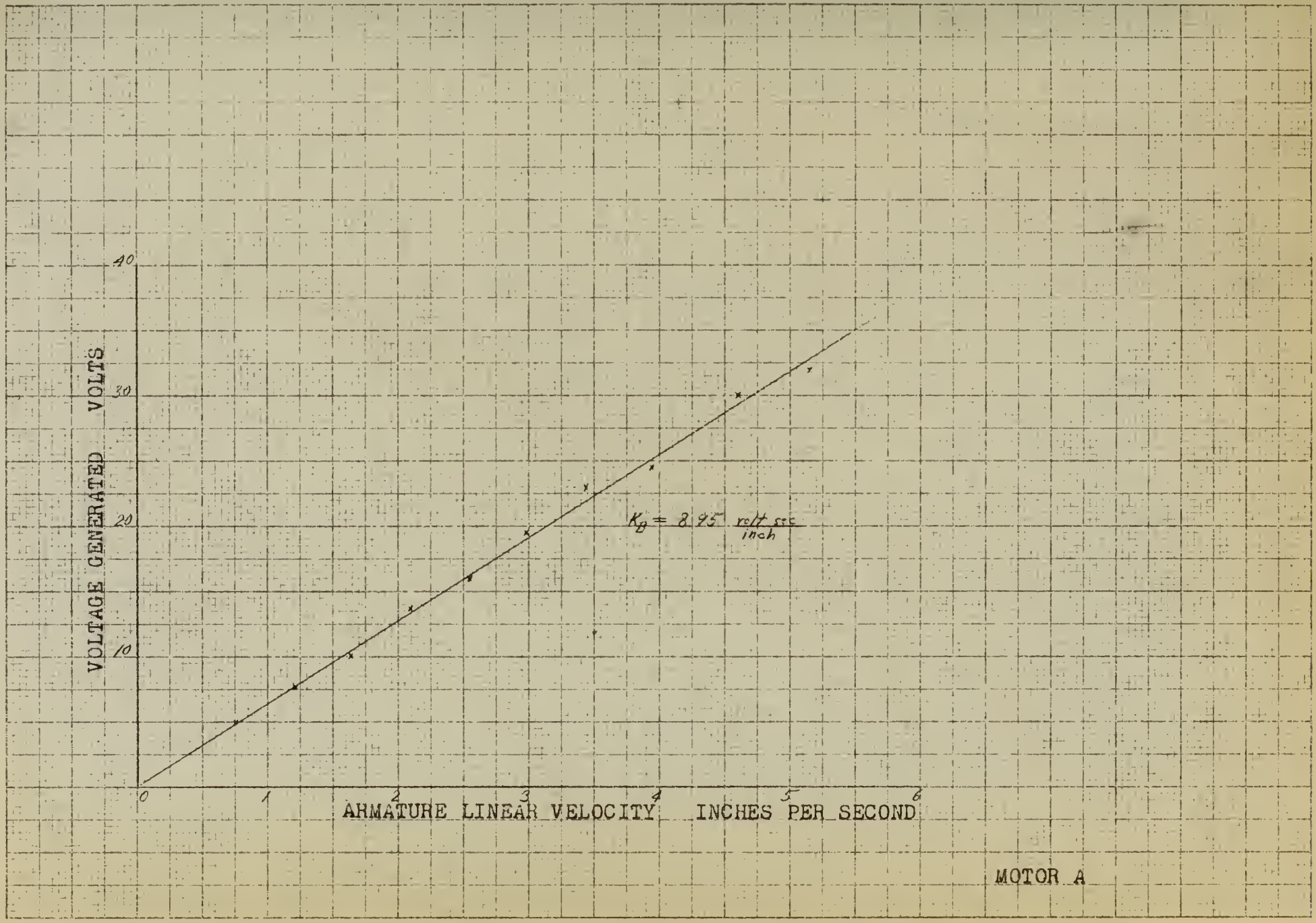

FIG.25 VOLTAGE GENERATED VERSUS ARMATURE LINEAR VELOCITY, A = 0.011 INCHES

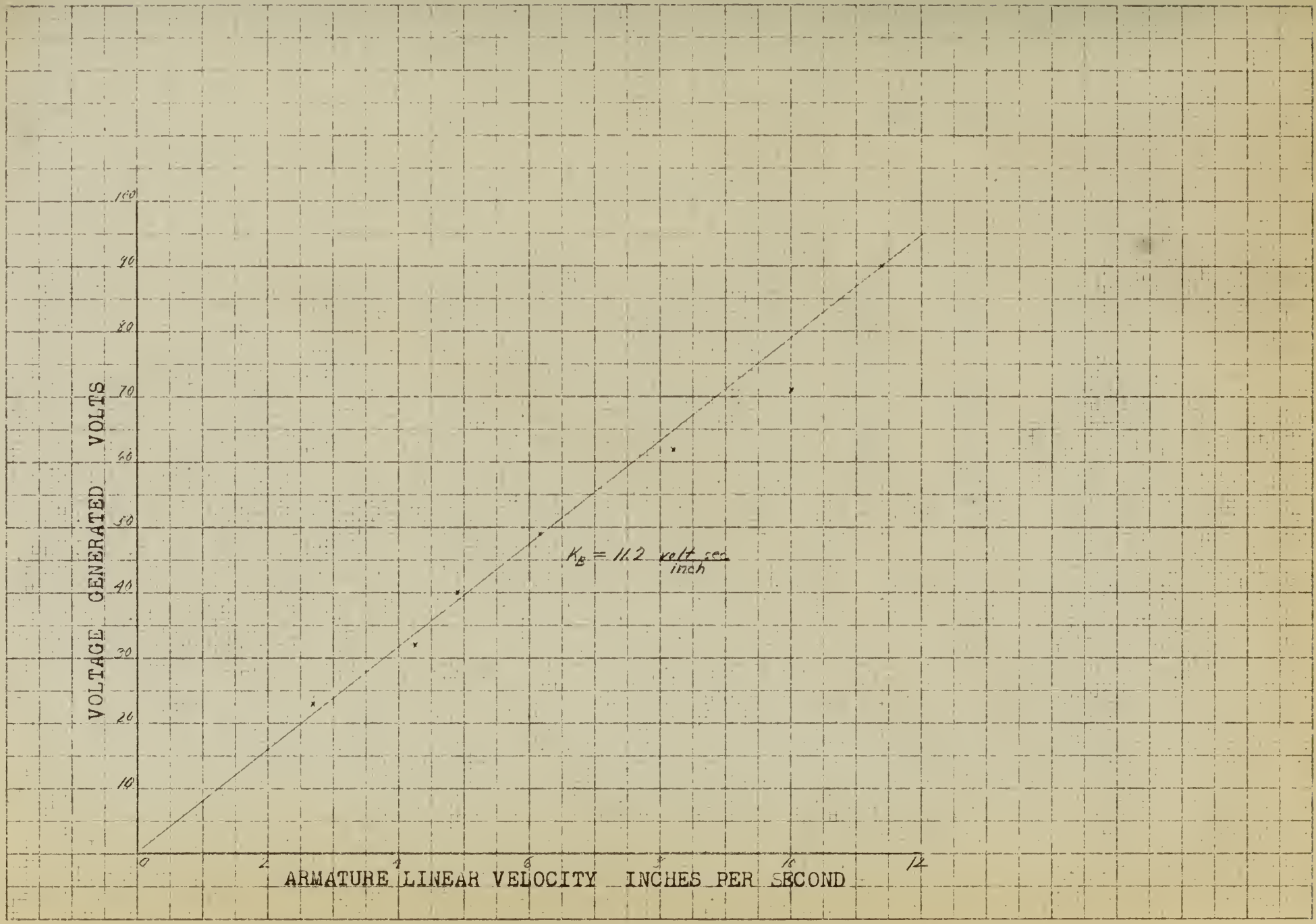

FIG. 26 VOLTAGE GENERATED VERSUS ARMATURE LINEAR VELOCITY, A = 0.0285 INCHES

TABLE VIII EXPERIMENTAL DATA FOR DETERMINATION OF BACK ELECTROMOTIVE FORCE

A = 0.00725 in			A = 0.011 in			A = 0.0285 in		
RPM	VOLTS	$\dot{x} = A\omega$ IN/SEC	RPM	VOLTS	$\dot{x} = A\omega$ IN/SEC	RPM	VOLTS	$\dot{x} = A\omega$ IN/SEC
4950	25.0	3.76	4475	32.0	5.15	5400	150	16.1
4500	21.9	3.41	4000	30.0	4.60	4900	130	14.7
3950	19.7	3.00	3420	24.5	3.94	3800	90	11.4
3450	16.5	2.62	2990	23.0	3.44	3330	71	10.0
2960	15.1	2.25	2600	19.5	2.99	2740	62	8.20
2450	12.4	1.86	2215	16.0	2.55	2060	49	6.16
2000	10.0	1.52	1820	13.8	2.09	1650	40	4.90
1550	7.4	1.17	1425	10.8	1.64	1330	32	4.25
1175	5.6	0.891	1050	7.8	1.21	900	23	2.68
890	4.2	0.674	655	5.0	0.75			
600	3.0	0.455						

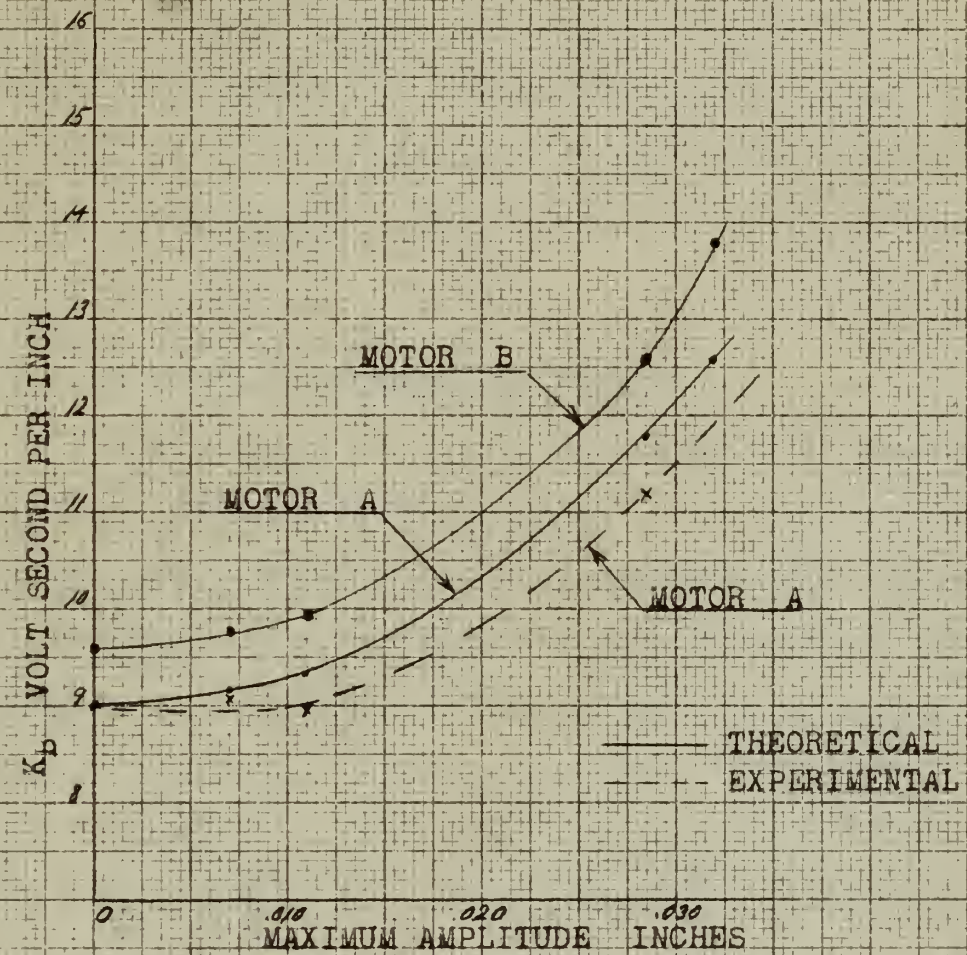

TABLE VIII-THEORETICAL AND EXPERIMENTAL VALUES OF K_B FOR DIFFERENT MAXIMUM AMPLITUDES

MAX AMPLITUDE	MOTOR A THEORETICAL	MOTOR A EXPERIMENTAL	MOTOR B THEORETICAL
0	9.01		9.64
.007	9.18	9.10	9.80
.011	9.34	8.95	9.98
.0285	11.82	11.2	12.6
.032	12.6		13.8

FIG 27 BACK ELECTROMOTIVE FORCE VERSUS ARMATURE DISPLACEMENT

gave the needed reference to enable the armature to be brought back to its center position each time a weight was added or subtracted to the armature arm. These data, as plotted in Fig. 28, gave a line whose average slope was determined to be 90.1 lbs/amp. for Motor A. The data for Motor B are plotted in Fig. 29, and $K_M = 100$ lbs/amp. The calculation data may be found in Tables IX and X for Motors A and B respectively. Currents i_1 and i_2 are the currents flowing in each of the motor coils and i is the differential current.

4.2 EXPERIMENTAL DETERMINATION OF IMPEDANCE

In order to determine the impedance of the motor experimentally a vacuum tube voltmeter was placed across one of the coils and a 27 ohm resistor was placed in series with it. By placing a second vacuum tube voltmeter across this known resistance, the current flowing in the coil was easily determined. The magnitude of the impedance was found by dividing the voltage across the coil by the current flowing in it. A plot of this experimental impedance as a function of alternating current frequency may be found in the section on the comparison of theoretical and experimental results in Fig. 44.

4.3 EXPERIMENTAL DETERMINATION OF PHASE AND AMPLITUDE CURVES

In determining experimentally the phase and amplitude characteristics as functions of frequency, the first problem encountered was that of measuring phase as accurately as possible. To do this a phase shift network was used as follows.

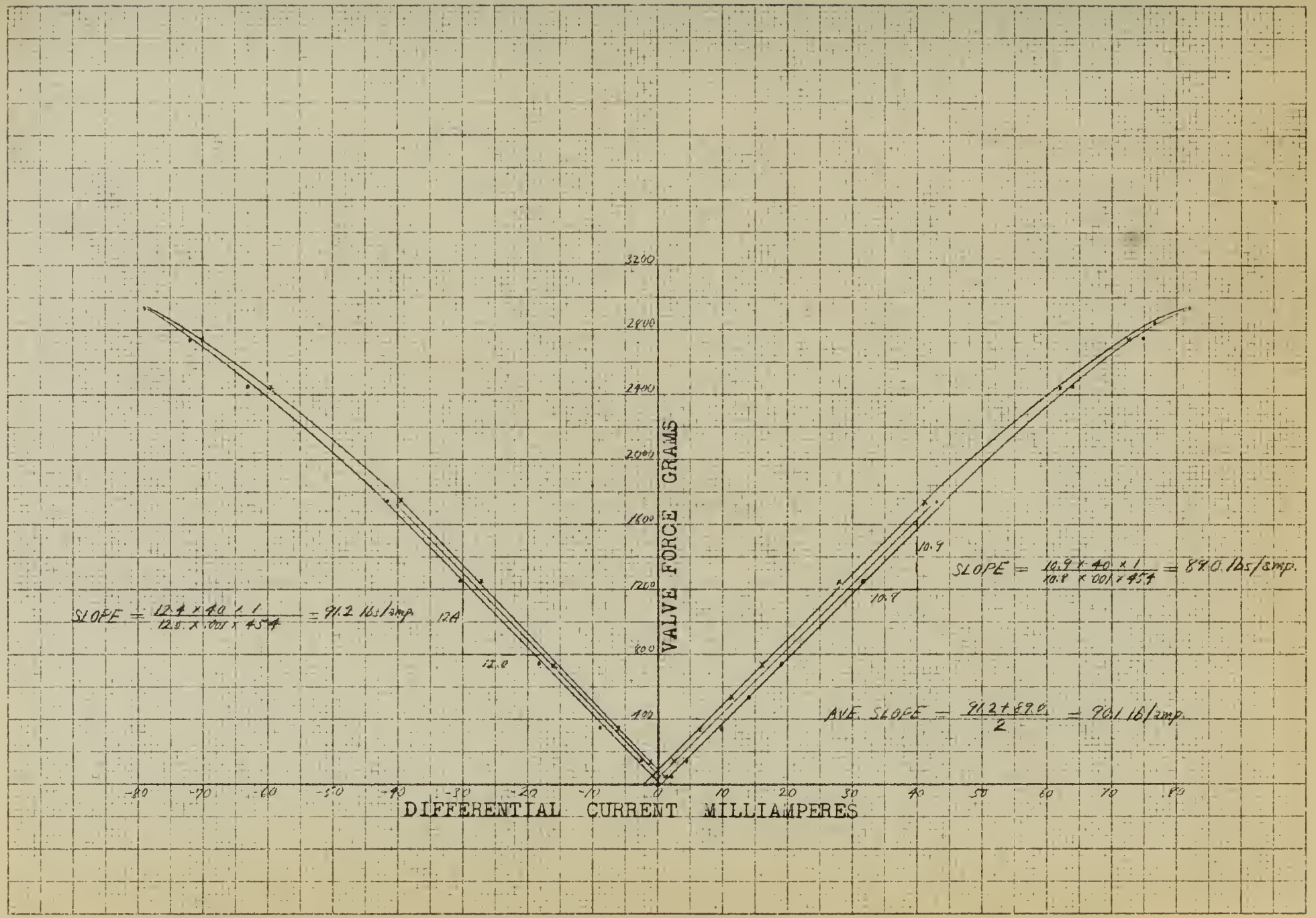

FIG 28 VALVE FORCE VERSUS DIFFERENTIAL CURRENT MOTOR A

FIG. 29 VALVE FORCE VERSUS DIFFERENTIAL CURRENT MOTOR B

TABLE IX EXPERIMENTAL DATA FOR DETERMINATION OF ELECTRO-MECHANICAL COUPLING CONSTANT FOR MOTOR A.

CURRENT (MILLIAMPERES)			FORCE	CURRENT (MILLIAMPERES)		
i_1	i_2	i	GRAMS	i_1	i_2	i
24.0	24.0	0.0	0	28.5	30.5	-2.0
25.0	24.0	1.0	50	29.5	30.0	-0.5
27.5	23.0	4.5	150	32.0	29.5	+2.5
31.0	21.0	10.0	350	32.0	25.5	6.5
34.5	20.5	14.0	550	36.0	24.5	11.5
38.5	19.5	19.0	750	37.5	21.5	16.0
44.0	13.5	31.5	1250	40.5	12.5	28.0
43.0	0.0	43.0	1750	41.0	0.0	41.0
64.0	0.0	64.0	2450	62.0	0.0	62.0
75.0	0.0	75.0	2750	72.5	0.0	72.5
76.5	0.0	76.5	2850			
82.0	0.0	82.0	2950			
24.0	24.0	0.0	0	24.0	22.0	+2.0
24.0	24.5	-0.5	50	23.0	21.5	+1.5
24.0	26.5	2.5	150	21.0	22.0	-1.0
18.0	27.0	9.0	350	18.0	24.0	6.0
10.5	29.0	18.5	750	11.0	27.0	16.0
1.5	32.0	30.5	1250	5.0	32.0	27.0
0.0	41.5	41.5	1750	0.0	39.5	39.5
0.0	63.0	63.0	2450	0.0	59.5	59.5
0.0	72.0	72.0	2750	0.0	70.0	70.0
0.0	79.0	79.0	2950			

TABLE X EXPERIMENTAL DATA FOR DETERMINATION OF ELECTRO-MECHANICAL COUPLING CONSTANT FOR MOTOR B.

CURRENT (MILLIAMPERES)			FORCE	CURRENT (MILLIAMPERES)		
i_1	i_2	i	GRAMS	i_1	i_2	i
24	24	0	0	19	21	-2
24	22	2	50	20	20	0
24	20	4	150	20	18	+2
26	16	10	350	21	16	5
27	13	14	550	24	14	10
29	10	19	750	24	10	14
32	3	29	1250	29	3	26
40	0	40	1750	36	0	36
54	0	54	2300	49	0	49
67	0	67	2800	63	0	63
76	0	76	3100	74	0	74
79	0	79	3200	78	0	78
80	0	80	3250			
24	24	0	0	23	20	+3
23	24	-1	50	23	22	+1
22	26	4	150	22	23	-1
20	28	8	350	21	26	5
18	31	13	550	20	29	9
17	33	16	750	18	31	13
14	40	26	1250	14	38	24
7	45	38	1750	8	43	35
2	53	51	2300	5	53	48
0	66	66	2800	0	62	62
0	76	76	3100	0	75	75
0	79	79	3200	0	79	79
0	82	82	3250			

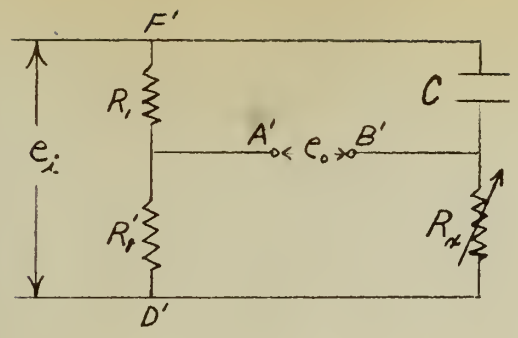

FIG. 30. SCHEMATIC OF PHASE SHIFT NETWORK

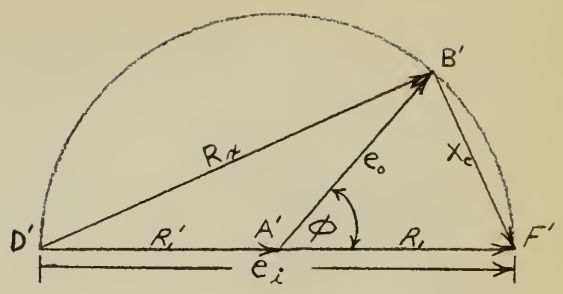

FIG. 31. VECTOR DIAGRAM FOR PHASE SHIFT NETWORK

A voltage, e_i, was put in across terminals D' and F' and a voltage, e_o, was taken off the terminals A' and B' as shown in Fig. 30. The phase angle, Ø, is equal to $2 \tan^{-1}\frac{X_c}{R_x}$ as can be seen from the vector diagram in Fig. 31. This phase shift network is discussed in Ref. 5, p. 30. Two matched resistances of 15,000 ohms each were used as R_1 and R_1'. A standard decade capacitor (Cornell-Dubilier Decade Capacitor, Model CDB-5) was used for the capacitance.

Fig. 32 shows how this phase shift network was used to measure the phase shift between the input voltage to the amplifier and the output of the torque motor. The input voltage, e_i, was fed into the amplifier and also into the phase shift network as shown in Fig. 32A. The signal from the amplifier actuates the motor and by means of the capacitor pickoff device a voltage representing the position of the armature arm is obtained. This voltage from the pickoff was fed into one pair of plates of a cathode ray oscilloscope. The signal, e_o, from the phase shift network was fed into the other pair of plates. As shown in Fig. 32B, when the two signals are out of phase the trace on the oscilloscope will appear as a loop. When by means of changing the resistance, R_x, in the phase shift network the two signals are brought into phase, the loop closes to a straight line. Thus by

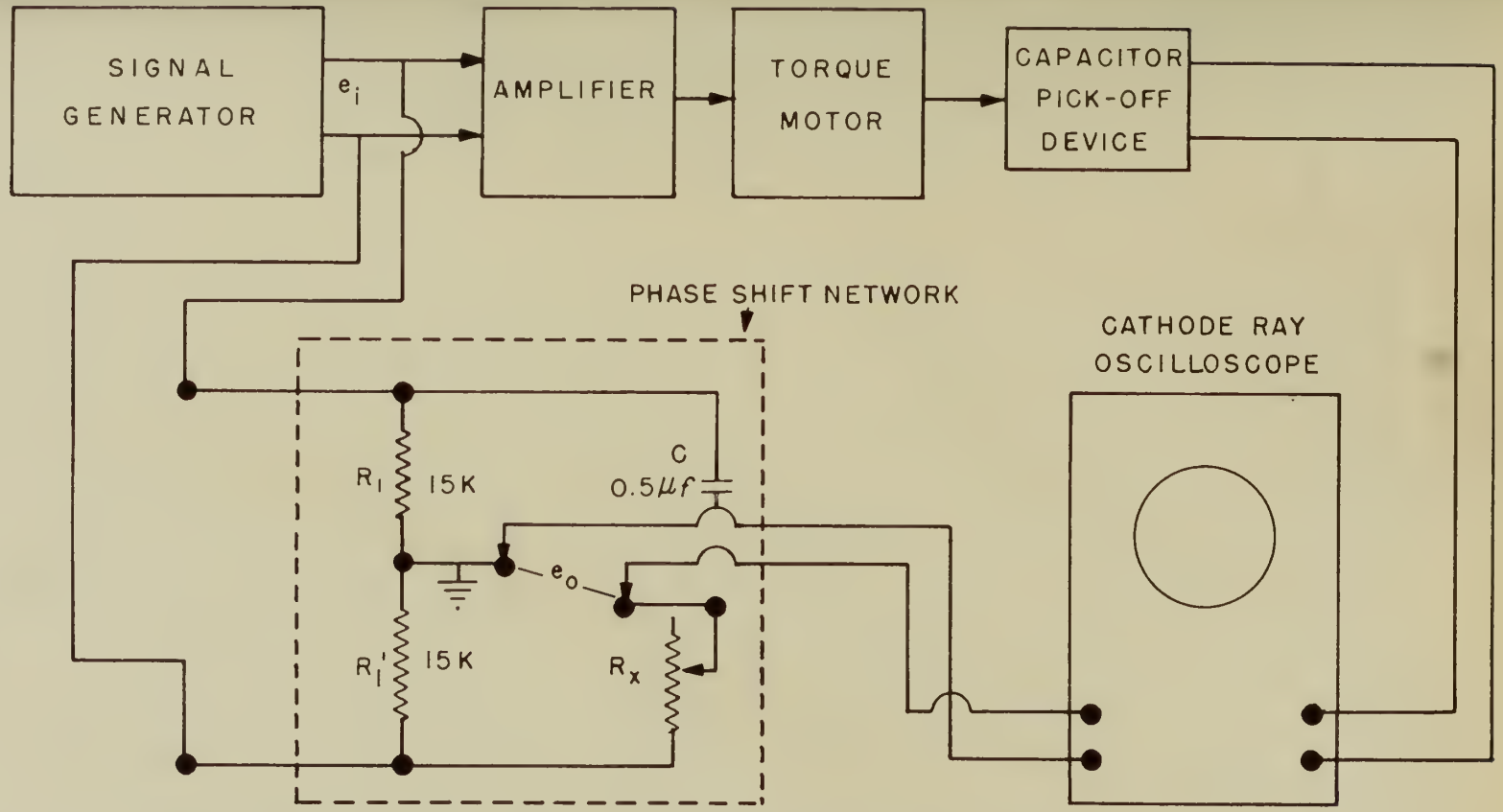

FIG. 32 A. PHASE SHIFT NETWORK USED TO MEASURE PHASE ANGLE LAG.

PHASE DIFFERENCE

AT NULL

CATHODE RAY OSCILLOSCOPE TRACE

FIG. 32 B. APPEARANCE OF CATHODE RAY TUBE WITH PHASE DIFFERENCE AND AT NULL.

using the oscilloscope as a null detector in this manner, one is able to measure the phase difference between input voltage and the displacement of the armature by recording the value of R_x necessary to close the loop at various discrete frequencies. The phase angle, ϕ, is as mentioned earlier $2 \tan^{-1}\frac{X_c}{R_x}$. A photograph of the actual experimental setup used to measure phase shift characteristics is shown in Fig. 33.

The capacitor pickoff deserves especial mention as it is a very sensitive device for changing the position of the armature arm into a voltage so that one may measure accurately its position. The circuit for the armature pickoff is given schematically in Fig. 34 and a photograph of the device as mounted on the motor is shown in Fig. 35. The pickoff is shown connected to the armature arm by a wire as it was connected during some early tests. However, in all the runs actually reported on the capacitor pickoff was mounted directly on the armature arm. The fan shaped piece moving between the stationary plates in accordance with the motion of the armature changes the capacitance, thus giving rise to the signal voltage. A plot illustrative of the linearity of this pickoff is given in Fig. 36.

The amplitude of the armature motion was obtained from the photographic record taken with a Model H, Multi-channel Oscillograph manufactured by the William Miller Corporation, Pasadena, California. An input signal was fed in by means of the signal generator to the amplifier and the motion of the armature of the motor was recorded on the oscillograph. Care was taken that the amplitude of the armature displacement remained within the linear range of our K_B factor. Also the voltage across the tube itself was kept above 65 volts at all times. The reason for this will be discussed in section 5.21. The Miller record gave a picture of the movement of the armature in response to the sinusoidal input. The experimental setup used

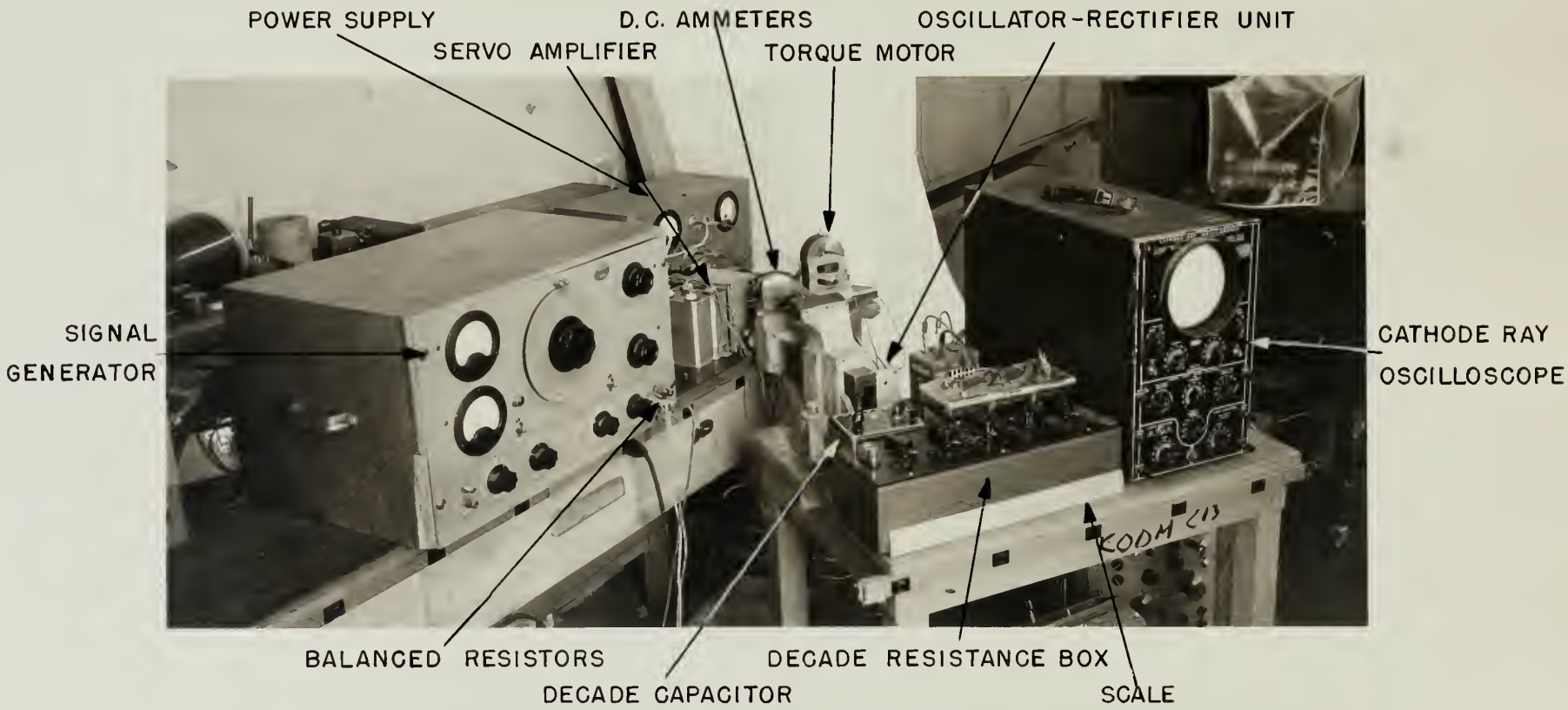

FIG.33. EXPERIMENTAL SET-UP USED TO MEASURE PHASE SHIFT CHARACTERISTICS.

APPLIED PHYSICS LABORATORY
THE JOHNS HOPKINS UNIVERSITY
8621 GEORGIA AVENUE
PHOTO NUMBER DATE PRINTED
9618

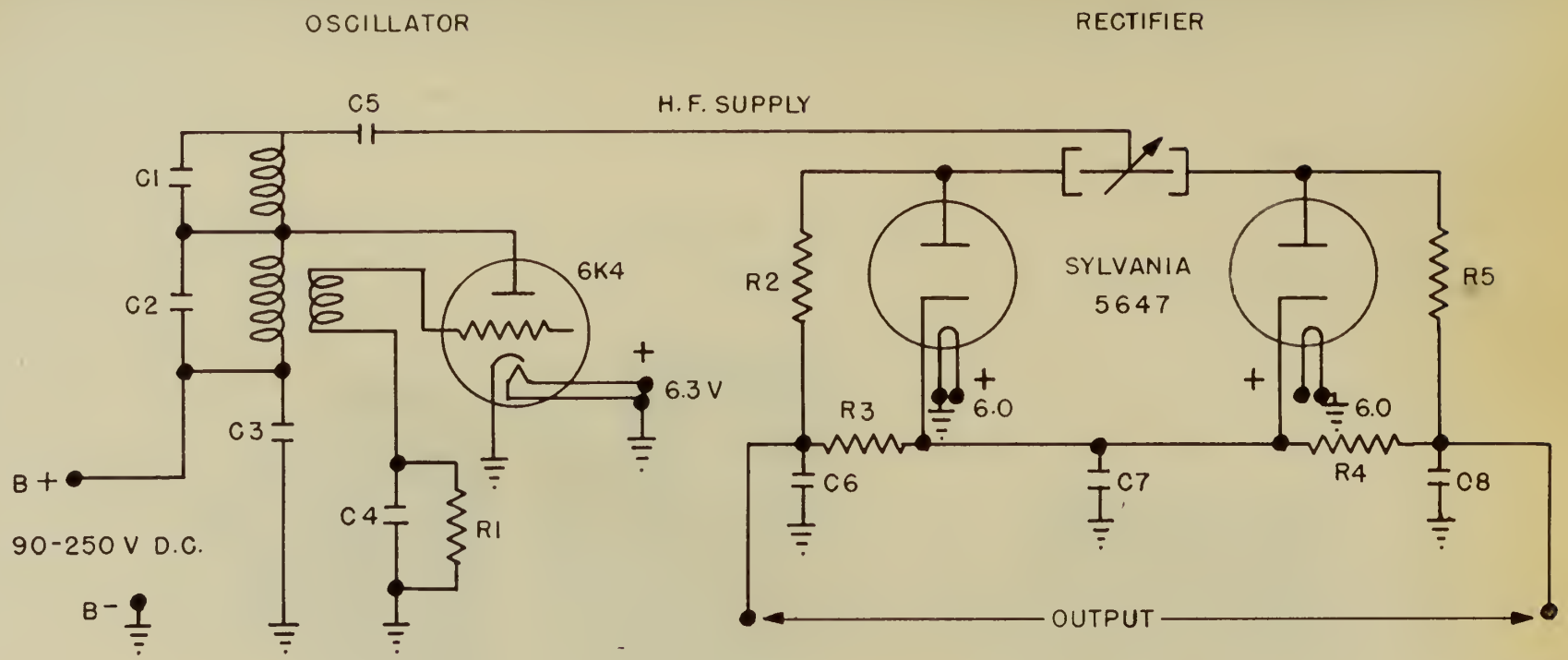

C1, C2, C3, C4	175 $\mu\mu f$ 400 VOLTS	
C5, C6, C7, C8	CAPACITORS	
R1	—— 8200 Ω	1/2 WATT
R2, R5	—— 56 K Ω	"
R3, R4	—— 200 K Ω	"

APPROXIMATE OSCILLATOR FREQUENCY 3.5 M.C.

FIG. 34. CAPACITOR PICKOFF CIRCUIT— KENYON GYRO AND ELECTRONICS CORPORATION, NEW YORK.

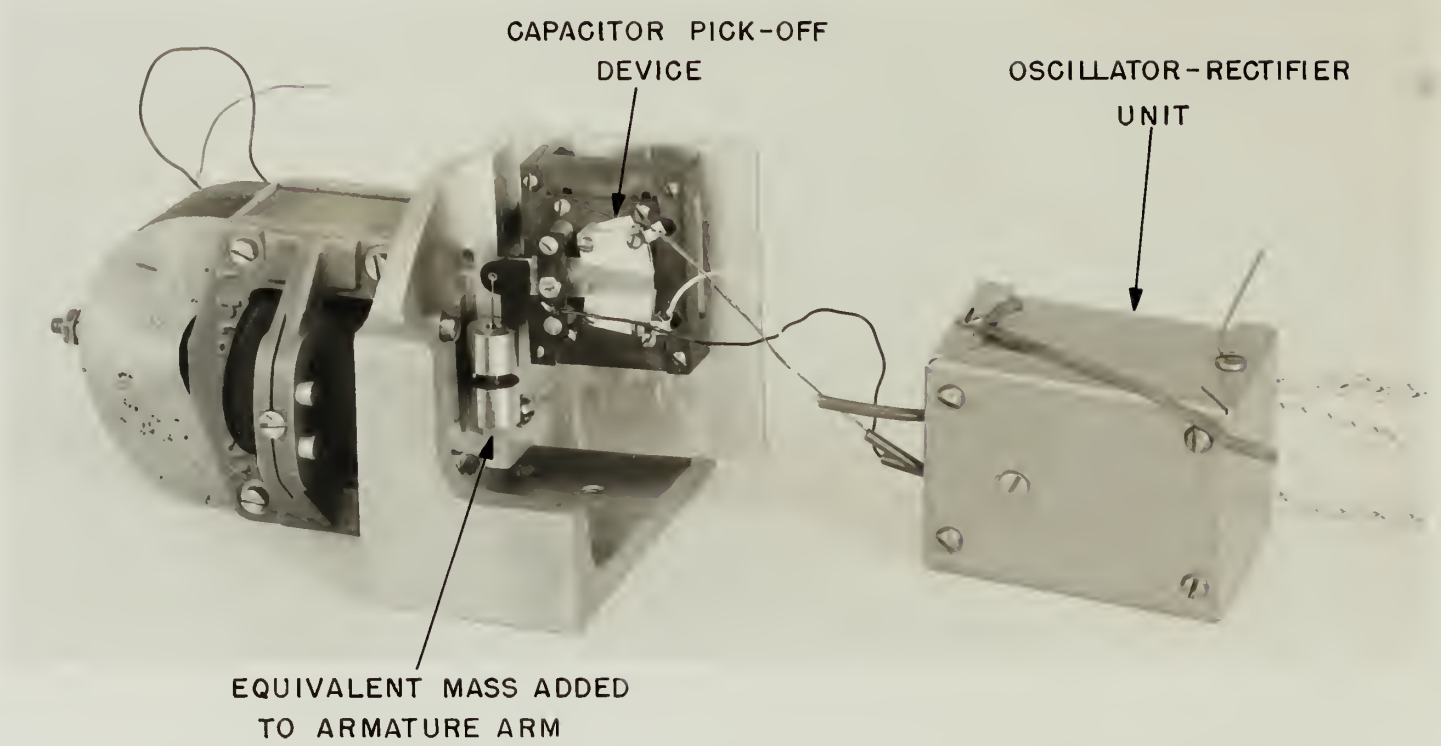

FIG.35. CAPACITOR PICK-OFF DEVICE AS MOUNTED ON TORQUE MOTOR FOR EARLY TESTS.

APPLIED PHYSICS LABORATORY
THE JOHNS HOPKINS UNIVERSITY
THIS PHOTOGRAPH ON FILE AT
8621 GEORGIA AVENUE
PHOTO NUMBER DATE PRINTED
8605

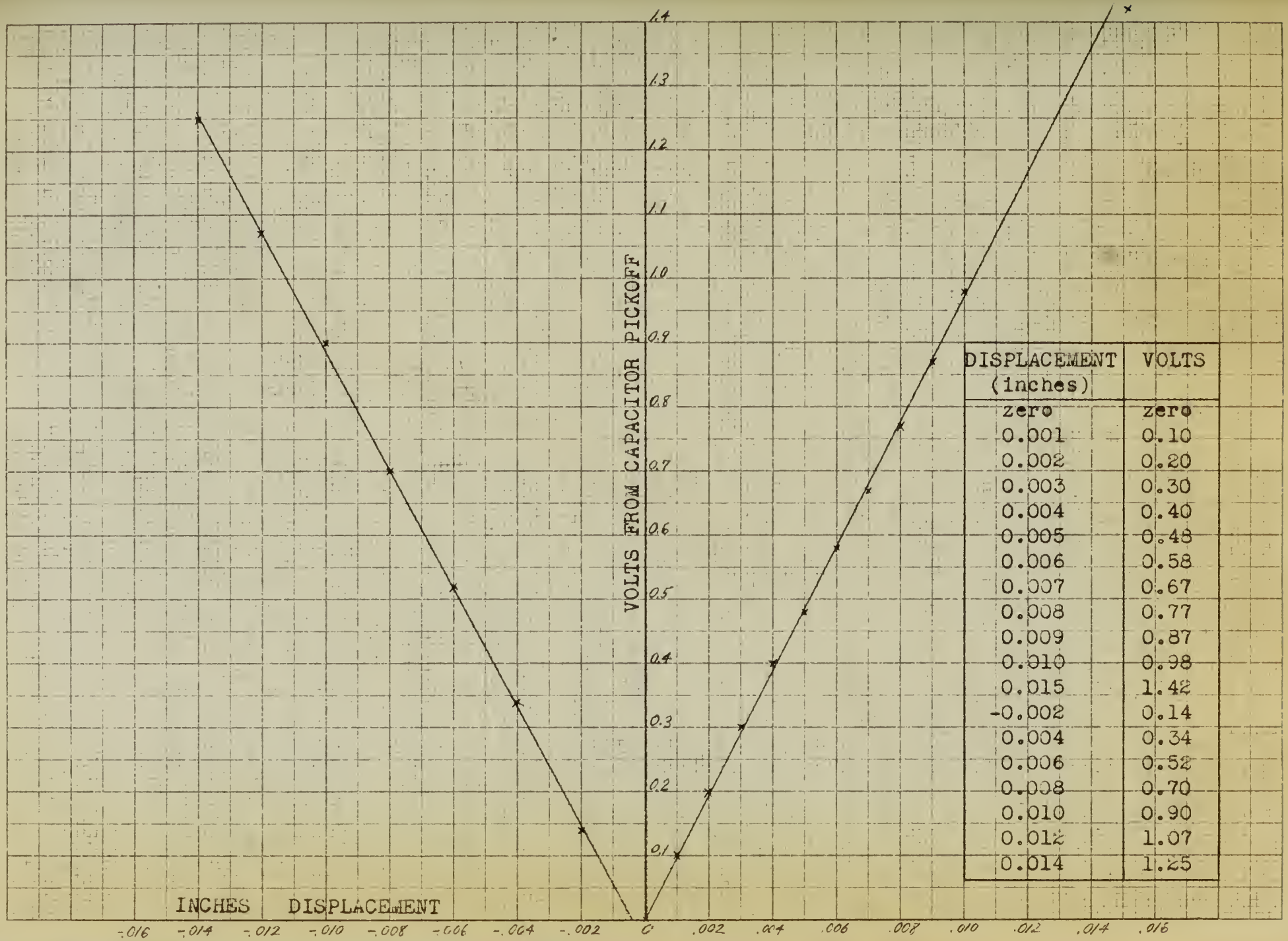

DISPLACEMENT (inches)	VOLTS
zero	zero
0.001	0.10
0.002	0.20
0.003	0.30
0.004	0.40
0.005	0.48
0.006	0.58
0.007	0.67
0.008	0.77
0.009	0.87
0.010	0.98
0.015	1.42
-0.002	0.14
0.004	0.34
0.006	0.52
0.008	0.70
0.010	0.90
0.012	1.07
0.014	1.25

FIG. 36 LINEARITY OF CAPACITOR PICKOFF

to measure the amplitude characteristic is shown in Fig. 37 and a sample portion of a record is enclosed as Fig. 38.

The amplifier used to drive the motor is shown schematically in Fig. 39.

In Fig. 40 the variation of phase lag versus frequency for three different initial values of amplitude is shown. It had been noted in performing tests on phase lag characteristics that the shape of the curve was easily reproducible but that the initial value of phase lag varied. Initial values of the amplitude of the input of 0.0025 in., 0.005 in., and 0.010 in. were taken and the resulting phase characteristics plotted. At low frequencies there is less phase lag for the larger values of sinusoidal input. This is due to some non-linear effect; perhaps hysteresis which would cause more phase lag percentagewise for small displacements than large ones. As the frequency increases all the curves come closer together until beyond resonance the curves of the larger values of initial amplitude exhibit more phase lag than the smaller ones. A valid reason for the reversal at high frequencies is not known at present.

The experimental values of phase lag of Motor B, both with and without the 0.1 microfarad condensers are shown in Fig. 41. It is seen that the addition of the condensers introduces an additional phase lag above resonance.

In Fig. 42, a plot of the amplitude ratio (output to input) versus frequency has been made for Motor B, both with and without the 0.1 microfarad condensers. In the same figure the theoretical values of amplitude ratio for the motor have been plotted for $\int = 0.1$. The experimental data for these curves may be found in Tables XI and XII and the theoretical value of amplitude ratio in Table XIV.

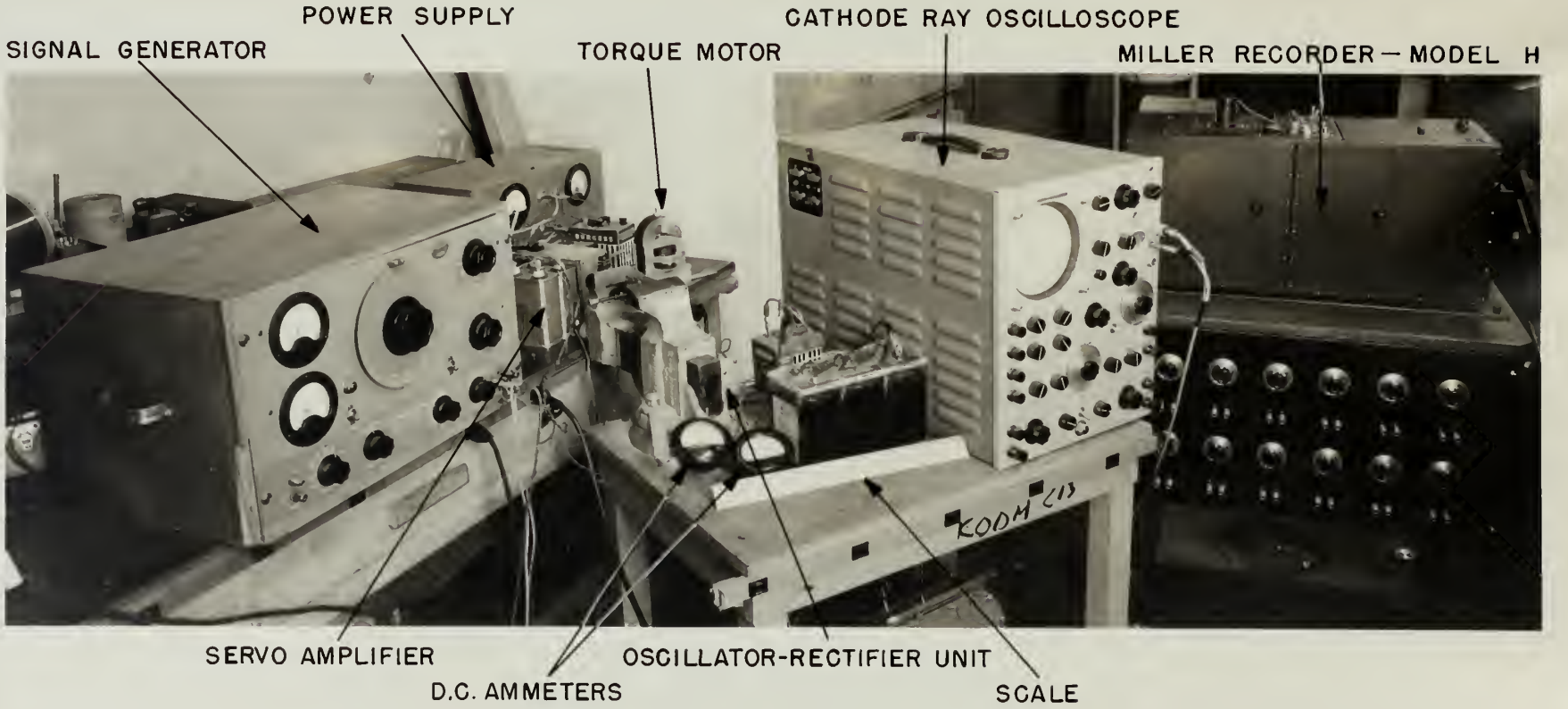

FIG. 37. EXPERIMENTAL SET-UP USED TO MEASURE AMPLITUDE CHARACTERISTICS.

9517

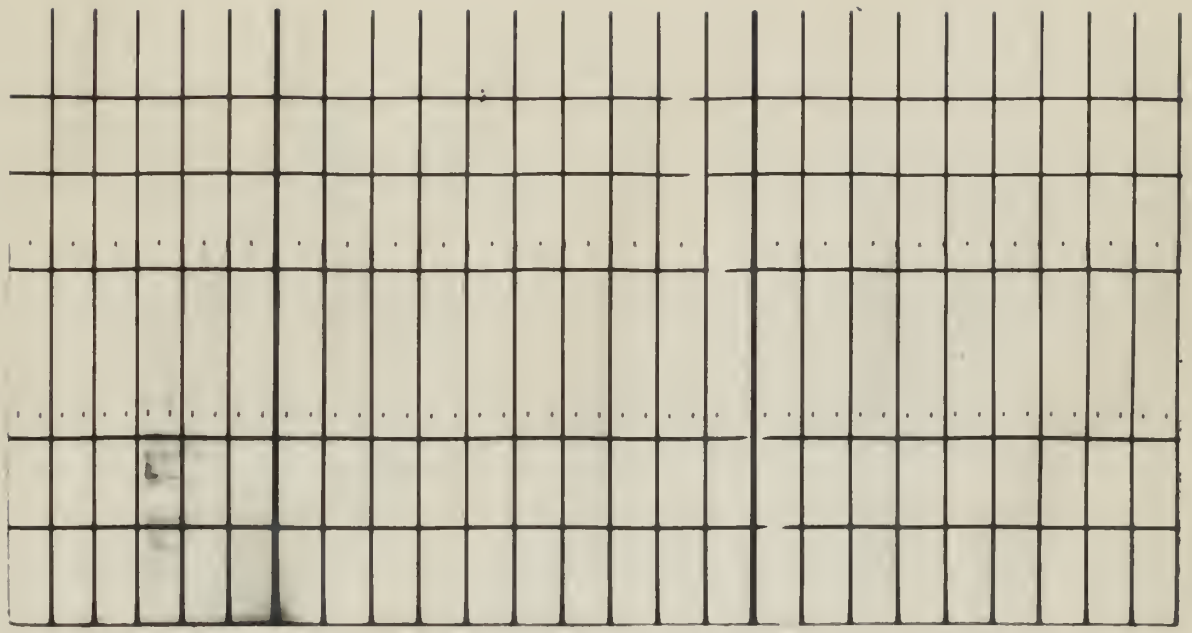

FIG. 38 SAMPLE PORTION OF MILLER OSCILLOGRAPH RECORD OF ARMATURE RESPONSE TO A SINUSOIDAL INPUT VOLTAGE

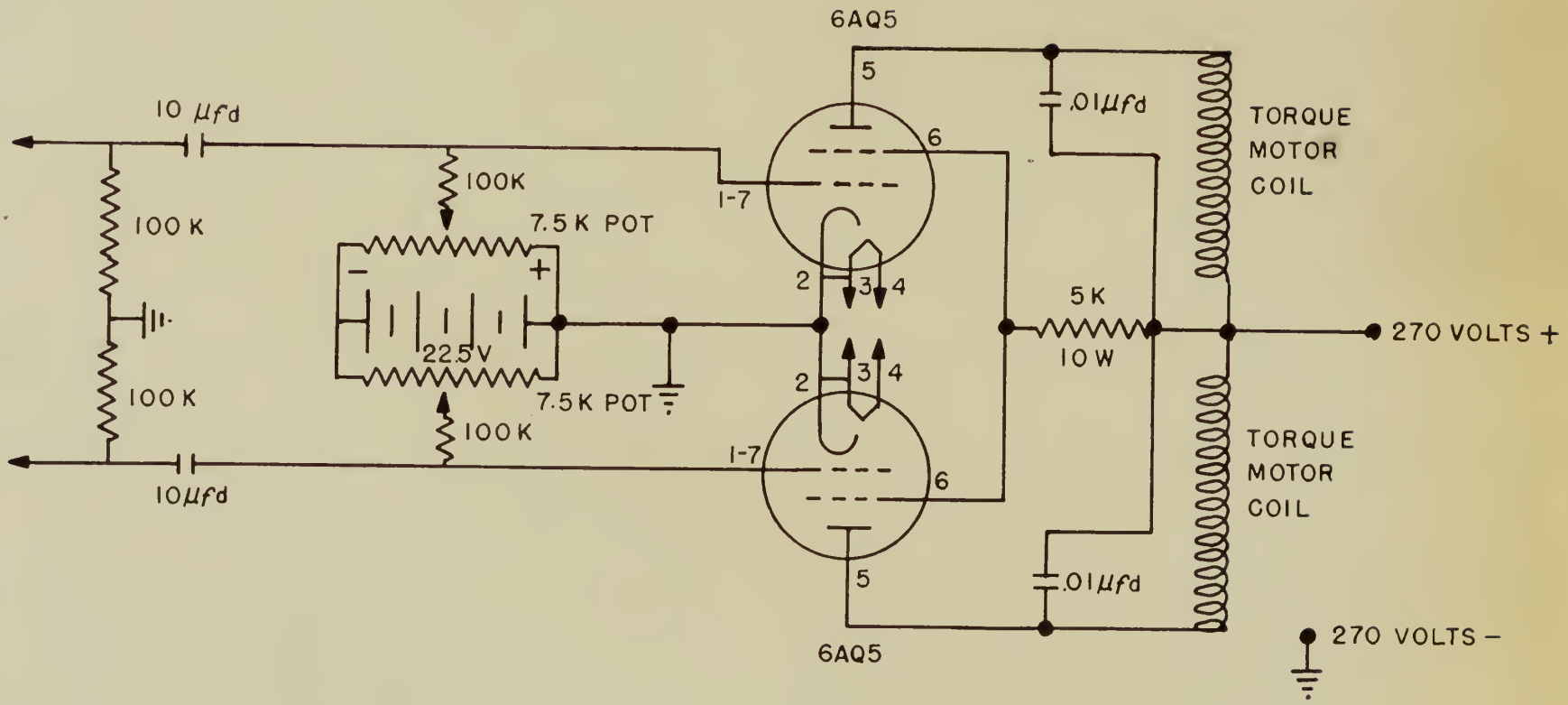

FIG.39. CIRCUIT DIAGRAM OF SERVO AMPLIFIER.

f	Ø ±0.005 in	Ø ±0.0025 in	Ø ±0.010 in
10	7.4	7.4	3.6
15	8.2	11.0	5.6
19.2	8.4	14.0	7.0
20	8.8	14.6	7.4
38	15.0	18.0	13.8
47.5	17.4	19.0	17.4
66.3	24.0	28.6	24.0
85	30.4	33.4	33.4
104	43.6	43.6	46.8
122	57.4	53.8	60.8
141	78.2	71.6	78.4
159	103.6	99.2	99.2
178	138.2	131.6	131.6
185	151.8	148.2	148.2
192	159.6	153.8	157.2
210	180.0	180.0	180.0
239	193.0	188.8	199.0
246	208.4	197.8	215.0
275	232.2	218.8	235.6
301	253.2	240.0	255.2
338	271.6	268.6	274.6
375	290.6	280.4	294.8
411	295.4	285.6	306.4

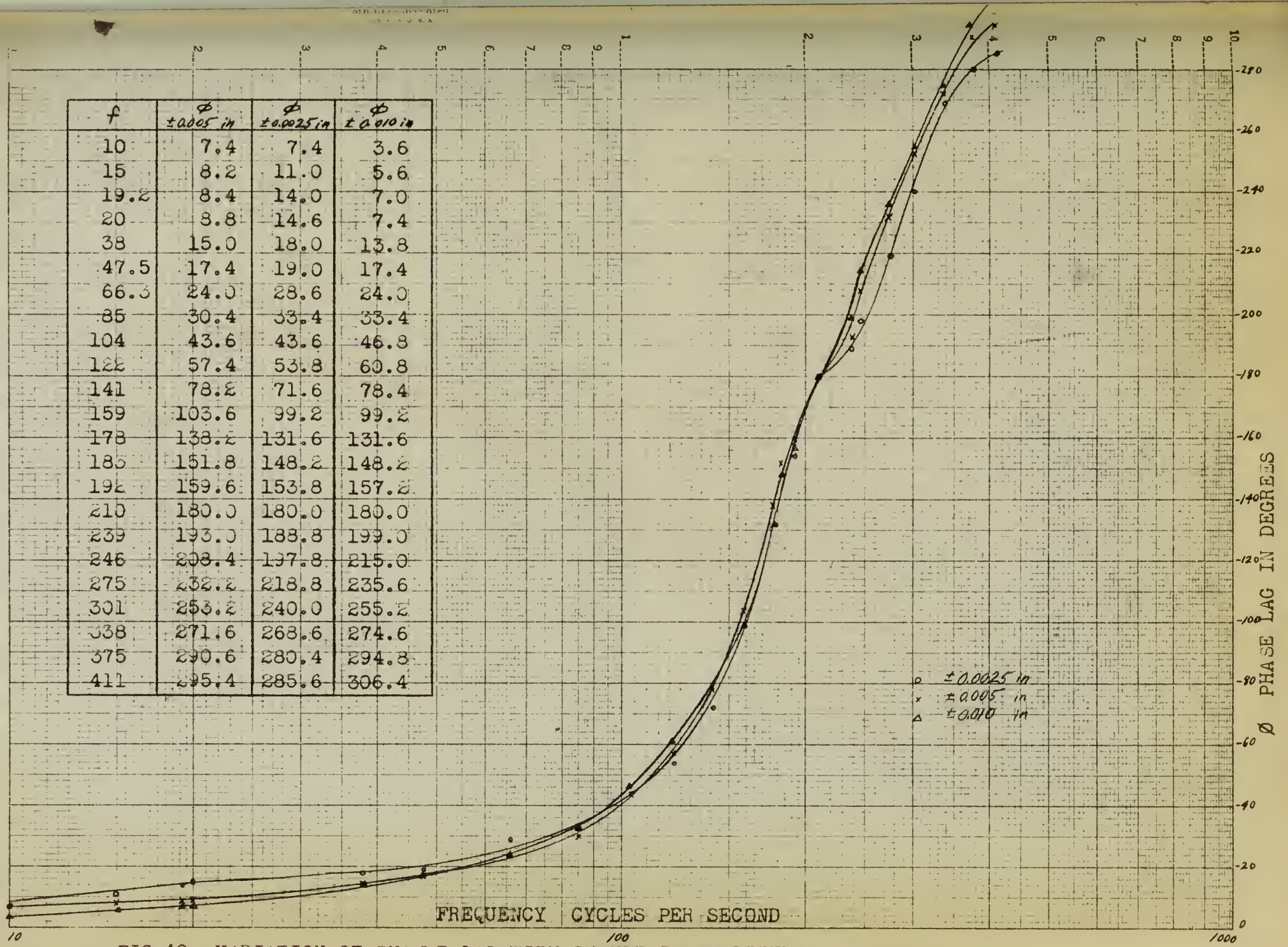

FIG.40 VARIATION OF PHASE LAG WITH CHANGE IN AMPLITUDE

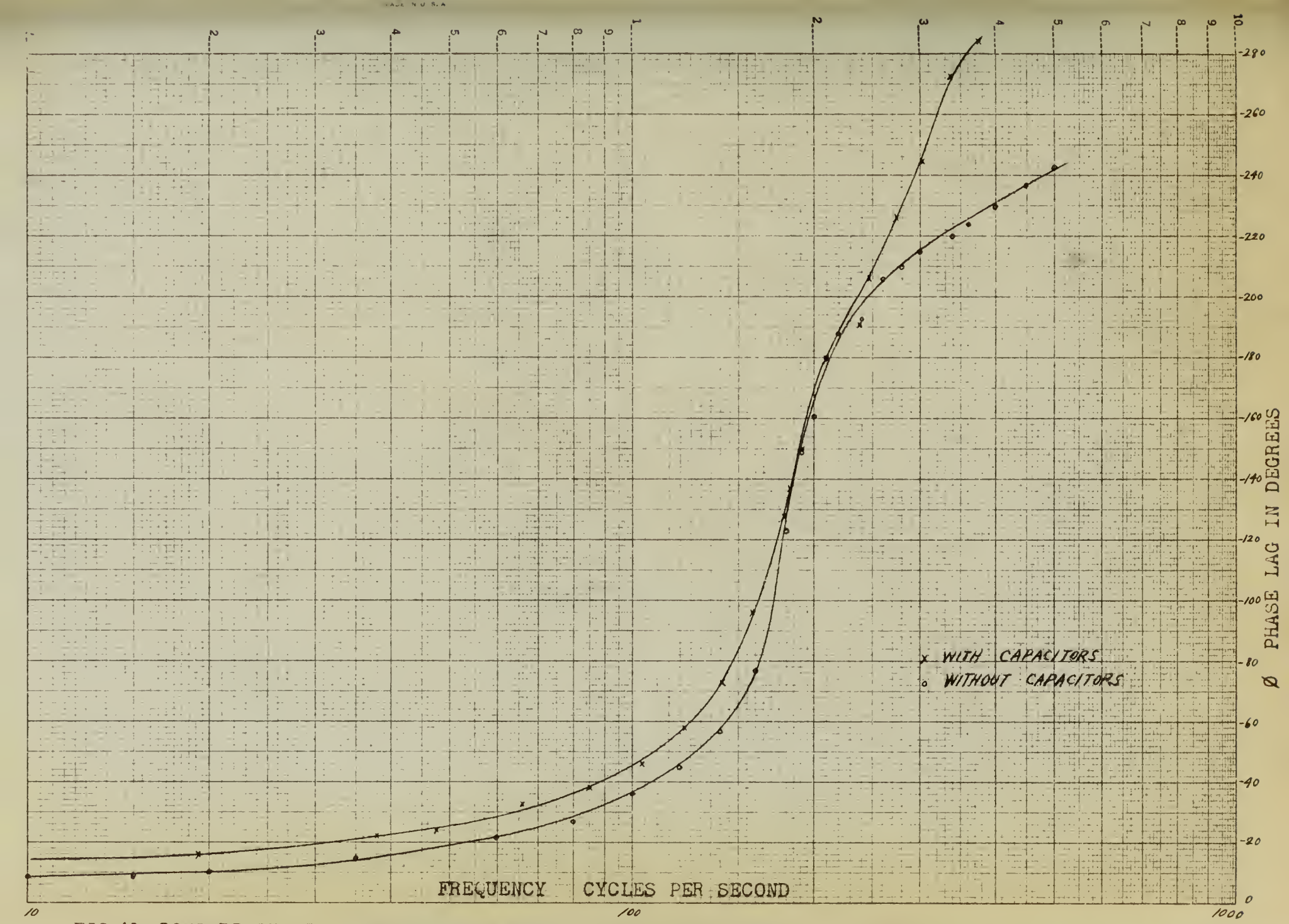

FIG.41 COMPARISON OF PHASE LAG FOR MOTOR B WITH AND WITHOUT CAPACITORS

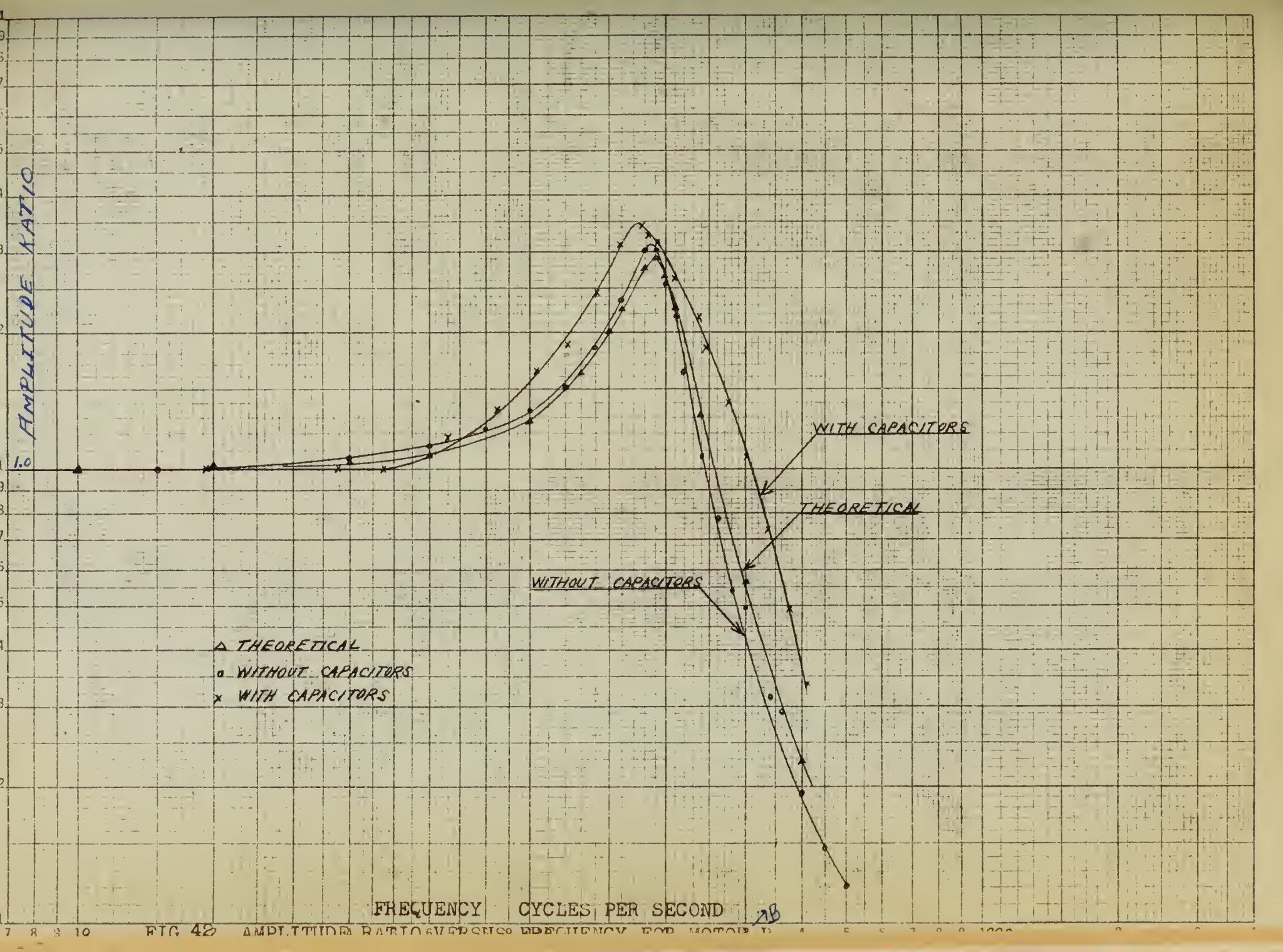

FIG 42 AMPLITUDE RATIO VERSUS FREQUENCY FOR MOTOR D

TABLE XI EXPERIMENTAL DATA FOR PHASE AND AMPLITUDE FREQUENCY CHARACTERISTICS OF MOTOR B WITHOUT CONDENSERS ACROSS MOTOR COILS

f	R_X	X_C	ϕ $(2\tan^{-1}\frac{X_C}{R_X})$	x (from Miller)	AMPLITUDE RATIO	$\frac{x}{\mu e} \times 10^{-6}$
cps	ohms	ohms	degrees	inches		in/volt
10	2400	31200	8.8	0.41	1.00	9.35
15	1700	20800	9.4	0.41	1.00	9.35
20	1400	15600	10.2	0.42	1.02	9.57
40	1000	7800	14.6	0.44	1.06	10.0
60	1000	5200	21.8	0.46	1.12	10.5
80	940	3900	27.2	0.50	1.22	11.4
100	1000	3120	35.6	0.55	1.34	12.6
120	1070	2600	44.8	0.62	1.51	14.2
140	1220	2230	57.4	0.76	1.85	17.3
160	1550	1950	76.8	0.97	2.36	22.1
180	3200	1731	123.2	1.24	3.02	28.3
190	6000	1641	149.4	1.24	3.02	28.3
200	19000	1559	161.2	1.05	2.56	23.9
210	100000	1486	180.0	0.90	2.19	20.5
220	100	1419	183.0	0.67	1.63	15.3
240	220	1300	192.8	0.44	1.07	10.0
260	280	1200	206.2	0.32	0.777	7.30
280	300	1113	210.2	0.24	0.584	5.48
300	330	1040	215.2	0.20	0.485	4.56
340	330	919	219.6	0.13	0.316	2.96
360	350	866	224.0	0.12	0.292	2.74
400	360	780	229.6	0.08	0.194	1.83
450	380	694	237.4	0.06	0.146	1.37
500	380	624	242.8	0.05	0.121	1.14

TABLE XII EXPERIMENTAL DATA FOR PHASE AND AMPLITUDE FREQUENCY CHARACTERISTICS OF MOTOR B WITH CONDENSERS ACROSS MOTOR COILS

f	R_x	X_c	ϕ $(2\tan^{-1}\frac{X_c}{R_x})$	x (from MILLER)	AMPLITUDE RATIO
cps	ohms	ohms	degrees	inches	
19.2	2300	16600	15.8	0.325	1.00
38.0	1600	8380	21.6	0.325	1.00
47.5	1400	6700	23.6	0.325	1.00
66.3	1400	4800	32.6	0.385	1.18
85.0	1300	3740	38.4	0.440	1.35
104.0	1300	3060	46.0	0.530	1.63
122.0	1400	2600	57.6	0.610	1.88
141.0	1680	2260	73.2	0.790	2.43
159.0	2230	2000	96.2	1.010	3.11
178.0	3700	1790	128.4	1.120	3.43
188.0	4400	1740	136.8	1.070	3.29
192.0	6200	1660	150.0	1.020	3.14
210.0	40000	1510	180.0	0.855	2.63
239.0	130	1330	191.2	0.705	2.17
246.0	300	1290	206.2	0.600	1.85
275.0	500	1160	226.6	0.455	1.40
301.0	670	1060	244.3	0.345	1.06
338.0	900	941	272.6	0.240	0.739
375.0	1130	849	286.2	0.160	0.493
411.0	1360	775	300.6	0.110	0.338

4.4 EXPERIMENTAL DETERMINATION OF TRANSIENT RESPONSE

In order to determine the transient response of the motor, a step input was applied to the grids by inserting a double pole, double throw switch across a variable voltage source. When the switch was thrown a small step input was applied. The output of the motor was recorded on the Miller oscillograph. A sample record is shown in Fig. 43. As can be seen from the sample record, it is very difficult to read exact values from such a picture. A comparison of the experimental and theoretical results is made in section 5.3 and the experimentally determined transient response is plotted in Fig. 48.

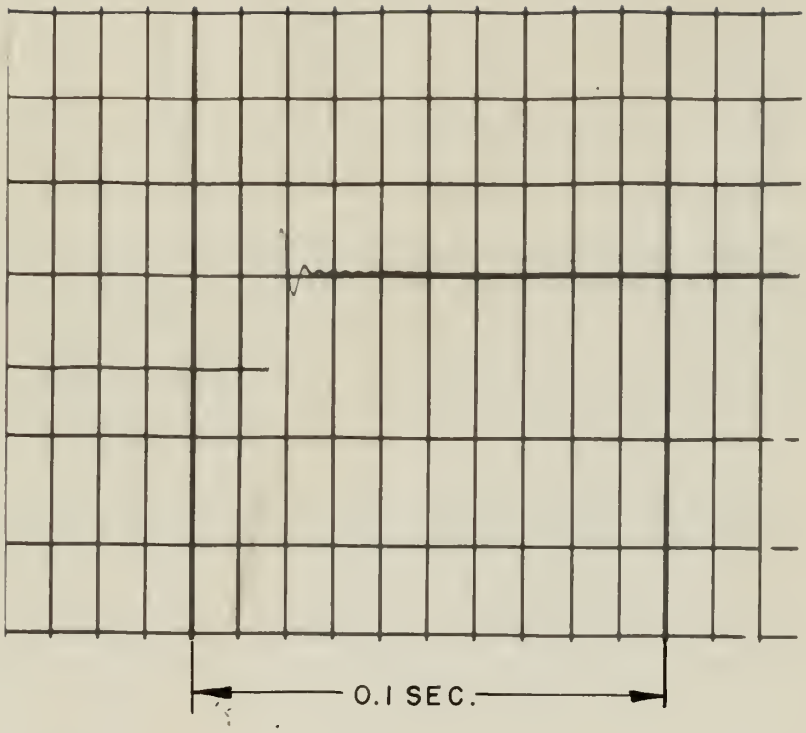

FIG. 43 SAMPLE OF MILLER OSCILLOGRAPH RECORD OF TRANSIENT RESPONSE TO A STEP INPUT

5.0 COMPARISON OF THEORETICAL AND EXPERIMENTAL RESULTS

In this section the theoretical results obtained in section 3.0 will be compared with those obtained in section 4.0 by actual experiment.

5.1 COMPARISON OF THEORETICAL AND EXPERIMENTAL IMPEDANCE CURVES

In Fig. 44 has been plotted the theoretical impedance curve for Motor B assuming a value of $\zeta = 0.1$. In the same figure, the impedance curve obtained experimentally is plotted. Data for these curves are given in Table XIII. The agreement of the theoretical and experimental curves is fair except at low frequencies. The reason for this disagreement below resonance is not known but may be due to invalid data at the low frequencies or harmonic distortion since the data was taken from one coil only. The theoretical curve was calculated assuming Class A push-pull operation of the amplifier. Since the phase and amplitude curves fit so nicely in the next section, it is felt that the difficulty lies in the experimental techniques used in measuring the impedance curve.

5.2 COMPARISON OF THEORETICAL AND EXPERIMENTAL PHASE AND AMPLITUDE CURVES

In Fig. 45 the theoretical amplitude characteristic for $\zeta = 0.1$ and the actual experimental curve for Motor B are plotted for the purpose of comparison. The calculation data for these curves may be found in Tables XI and XIV. The correlation between the two curves is excellent.

In Fig. 46 are plotted the phase characteristic curves corresponding to these amplitude curves. The agreement between theoretical and experimental curves is remarkable as the curves would lie one on the other out to 60 cycles if we ignore the constant phase lag difference of 6 degrees of the experimental curve. This lag appears to be caused by the initial value of displacement of the armature (section 4.3) or by some delay in the phase

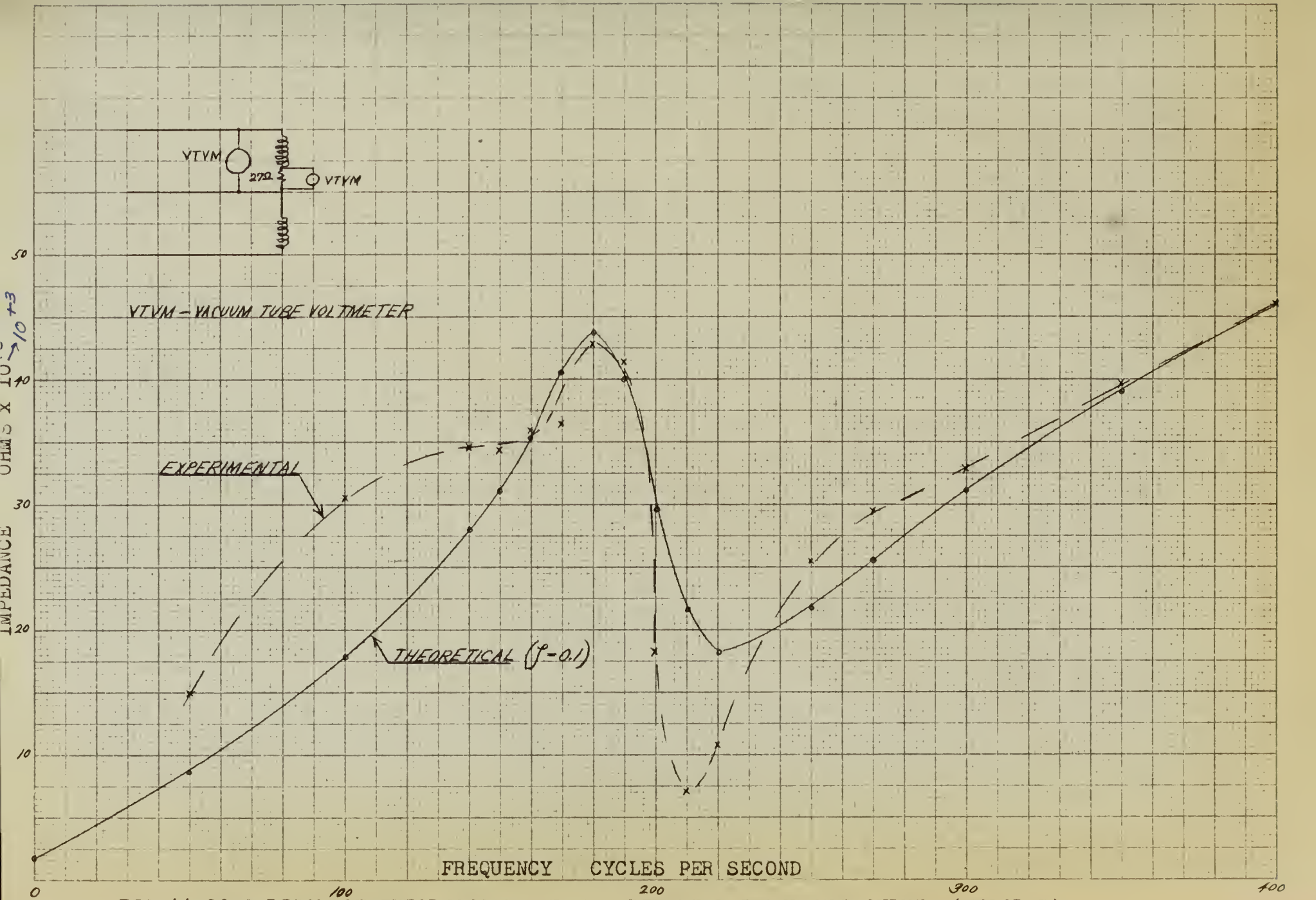

FIG.44 COMPARISON OF THEORETICAL AND EXPERIMENTAL IMPEDANCE CURVES (MOTOR B)

TABLE XIII THEORETICAL ($f=0.1$) AND EXPERIMENTAL DATA FOR IMPEDANCE CURVES OF MOTOR B

THEORETICAL		EXPERIMENTAL			
f cps	$Zx10^3$ ohms	Voltage(27Ω) volts	Current ma	Voltage(coil) volts	$Zx10^3$ ohms
0	1.80				
50	8.56	.072	2.67	40.0	15.0
100	17.9	.075	2.78	85.0	30.6
140	28.1	.082	3.04	105.0	34.6
150	31.3	.083	3.08	106.0	34.4
160	35.4	.081	3.00	108.0	36.0
170	40.5	.074	2.74	100.0	36.5
180	43.9	.059	2.19	94.0	42.9
190	40.0	.045	1.67	69.0	41.4
200	29.6	.052	1.96	36.0	18.4
210	21.6	.065	2.40	17.0	7.1
220	18.2	.074	2.74	30.0	10.9
250	21.8	.090	3.33	85.0	25.5
270	25.6	.094	3.46	102.0	29.5
300	31.2	.097	3.60	118.0	32.9
350	39.1	.081	3.00	119.0	39.7
400	46.2	.062	2.30	106.0	46.1

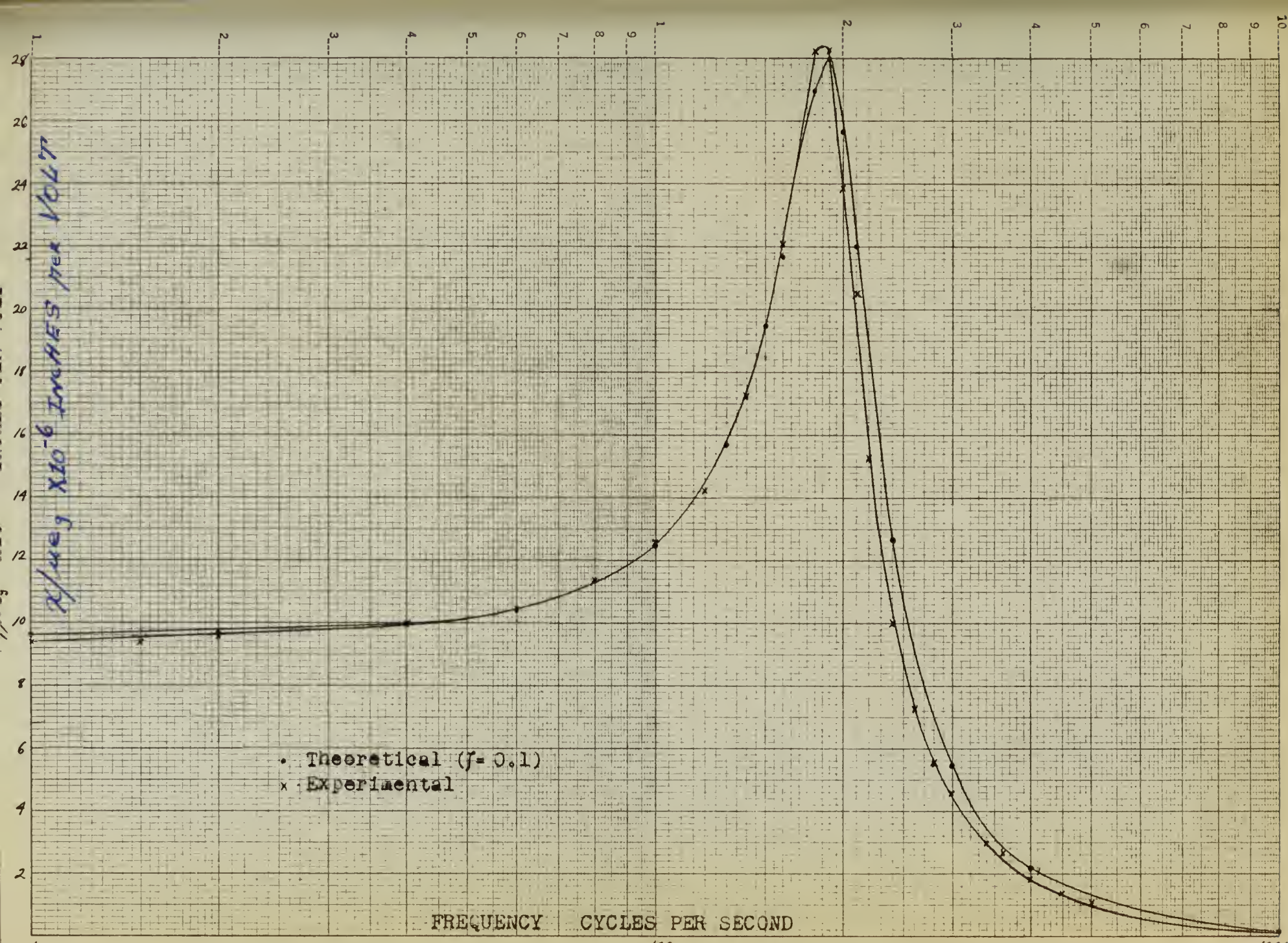

FIG.45 THEORETICAL AND EXPERIMENTAL AMPLITUDE CHARACTERISTIC FOR MOTOR B

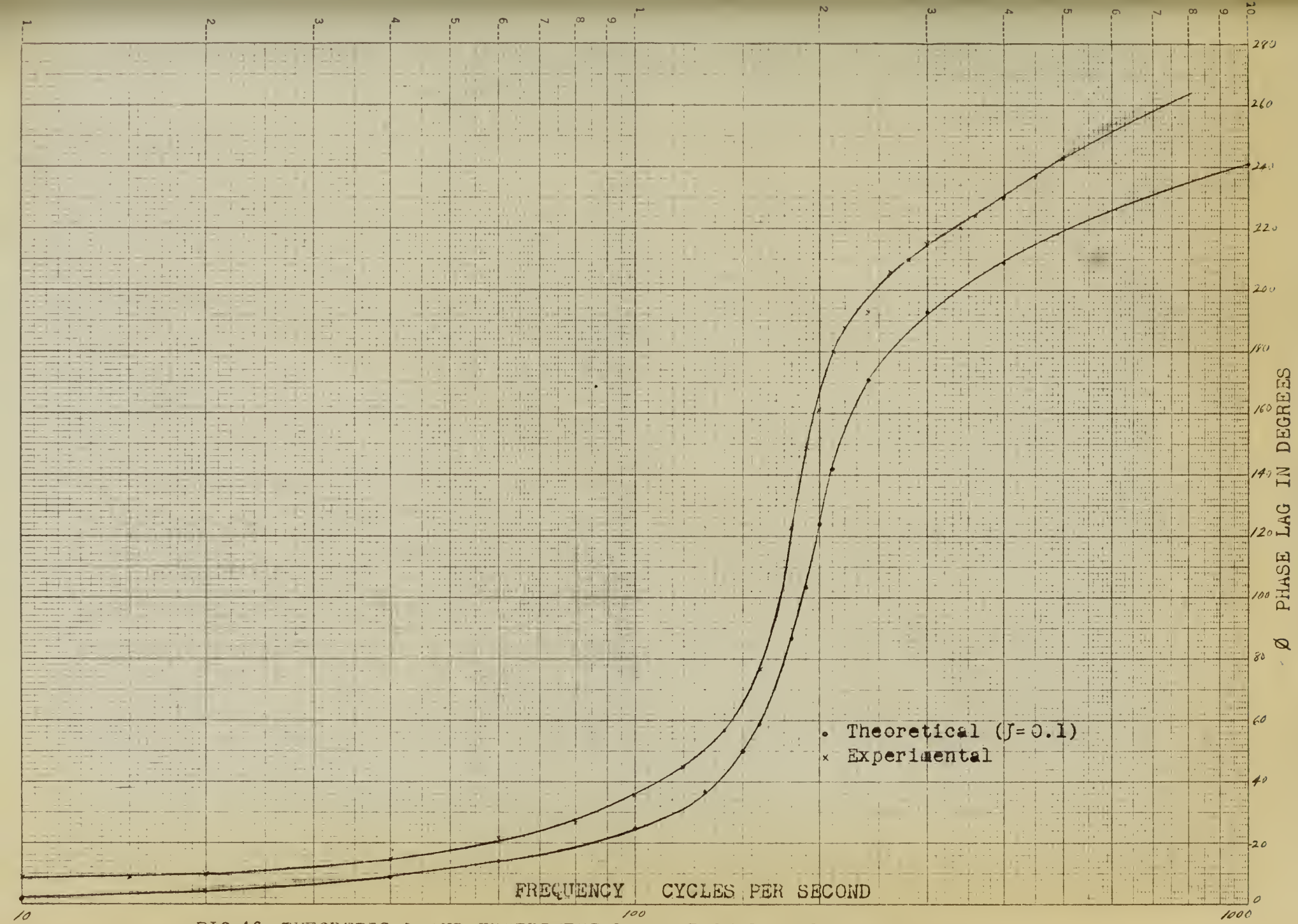

FIG.46 THEORETICAL AND EXPERIMENTAL PHASE CHARACTERISTIC FOR MOTOR B

TABLE XIV THEORETICAL DATA FOR PHASE AND AMPLITUDE FREQUENCY CHARACTERISTICS OF MOTOR B

f	$x/\mu e_b$	Ø	AMPLITUDE RATIO
cps	in/volt	degrees	
0	9.61	0.0	1.00
10	9.64	2.2	1.00
20	9.74	4.4	1.01
40	9.97	8.9	1.03
60	10.4	14.3	1.08
100	12.5	24.9	1.29
130	15.7	37.0	1.63
150	19.5	49.7	2.02
160	21.7	58.6	2.25
180	27.0	86.7	2.79
190	28.0	103.5	2.91
200	25.7	124.4	2.66
210	22.0	141.7	2.28
240	12.7	170.5	1.32
300	5.46	193.0	0.567
400	2.20	203.9	0.228
1000	0.16	241.1	0.017

measuring circuit or both. At 100 cycles per second the actual phase lag differs from the theoretical by only 12 degrees and the absolute phase lag is only 36 degrees. Beyond resonance there is more phase lag but this is accounted for by the fact that theoretically the system was assumed to be third order. For a third order system the phase lag should be asymptotic to the 270 degree axis. Actually, as shown in section 3.115, taking the elastance of the connection of the torque motor to the transfer valve into account the system is fifth order and therefore asymptotic theoretically to the 450 degree axis.

It is interesting to check the value of effective mass of the system found in section 4.1.

$$\omega_n = \sqrt{\frac{k}{M}} \qquad \text{or} \qquad M = \frac{k}{\omega_n^2}$$

but $$\omega_n = \frac{\omega_p}{\sqrt{1-2\zeta^2}}$$

where ω_p is the frequency of maximum response
ζ is damping ratio = 0.1

The value of ω_p from Fig. 45 is $(2\pi 188)$ radians per second. Substituting into the formula for M,

$$M = \frac{168}{\left(\frac{2\pi 188}{0.99}\right)^2} = 1.188 \times 10^{-4} \text{ lb sec}^2/\text{in} \quad (20.8 \text{ grams}).$$

5.21 Survey of Linear and Non-linear Regions

In performing the experimental tests for phase and amplitude characteristics on the torque motor, one must be careful to avoid voltage limiting, i.e. not allow the voltage on the tube to drop below approximately 65 volts so that the tube goes into its non-linear region and thereby introduces non-linearities into the system. The tube characteristics are shown in Fig. 47. Expressed differently, one must exercise care not to drive the tube from pentode into triode operation. To ensure that in running the experimental tests data were secured that could be compared directly with

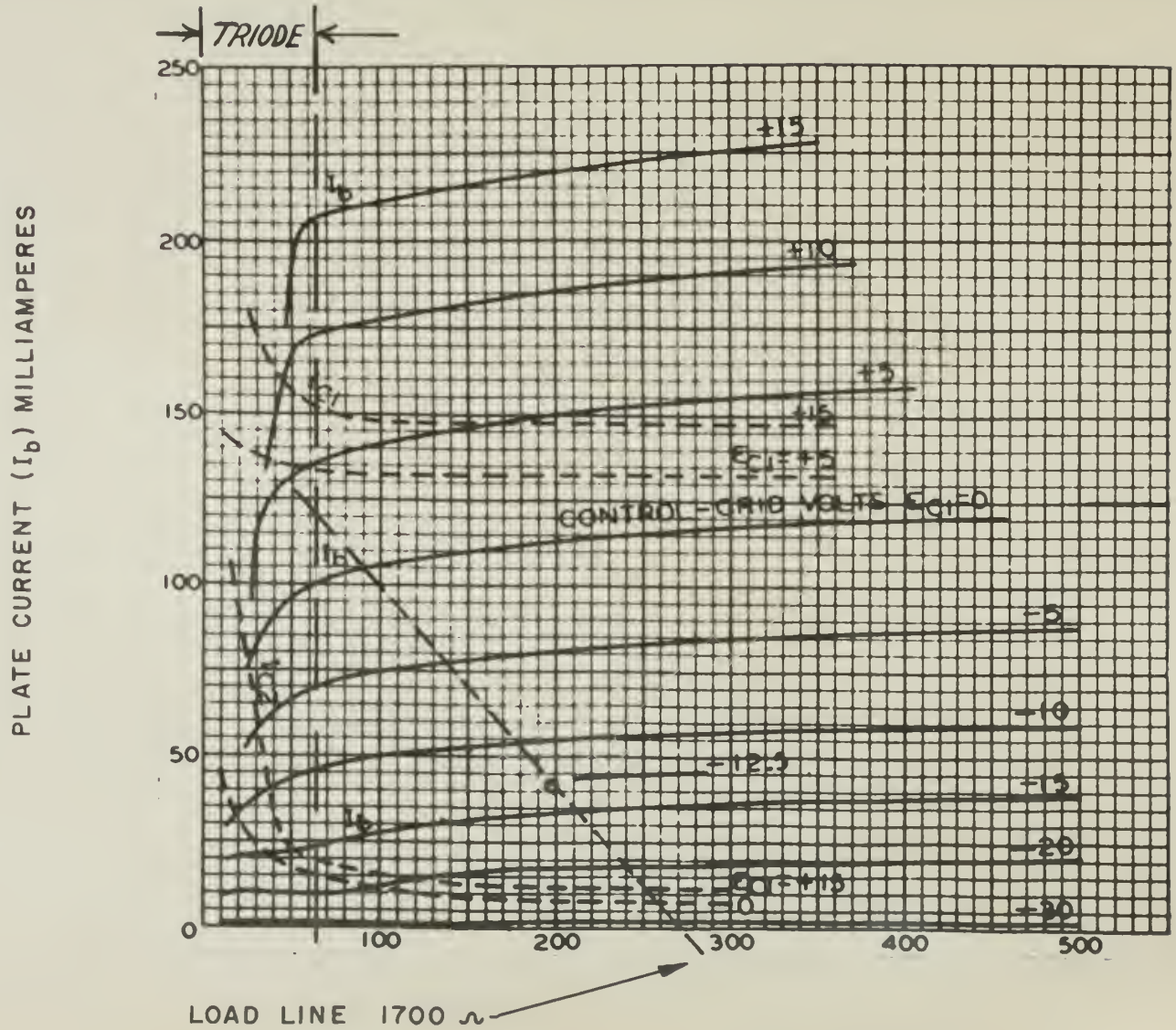

FIG. 47 TUBE CHARACTERISTICS OF THE 6AQ5 PENTODE

that of the analytical analysis, an oscilloscope was placed across the tube as a voltmeter. The voltage across the tube was kept at all times above 65 volts. Also an initial value of amplitude of armature movement of ±0.005 was used to avoid any non-linear effects due to the back electromotive force, K_B. Avoiding these non-linearities accounts for the fine correlation between the theoretical and experimental data.

5.3 COMPARISON OF THEORETICAL AND EXPERIMENTAL TRANSIENT RESPONSE CURVES

In Fig. 48 is plotted the theoretical transient response to a unit step function. Also the experimental response to a step input with the amplifier connected and no 0.1 microfarad capacitors across the motor coils. The experimental curve was taken off the photographic record from the Miller oscillograph and was blown up proportionally to the scale of the theoretical curve. The agreement is very good considering the difficulty in reading values off the record.

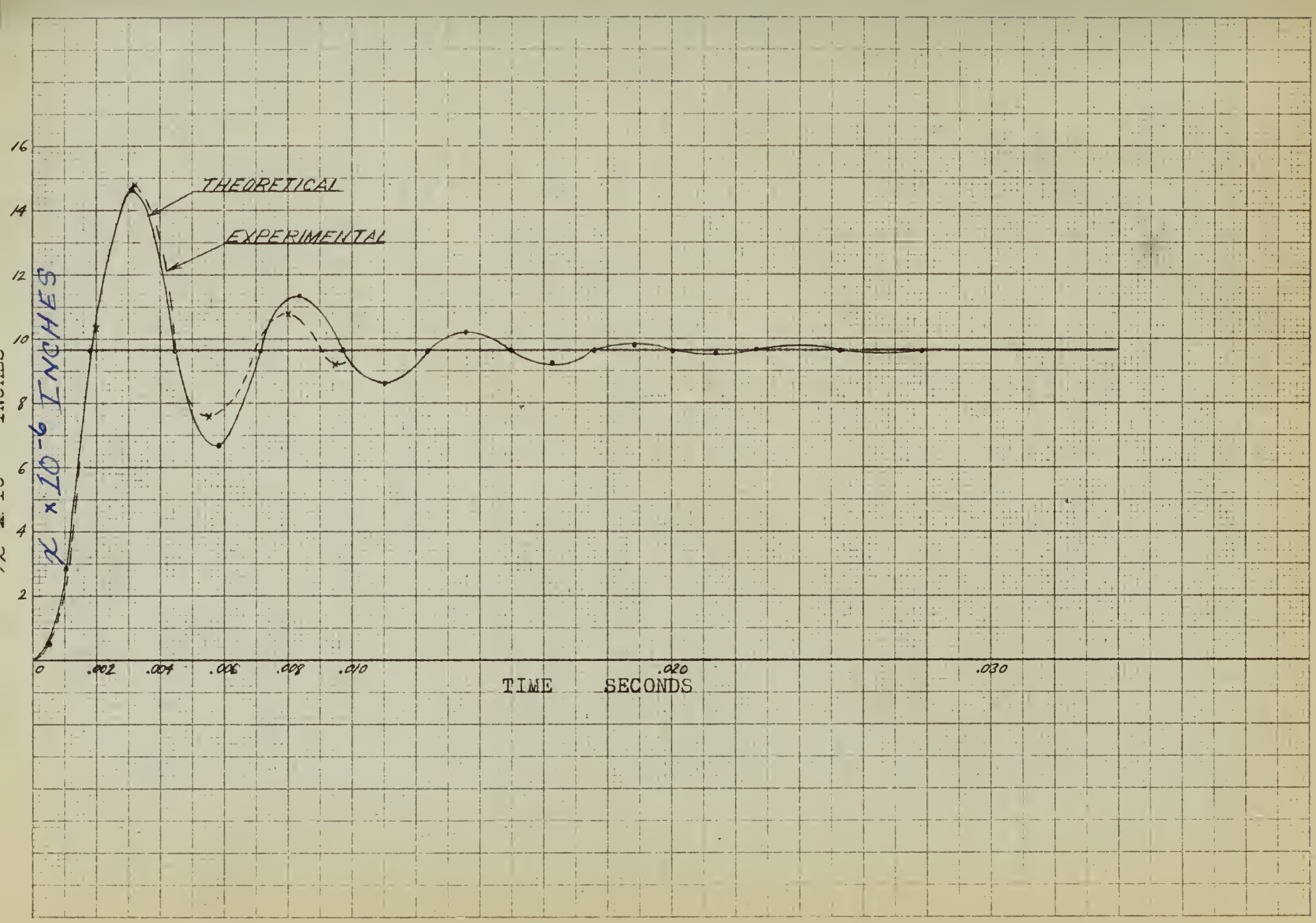

FIG. 48 COMPARISON OF THEORETICAL AND EXPERIMENTAL TRANSIENT RESPONSE CURVES (MOTOR B)

6.0 DISCUSSION OF EFFECT OF MOTOR STUDY ON CLOSED SERVO LOOP

In this section the effect of the motor on the functioning of the closed servo loop as shown in Fig. 1, will be discussed. The transfer function of the motor itself from section 3.23 is:

$$\frac{K_M/kR}{[s + 2950]\,[(s + 203) + j1190]\,[(s + 203) - j1190]}$$

If we place the motor in series with an integrating device such as a hydraulic transfer valve and actuator with transfer function K/s, as shown in Fig. 49,

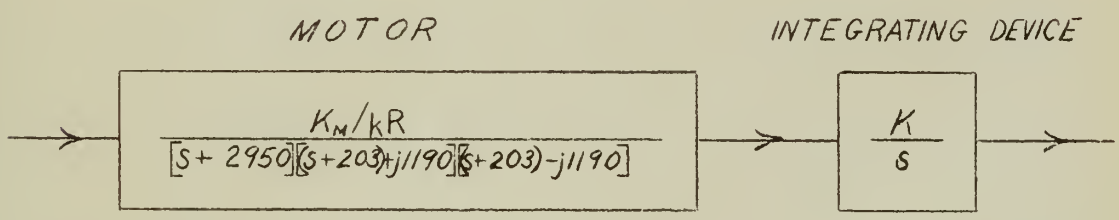

FIG. 49. BLOCK DIAGRAM OF MOTOR IN SERIES WITH INTEGRATING DEVICE

we have for the open loop transfer function,

$$\frac{K\,K_M/kR}{s\,[s + 2950]\,[(s + 203) + j1190]\,[(s + 203) - j1190]}$$

Substituting into this expression the values of the constants and multiplying out the quadratic term in the denominator, we may write the transfer function as

$$\frac{K\,(9.64\times10^{-6})}{s(s + 2950)(s^2 + 406s + 1.46\times10^{6})}$$

In terms of time constants this can be expressed as

$$\frac{1}{\tau_1 s(\tau_2 s + 1)\left((\tau_3 s)^2 + 406\,\tau_3 s + 1\right)}$$

where $\tau_1 = \dfrac{1}{K\times2.23\times10^{-15}}$

$\tau_2 = \dfrac{1}{2950}$

$\tau_3 = \dfrac{1}{1210}$, $\zeta = 0.168$

This open loop transfer function may be plotted by the use of non-dimensional gain phase diagrams which are included as Figs. 50 and 51. By making the plot, it was found that the locus crossed the minus 180 degree phase lag line at a value of ω equal to 1145 radians per second. The table below shows the values of the individual transfer functions for a value of ω equal to 1145 radians per second.

TRANSFER FUNCTION	GAIN db	ϕ degrees
$\frac{1}{(\tau_2 s + 1)}$	-0.5	-20
$\frac{1}{[(\tau_3 s)^2 + .406\tau_3 s + 1]}$	10.0	-70
$\frac{1}{(\tau_1 s)}$	?	-90
		-180

Since it is desired that the closed loop gain not exceed 3 decibels at minus 180 degrees, the total open loop gain must not exceed minus 4.5 decibels (see Fig. 52). It is evident then that the gain of the integrating network, $\tau_1 s$, must equal minus 14.0 decibels. From Fig. 50, u equals 5.0 for a gain of minus 14.0 decibels.

$$u = \frac{\omega}{2.23\times10^{-15}K} = 5.0$$

or $$K = \frac{1145}{2.23\times10^{-15}\times5.0} = 102.5\times10^{15} \text{ volts/in-sec.}$$

Therefore, $K_{loop} = 2.23\times10^{-15}\times102.5\times10^{15} = 228/\text{sec.}$

It can be seen that the motor allows extremely high values of gain to be used which is of great practical importance. In regard to this it is interesting to note the effect of increasing the damping term, ζ, in the quadratic term of the transfer function. For $\zeta = 0.168$ there resulted an open loop gain of 228; but, if ζ is increased to a value of 0.300, the open

FIG. 50 GAIN PHASE DIAG

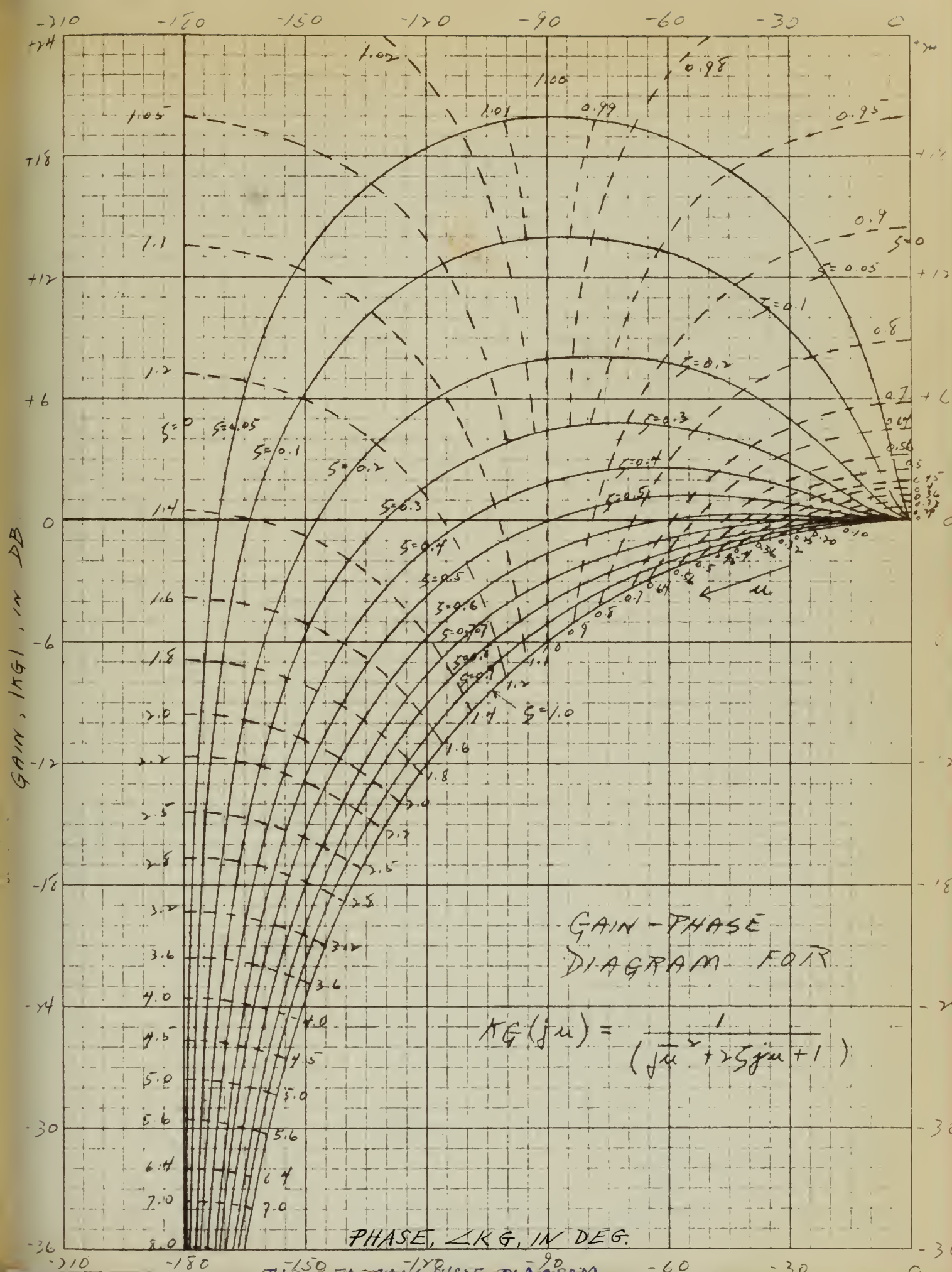

FIG. 51 GAIN-PHASE DIAGRAM

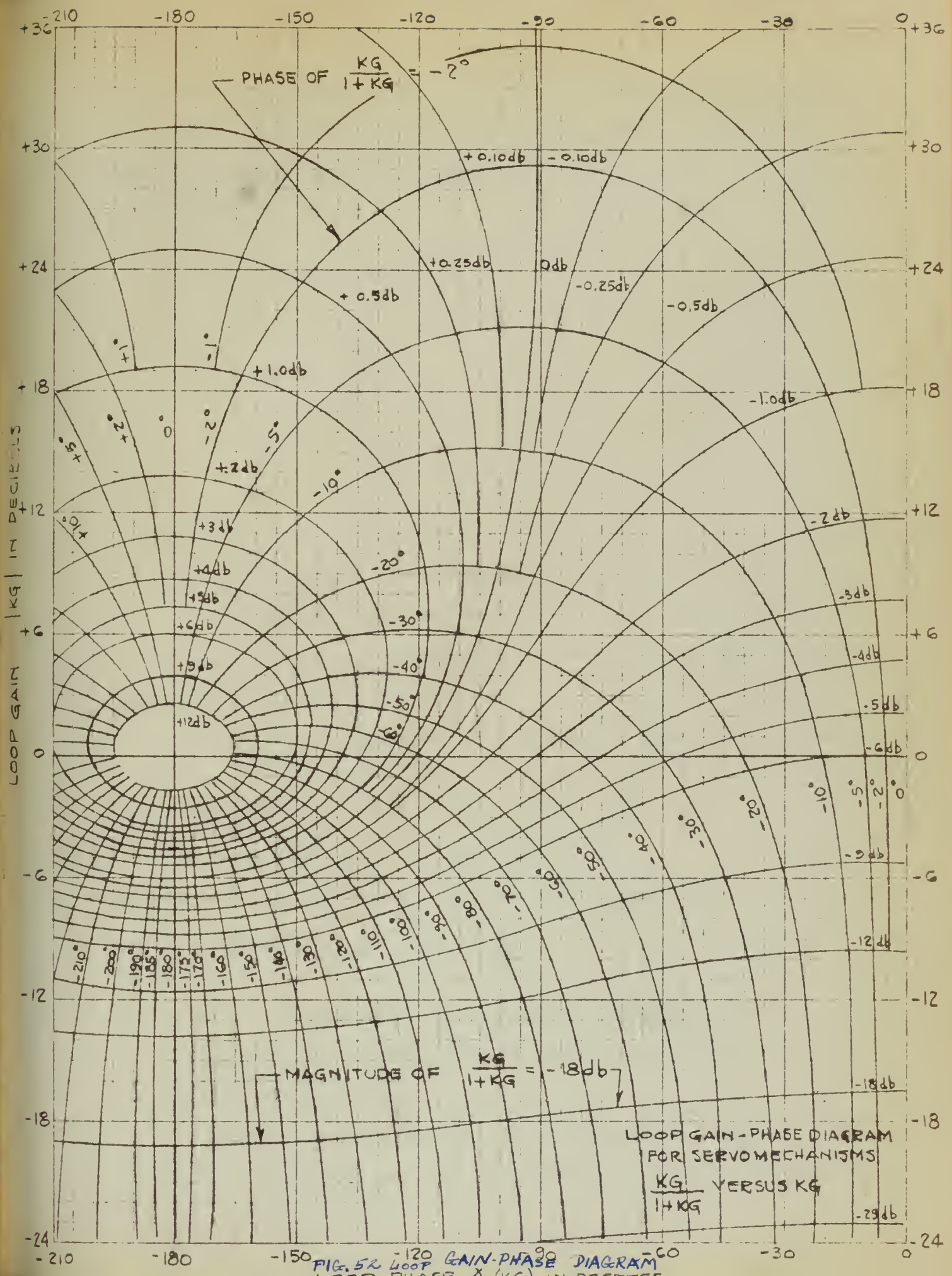

FIG. 52 LOOP GAIN-PHASE DIAGRAM

loop gain, K_{loop}, becomes equal to 456. This is closer to the values of gain actually realized in the closed loop shown in Fig. 1, since the hydraulic transfer valve adds a considerable amount of viscous damping to the system.

6.1 EFFECT OF CURRENT AND VOLTAGE FEEDBACK

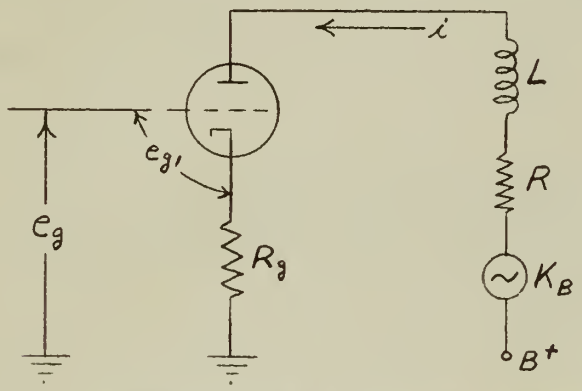

FIG. 53. SCHEMATIC SHOWING CURRENT FEEDBACK CIRCUIT

To understand what happens if we put in a resistor, R_g, to ground forming a current feedback path, let us first write the voltage equation by Kirchhoff's law

$$\mu e_{g1} = Ri + L\frac{di}{dt} + K_B\frac{dx}{dt} \qquad \text{where } R = r_p + R_c \text{ (Section 3.113)}$$

The voltage input to the grid, e_g, is the sum of e_{g1} and $R_g i$,

$$e_g = e_{g1} + R_g i \quad \text{or} \quad e_{g1} = e_g - R_g i$$

Substituting this value for e_{g1} into the initial equation,

$$\mu e_g = (R + R_g\mu)i + L\frac{di}{dt} + K_B\frac{dx}{dt}$$

The effect of current feedback is to increase the amount of resistance in the circuit by $R_g\mu$, which makes the tube look even more like a constant current source than before.

Voltage feedback has just the opposite effect tending to reduce the resistance and making the tube appear more like a constant voltage source.

7.0 CONCLUSIONS

This motor, operating on the polarized relay principle, provides high frequency response and by reducing the motor-valve time delay improves the servo stability, allows a higher servo loop gain, and results in a higher performance servo system.

The high resonant frequency makes for good servo stability and keeps transient oscillations of the motor from appearing at the output of the servomechanism.

Motors of this type will have many applications where small proportional displacements and large torques with low inertia are prime requisites.

8.0 APPENDIX

8.1 MOMENT OF INERTIA OF ARMATURE CALCULATION

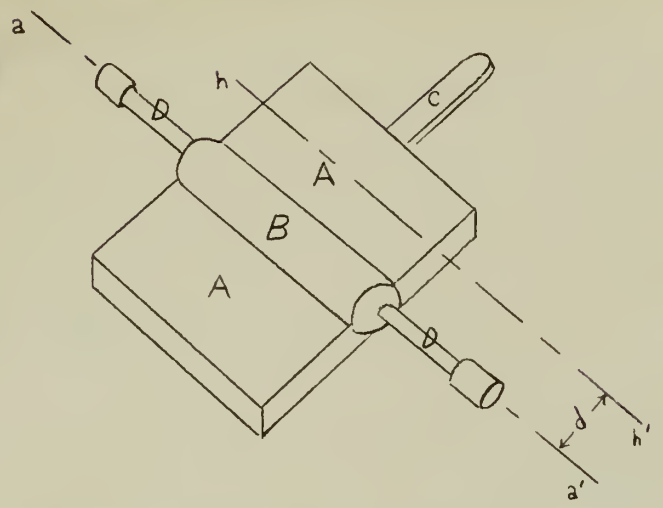

FIG. 54. MOTOR ARMATURE DIVIDED INTO SIMPLE GEOMETRIC SHAPES

The armature was divided up into simple geometric shapes as shown in Fig. 54 and listed below.

Part	Volume Cu. In.	Mass Grams	I^* gm-cm^2	I gm-cm^2
A (Rectangular parallelepiped)	2(0.0927)	2(8.95)	2(2.26)	2(17.16)
B (Circular cylinder)	0.1251	16.17	---	1.54
C (Rectangular parallelepiped)	0.0114	1.47	0.264	12.26
D (Circular cylinder)	2(0.0238)	6.13	---	---
		Total		$I_a = 48.12$

Sample calculation for one body (rectangular parallelepiped A)

Volume = (0.6715 x 1.047 x 0.132) = 0.0927 cu. in.

Mass = 0.0927 cu. in. x 0.284 lbs/in^3 (density of steel) x 454 gr/lb x 0.75 (staking factor)

= 8.95 grams

I^*(Moment of inertia about axis h-h′) $= \frac{8.95\ (1.708^2 + 0.336^2)}{12} = 2.26$ gm-cm^2

Using the parallel axis theorem

$$I_{a-a,} = I^{*} + md^2 = 2.26 + (8.95 \times 1.665) = 17.16 \text{ gm-cm}^2$$

This procedure was followed for each part of the armature and the result tabulated above. The moment of inertia of armature, I_a, equals 48.12 gm-cm^2.

8.2 FLUX DENSITY IN AIR GAP DUE TO CURRENT IN ARMATURE COILS

The reluctance of the air gap is

$$\mathcal{R} = \frac{g}{\mu_o S} = \frac{0.145}{1.259 \times 1.69} = 0.0683 \text{ NI/maxwell}$$

where g = length of gap, 0.145 cm.
S = area of gap, 1.69 sq. cm.
μ_o = magnetic permeability, 1.259 maxwell-cm/NI

The flux in each air gap due to the current in the armature coils is

$$\phi_a = \frac{\mathcal{F}}{\mathcal{R}} = \frac{\frac{NI_A}{2}}{\mathcal{R}}$$

where $\frac{NI_A}{2}$ is the armature ampere-turns acting at each gap.

The flux density is

$$B = \frac{\phi_a}{S} = \frac{NI_A}{2\mathcal{R}S} = \frac{NI_A}{2 \times 0.0683 \times 1.69} \text{ gauss}$$

If we denote this flux density by the symbol B_{ga}, then

$$B_{ga} = \frac{NI_A}{2 \times 0.1152} \text{ gauss}$$

where N = 7650 turns
B_{ga} = flux density in gap due to armature, gauss.

The measured values of the flux density were obtained by removing the permanent magnet from a motor and measuring the flux present in the gap for different values of current in the armature coils. The actual physical measurement of the flux density in the air gap presented quite a problem because of the small physical dimensions involved. A special test coil was wound by Mr. Loran A. Wenrich and imbedded in a piece of lucite. This search coil and the fluxmeter used were then calibrated together at the National Bureau of Standards and the combination was used in making all flux measure-

ments. A plot of calculated and experimental air gap flux density versus armature ampere-turns may be found in Fig. 55. The calculated and measured data are given in Table XV.

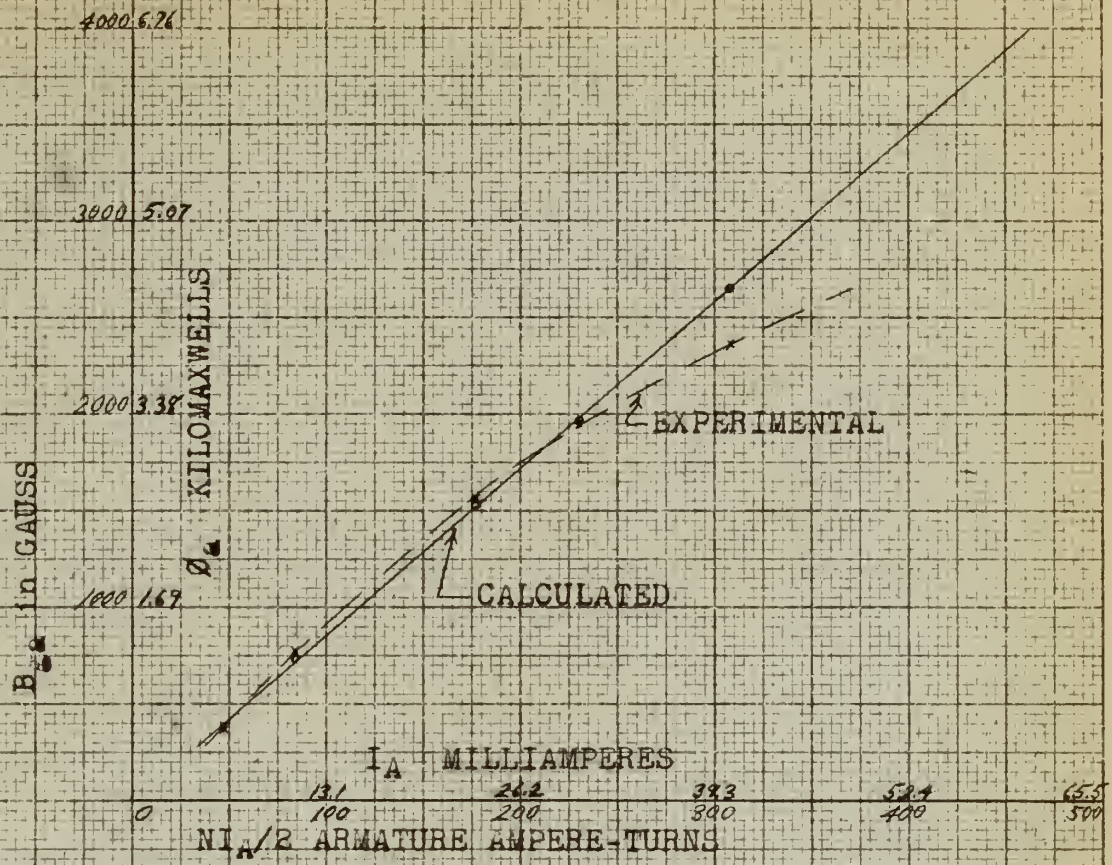

FIG. 55 PLOT OF CALCULATED AND EXPERIMENTAL AIR GAP DENSITY VERSUS ARMATURE AMPERE-TURNS.

TABLE XV FLUX DENSITY IN AIR GAP DUE TO ARMATURE AMPERE-TURNS.

aa	$NI_A/2$	B_{g_a} (Calc)	B_{g_a} (Meas)
12	46	398	394
22	84	729	787
46	176	1525	1574
60	230	1992	1966
80	306	2650	2360

8.3 TABLE XVI CONSTANTS OF MOTORS A AND B USED IN STUDY

CONSTANT	MOTOR A	MOTOR B
R resistance (R_c+r_p), ohms	61800	61800
R_c coil resistance, ohms	1800	1750
r_p plate resistance, ohms	60000	60000
L inductance, henries	15	20
K_M electromechanical coupling constant, lbs/amp	90.1	100
k spring coefficient, lbs/in	207	168
K_b back electromotive force, volt sec/in	9.0	9.6
f/M damping parameter /sec	300	264
M mass, lb sec^2/in	$1.188x10^{-4}$	$1.188x10^{-4}$
ζ critical damping ratio	0.113	0.100
f viscous friction, lb sec/in	0.0354	0.0283

8.4 COMPLETE LIST OF SYMBOLS

a	Constant
A	Maximum displacement of armature from neutral
A'	Terminal point in phase shift network
A*	Special constant used in section 3.115
b	Constant
B	Flux density
B_{ga}	Flux density in air gap due to armature ampere-turns
B_p	Flux density in any gap due to permanent magnet
B'	Terminal point in phase shift network
B*	Special constant used in section 3.115
C	Capacitance
C*	Special constant used in section 3.115
D'	Terminal point in phase shift network
D*	Special constant used in section 3.115
e	Voltage applied to armature coil
e_g	Grid voltage
e_i	Voltage input
e_o	Voltage output
E	Voltage
E*	Special constant used in section 3.115
f	Viscous friction coefficient and also frequency (no ambiguity)
f_v	Viscous friction of valve
F	Force
F_v	Force of valve
F'	Terminal point in phase shift network
F*	Special constant used in section 3.115
F_1, F_2, F_3, F_4	Forces acting at air gaps 1, 2, 3, and 4
$\mathcal{F}$	Magnetic potential difference
g	Gap length with armature centered
g_1, g_2, g_3, g_4	Gap lengths of air gaps 1, 2, 3, and 4
i	Differential current
i_1, i_2	Individual currents flowing in each of the two coils
I	Current
I_a	Moment of inertia of armature
I_A	Current in armature coil
k	Effective spring coefficient
k_f	Anti-spring rate
k_s	Actual spring rate of torsional centering spring
k_v	Spring coefficient of valve
k_1	Spring coefficient of connection
K	Gain of integrating device
K_B	Back electromotive force
K_{loop}	Open loop gain of system
K_M	Electromechanical coupling constant
K*	Step input voltage
l	Length of armature suspension
ln	Natural logarithm
L	Inductance of armature coil
M	Total effective moving mass

M_a	Mass of armature
M_e	Mass equivalent of armature
M_v	Mass of valve piston and piston rod
N	Number of turns on armature coil
NI	Ampere-turns of permanent magnet
NI_A	Ampere-turns of armature
P	Pivot point of armature
$\mathcal{P}$	Magnetic permeance
$\mathcal{P}_1, \mathcal{P}_2, \mathcal{P}_3, \mathcal{P}_4$	Permeances at air gaps 1, 2, 3, and 4
Q	Force of valve and rod acting on motor
r	Distance from point of application of valve force to pivot point P
r_p	Plate resistance
R	Total resistance of plate and coil
R_c	Resistance of armature coil
R_x	Variable resistance
R_1, R_1'	Matched resistances in phase shift network
$\mathcal{R}$	Magnetic reluctance
$\mathcal{R}_a$	Reluctance of armature
$\mathcal{R}_1, \mathcal{R}_2, \mathcal{R}_3, \mathcal{R}_4$	Reluctances at air gaps 1, 2, 3, and 4
s	Laplace operator
S	Area of gap
T	Period of oscillation
u	Dimensionless frequency variable
V_g	Voltage generated by motion of armature in magnetic field
V_1, V_2, V_3	Voltages
w	Half suspension width
x	Armature displacement at point of application of valve force
x_1	Displacement of piston rod
X	Length of armature from pivot point to center of air gap
X_c	Capacitive reactance
y	Armature displacement in air gap
y_1, y_2	Two consecutive values of amplitude of same sign from oscillographic record of transient response
Y	Length of armature from center of air gap to point of application of valve force
Z	Impedance
Z_c	Impedance of armature coil
Z_o	Source impedance

α	Logarithmic decrement
Δt	Time interval
ϵ	Error signal
ζ	Ratio of actual damping to critical damping
θ_i	External input signal
θ_o	Output signal
μ	Amplification factor
μ_o	Magnetic permeability
τ_1, τ_2, τ_3	Time constants

ϕ	Phase angle
ϕ_a	Armature flux
ϕ_L	Leakage flux
ϕ_o	Flux at any gap
ϕ_p	permanent field flux
ϕ_1, ϕ_2, ϕ_3, ϕ_4	Total flux at air gaps 1, 2, 3, and 4
ϕ_1', ϕ_2', ϕ_3' ϕ_4'	Loop fluxes used to calculate leakage flux
ω	Angular velocity
ω_n	Angular velocity at undamped natural resonant frequency
ω_o	Angular velocity at damped resonant frequency
ω_p	Angular velocity at peak resonance
Ω	Ohms

$\bar{\ }$	Bar over a quantity means the Laplace transform of that quantity
$\dot{\ }$	Single dot over quantity indicates the first derivative of that quantity with respect to time
$\ddot{\ }$	Double dot over quantity indicates the second derivative of that quantity with respect to time

8.5 REFERENCES

1. ELECTROMAGNETIC DEVICES by H. C. Roters, John Wiley and Sons, New York, 1941.

2. PRINCIPLES OF SERVOMECHANISMS by Gordon S. Brown and Donald P. Campbell, John Wiley and Sons, New York, 1948.

3. DESIGN OF A POLARIZED RELAY WITH A FREQUENCY RESPONSE FROM 0 TO 200 CYCLES PER SECOND by R. B. Higley and J. Wheeler, R47-3, July 31, 1947. UNCLASSIFIED.

4. ADVANCED EXERCISES IN PRACTICAL PHYSICS by Arthur Schuster and Charle H. Lees, Cambridge University Press, London, 1901.

5. ELECTRONIC CIRCUITS AND TUBES by Cruft Laboratory, War Training Staff, McGraw-Hill, New York, 1947.

V I T A

Robert Joseph McNICHOLAS was born in Boston, Massachusetts, April 8, 1925. He attended Boston Public Latin High School and was graduated in June, 1942. He was employed by the Boston Edison Company until enlisting in the U. S. Naval Reserve and in November, 1943, was assigned to the Naval V-12 unit at the Massachusetts Institute of Technology. Upon acceptance as a member of the Naval Reserve Officer Training Corps, he was assigned to the naval unit at Tufts College, Medford, Massachusetts. At Tufts he was elected to membership in Tau Beta Pi. In February, 1946, he was commissioned a second lieutenant in the U. S. Marine Corps Reserve and was awarded the degree of Bachelor of Science in Engineering magna cum laude. Following assignment at Parris Island, South Carolina, and Quantico, Virginia and upon completion of the U. S. Marine Corps Basic School, he was commissioned a second lieutenant in the U. S. Marine Corps.

He served as a rifle platoon commander in the Fifth Marines in North China until the withdrawal of Marine forces to Guam in May, 1947. Following assignments as Transport Quartermaster and Battalion S-4, he returned to the United States and attended the Basic Artillery Officers' Course given by the U. S. Army at Ft. Sill, Oklahoma, and Ft. Bliss, Texas. In July, 1949, he was assigned to the U. S. Naval Postgraduate School, Annapolis, Maryland, where he was awarded the degree of Bachelor of Science in Electrical Engineering in June, 1951.

OCT 2 BINDERY

18047

Thesis
M265

McNicholas
Theoretical & experimental study of a new, small, high speed, linear torque motor ...

OCT 2 BINDERY

Thesis
M265

18047

McNicholas
Theoretical & experimental study of a new, small, high speed, linear torque motor (polarized relay type).

Library
U. S. Naval Postgraduate School
Monterey, California

thesM265
Theoretical and experimental study of a
3 2768 001 01202 4
DUDLEY KNOX LIBRARY